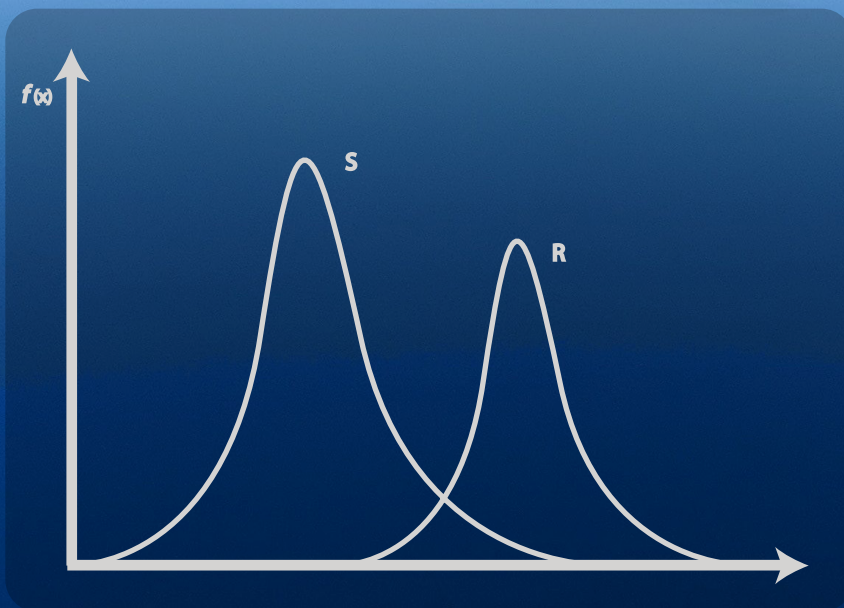# Reliability analysis of Submerged Floating Tunnels

F.E.M. Swaalf

Reliability analysis of Submerged Floating Tunnels

by

F.E.M. Swaalf

to obtain the degree of Master of Science
at the Delft University of Technology,
to be defended publicly on June 16, 2020 at 10:30 AM.

An electronic version of this thesis is available at `http://repository.tudelft.nl/`.
Cover credits: Eugene Kopich

Preface

Dear reader,

This thesis is written as part of the Master of Science in Structural Engineering (Hydraulic Structures) at the Technical University of Delft. In this work I present the findings of the reliability analysis performed for an SFT. This topic triggered me from the beginning, because of the practical application and my personal interest in probabilistic design. Through probabilistic design, the SFT can be optimized and an economical design can be made. This is not only the case for an SFT, but this also holds for many other (new) structures.

"Doubt is an uncomfortable condition, but certainty is a ridiculous one." - Voltaire

Delft, 9th of June 2020

Abstract

A submerged floating tunnel (SFT) can be a promising solution for crossing a deep or wide waterway. This tunnel concept will consist of an immersed tube, either attached with anchor cables to the seabed or attached to pontoons floating on the water surface. The reliability of the tether-stabilized SFT is assessed in this research. A suitable target reliability is determined in order to design a full probabilistic SFT. Subsequently, a calibration of partial factors from Eurocode is performed. The robustness of the structure is also analyzed and improvements are suggested.

Important failure mechanisms are defined as yielding and slackening of the tethers, longitudinal failure and transverse shear failure of the tube. A first-order reliability method (FORM) and a Monte Carlo simulation (MC) are performed for the limit state functions of these mechanisms. Design parameters are determined so that a target reliability index of 3.8 is met, because of consistency with Eurocode. Consequently, the design points from FORM are used to calculate partial factors for different loading types. The calculated factors and the general partial factors from Eurocode are compared.

Slackening of the tethers proved to be the governing failure mechanism in this analysis. The resistance against slackening depends on the force equilibrium, whereas the resistance of the other mechanisms depends on structural strength. The influence factors from the FORM analysis indicated that permanent loading parameters were dominant, i.e. concrete density, water density and tube diameter. It was found that for the strength (STR) mechanisms, the factors from Eurocode result in an overly safe design of the SFT. The calculated partial factors for unfavorable permanent load and variable load are significantly lower than the corresponding general factors from Eurocode. For the equilibrium (EQU) case, Eurocode is not safe to be applied. The general partial factor for the unfavorable permanent loading is insufficient.

The robustness of the structure is assessed by considering important scenarios. Excessive leakage has large consequences and will result in global structural failure. However, it has a low probability of occurrence. Mitigating measures are available to prevent failure due to leakage. Furthermore, an SFT will be constructed at a specific location. Wave conditions and geolocation need to be taken into account to reach an optimal design. At a depth of 30 meters, the impact of waves becomes insignificant. Lastly, failure of a single tether should not result in failure of adjacent tethers (i.e. progressive failure). A redundant system can be created by installing more or higher quality tethers. Consequently, when all four tethers of one element fail at the same time, this does not result in longitudinal failure.

Overall, it was demonstrated that the reliability requirements of the SFT can be met in the design. Moreover, the design can be optimized by a full probabilistic calibration of partial factors.

Keywords: submerged floating tunnels, tether-stabilized, partial factor method, first-order reliability method, Monte Carlo simulation, tether yielding, tether slackening, Eurocode

Samenvatting

Een onder water drijvende tunnel, ookwel een Submerged Floating Tunnel (SFT) genoemd, kan een veelbelovende oplossing zijn om een diepe of brede waterweg over te steken. Deze tunnel zal bestaan uit een buis onder het wateroppervlak, ofwel bevestigd met ankerkabels aan de zeebodem of bevestigd aan pontons die op het wateroppervlak drijven. In dit onderzoek is de betrouwbaarheid van de SFT-variant met ankerkabels onderzocht. Een geschikt betrouwbaarheidsniveau is bepaald om de SFT volledig probabilistisch te ontwerpen. Vervolgens is een kalibratie uitgevoerd met de algemene partiële veiligheidsfactoren van de Eurocode. De robuustheid van de constructie is ook geanalyseerd en er zijn methodes voorgesteld om de robuustheid te verhogen.

Belangrijke faalmechanismen zijn gedefinieerd als het vloeien en slap hangen van de ankerkabels, het in langsrichting en dwarsrichting falen van de buis. Een eerste-orde betrouwbaarheidsmethode (FORM) en een Monte Carlo-simulatie (MC) zijn uitgevoerd voor de grenstoestanden van deze mechanismen. Ontwerpparameters zijn zo bepaald dat aan een betrouwbaarheidsindex van 3.8 is voldaan, vanwege consistentie met de Eurocode. Vervolgens zijn de ontwerppunten vanuit FORM gebruikt om partiële factoren voor verschillende soorten belasting te berekenen. De berekende factoren zijn vergeleken met de algemene partiële factoren uit de Eurocode.

In dit onderzoek bleek het slap hangen van de ankerkabels het belangrijkste faalmechanisme te zijn. De weerstand hiervan hangt af van het krachtenevenwicht, terwijl de weerstand van de andere mechanismen afhangt van materiaalsterkte. De invloedsfactoren uit de FORM-analyse demonstreerden dat de parameters van de permanente belasting dominant waren, zoals betondichtheid, waterdichtheid en buisdiameter. De hieruitvolgende partiële factoren weken af van de algemene factoren van de Eurocode. De toepassing van de Eurocode vergt dus een aparte kalibratie om specifiek voor SFT's een goede relatie tussen partiële factoren en veiligheid te bereiken. Voor de sterkte (STR) gevallen kan de Eurocode veilig worden toegepast. De algemene partiële factoren voor ongunstige permanente belasting en voor variabele belasting waren aanzienlijk conservatief ten opzichte van de berekende factoren. In het geval van evenwicht (EQU) is de Eurocode niet veilig om toe te passen. De algemene partiële factor voor de ongunstige permanente belasting was onvoldoende.

Verder is de robuustheid van de constructie beoordeeld aan de hand van belangrijke scenario's. Overmatige lekkage heeft grote gevolgen en zal leiden tot systeemfalen. Echter is de kans dat dit voorkomt klein. Er zijn mitigerende maatregelen beschikbaar om falen als gevolg van lekkage te voorkomen. Verder zal een SFT op een specifieke locatie worden gebouwd, waar rekening gehouden moet worden met golfcondities en geolocatie om tot een optimaal ontwerp te komen. Op een diepte van 30 meter wordt de impact van golven klein. Ten slotte mag het falen van een enkele ankerkabel niet leiden tot het falen van alle ankerkabels. De betrouwbaarheid kan worden verhoogd door meer of betere kwaliteit ankerkabels te installeren. Als alle vier de ankerkabels van één element dan tegelijkertijd falen, resulteert dit niet in het falen van de buis in langsrichting.

Over het algemeen is de veiligheid van een SFT gegarandeerd in het kader van dit onderzoek. De toegepaste methode is bruikbaar voor toekomstige betrouwbaarheidsanalyses van de SFT.

Contents

List of Figures

1

List of Tables

List of Symbols

α The importance or sensitivity factor of a parameter

β The reliability index

γ_c The unit weight of concrete

γ_f The partial factor for favorable loading

γ_R The partial safety factor for resistance

γ_S The partial safety factor for the load effect

γ_u The partial factor for unfavorable loading

γ_V The partial factor for the most important variable load

γ_v The partial factor for other variable loads

γ_w The unit weight of water

μ_x The mean value of X

Φ^{-1} The inverse normal distribution

σ_c The stress in the concrete cross-section

σ_x The standard deviation of X

θ_1 Model uncertainty for shear capacity

θ_R Model uncertainty for resistance

θ_S Model uncertainty for strength

$\theta_{\sigma R}$ Model uncertainty for the capacity of the cross-section

$\theta_{\sigma S}$ Model uncertainty for stresses in the cross-section

A_c The area of the concrete tube cross-section

A_p The area of prestressing steel

A_s The submerged area of the object

A_t The area of the steel tether cross-section

A_{strand} The area of one strand of the prestressing steel

C_D The drag coefficient

C_L The lift coefficient

D The outer diameter of the concrete tube

e The eccentricity of the post-tensioning

$f(x)$ The probability density function

f_s The average tension strength of the prestressing steel

f_y	The yield strength of steel
f_{cd}	The design value of the compressive strength
f_{ck}	The characteristic value of the compressive strength
f_{cm}	The mean value of the compressive strength
G	Permanent actions
g	The gravitational acceleration
M	The bending moment
N	The normal force
N_p	The normal force due to prestressing steel
P	Pretension
P_f	The probability of failure
Q	Variable actions
q_b	Distributed load due to buoyancy force
q_c	Distributed load due to self-weight of concrete
q_t	Distributed load due to traffic
$q_{asphalt}$	Distributed load due to asphalt
$q_{ballast}$	Distributed load due to ballast
$q_{equipment}$	Distributed load due to equipment
q_{marine}	Distributed load due to marine load
R_d	The design value of the resistance
R_k	The characteristic value of the resistance
R_m	The mean value of the resistance
S_d	The design value of the load
S_k	The characteristic value of the load
S_m	The mean value of the load
t	The thickness of the concrete tube
u_c	The wave-current flow velocity
u_x	The horizontal flow velocity
u_y	The vertical flow velocity
$V_{Rd,c}$	The design value of the shear resistance
$V_{Rm,c}$	The mean value of the shear resistance
W	The section modulus
Z	The limit state function

$\Large 1$

Introduction

In this chapter, the concept of submerged floating tunnels (SFTs) is explained. Hereby, the necessity for an innovative crossing is made clear. Subsequently, the problems concerning the SFT development are formulated. From this, the research objective and research questions follow. The research questions are divided into sub-questions, which will be elaborated on during the different chapters of the report.

1.1. Context

Tunnels under waterways, rivers and estuaries have limitations in depth and length. The distance between banks of shores and water depth are restricting variables in tunnel engineering. It is difficult to construct an immersed or bored tunnel at a large depth because of the necessary slope, the limitations of the techniques and the equipment. The Marmaray tunnel in Turkey is the deepest immersed tube tunnel in the world, with its deepest point located 60 meters below sea level. Bored tunnels can reach larger depths: Norway's Eiksund tunnel is the deepest bored undersea tunnel in the world, with a lowest elevation of 287 meters below sea-level. However, seas and fjords can have depths exceeding 500 meters. Furthermore, large widths make tunnel engineering more complex. A famous example of this is the Channel Tunnel between the United Kingdom and France. This tunnel has the largest underwater section, for which twelve tunnel boring machines of 200 meters in length were necessary. This was an extremely difficult operation. In addition, in case of a large width, (floating) bridges are not always an option either. Bridges restrain water traffic from passing and many columns and/or pontoons are needed. Furthermore, at the water surface the influence of wave-, current- and wind load is larger than below the surface, which causes problems for the stability of the bridge. The longest floating bridge is the The Evergreen Point Floating Bridge, with a length of 2350 meters. The longest segment of a bridge over water, for a non-floating bridge, is 38.3 km: The Lake Pontchartrain Causeway. This is a rare example, and is feasible because of its small depth. The lake has an average depth of four meters and a maximum depth of 20 meters.

A solution for crossing deep and wide waterways is a floating tunnel under the water level: a Submerged Floating Tunnel (SFT). This type of tunnel consists of an immersed (concrete) tube, either attached with anchor cables to the seabed or attached to pontoons floating on the water surface. These two variants can be seen in Figure 1.1. The concept of an SFT was patented in the United Kingdom in 1886, and the first Norwegian patent on the subject was issued in 1923. In the 1960's a small group of Norwegian experts started to evaluate the potentials of the SFT concept. More recent, the government of Norway has plans for the E39, a highway route crossing many fjords, to be ferry-free. This could be achieved by constructing SFTs crossing the fjords on this route.

At the same time, research is also conducted in other countries (China, Japan and Italy). In China, they have built over 500 underwater tunnels (both bored as well as immersed) over the past 20 years, and are quickly gaining experience in different technologies. Within the next few years, the SFT technology is likely to be further developed and may even be constructed. When this is the case, safety should be ensured.
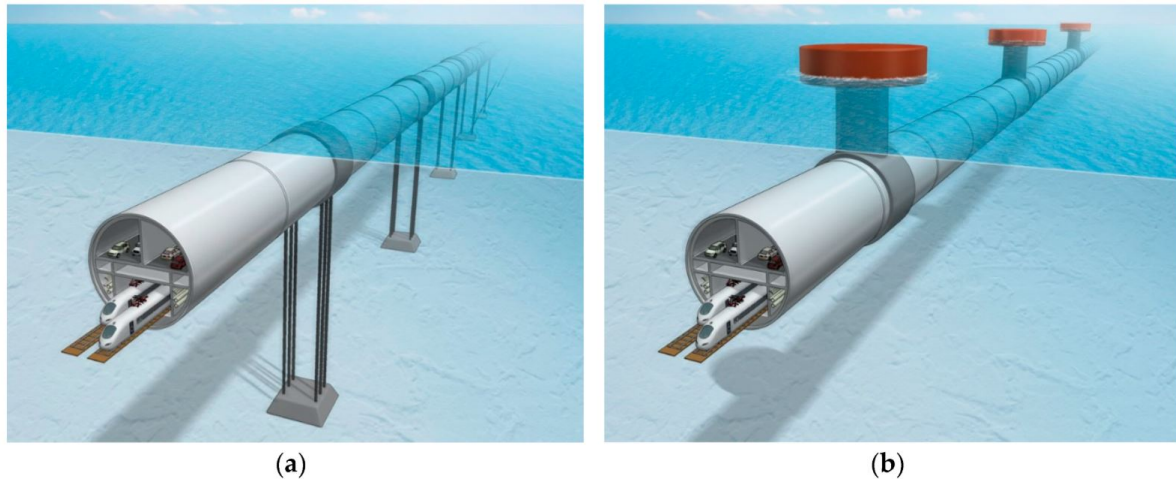
Figure 1.1: Impressions of an SFT: tether variant (a) and pontoon variant (b) [60]

1.2. Problem statement

Previous works focused mostly on the structural lay-out of the SFT. Few researchers have addressed the issue of safety. Safety and reliability are very important for every civil engineering structure. This is especially true for the SFT, since failure can have large consequences. The safety philosophy of civil structures has changed throughout the years. In the old Dutch standard, VB 74/78, a structure had to be able to carry 1.7 times the total loading. This included the uncertainty of the load as well as the uncertainty of the resistance. In new standards, partial factors are introduced, which depend on the material and type of loading [56]. In modern codes and standards, partial safety factors are available for standard civil structures, but it is uncertain if these factors can be applied to SFTs as well. The general partial factors from Eurocode, Appendix A of EN1990, are calibrated on forces acting on buildings, tunnels and bridges [13].

An SFT can fail in multiple ways and is exposed to different types of forces. The buoyancy force and wave forces can be of significant influence. The equilibrium of the system is determined by the buoyancy-weight ratio, which is not comparable to another type of tunnel. No SFT has been constructed up to today. Before the tunnel can be constructed, more has to be known about the reliability of the system. This is important for the end-users, that the structure does not fail during its use, as well as for the decision makers, so they know that they do not make an unbalanced investment.

Engineering optimum design copes with uncertainties. For the assessment and analysis of uncertainties, methods and concepts of reliability are necessary. For uniformity of design methods, it would be convenient if it is possible to apply the partial factor method from Eurocode to new structures like the SFT. The partial factors and their values are ideally obtained by a full-probabilistic calibration, accounting for a wide range of design situations (material types, failure modes, load combinations).

1.3. Research objective and questions
1.3.1. Research objective

The objective of this research is to assess the reliability of an SFT. An acceptable target reliability of the system should be set and a full probabilistic design needs to be made accordingly. Limit state functions for the most important failure mechanisms need to be defined. The full probabilistic design should be compared to a conventional design based on partial safety factors from Eurocode. The aim is to perform a full probabilistic calibration of partial factors for all relevant limit states. Furthermore, measures should be proposed for improving the robustness of the structure. These improvements can be implemented on the resistance part of the system, as well as on the loading part.

1.3.2. Research questions
The following four research questions are formulated to meet the research objective:

1. Which target reliability should be applied to SFTs?

2. How can a full probabilistic design of an SFT be made?

3. How can a full probabilistic calibration of partial factors be performed?

4. How could the structure's robustness be assessed and improved?

1.3.3. Sub questions
To support the research questions, several sub questions are formulated. These questions address the most important topics of this research and will be answered in the corresponding chapters.

1. Literature review

(a) What does failure, availability and survival mean in the case of SFTs?

(b) What are target reliabilities for geotechnical- and hydraulic structures, buildings and bridges?

(c) What is the effect of the spatial variability on the design of flood defences?

2. Framework for reliability analysis

(a) Which properties should be taken into account to determine the target reliability?

(b) How does failure of one component relate to system failure?

(c) Which failure mechanisms should be considered to assess the reliability?

3. Full probabilistic design and calibration of partial factors

(a) Which parameters are dominant?

(b) How can the required reliability level be met?

(c) How can partial factors for resistance and loading be derived?

(d) What can be gained from the full probabilistic calibration of the partial factors?

4. Robustness

(a) What influence does the spatial variability have on the system's reliability?

(b) Which methods can be used to make the structure more robust?

1.4. Scope and approach
1.4.1. Scope
The following assumptions and constraints are set in order to conduct this research:

- A reference model of an SFT will be defined in Chapter 3, Case study. The key figures of the Bjørnafjorden design will be used as a basis for the calculation model (the diameter, thickness and length of the tube, and the concrete- and steel properties). [35]

- For this research, one tube (with a governing diameter of 15 meters) is taken into account, instead of the original design with two tubes, crossbeams and diagonals.

- For the Bjørnafjorden study, a pontoon and tether variant were investigated. However, the pontoon variant turned out to be less feasible and more wave calculations are necessary. Therefore, this research only focuses on the tether variant. [35]

- The alignment of the tunnel profile will be considered straight, not curved.

- Accidental loads are defined as the impact of a submarine or a whale, sinking ship, falling anchor, heavy vehicles, collisions inside the tube, fire, explosion, vandalism, terrorism, earthquakes and tsunamis. These mechanisms are out of scope, and will thus not be investigated in detail.

- The focus lies on the continuous floating tunnel part, not on the land bored tunnel part.

- The exploitation stage will be investigated. The construction phase will not be taken into account, because it deals with temporary conditions which are less known. Necessary equipment can cause additional loading on the structure, and the available machinery and quantities are hard to predict. This is mainly because SFTs have never been built.

- Level I, Level II and Level III reliability methods are used in this study. A level IV analysis will not be performed, because this involves costs and risks of failure mechanisms. Specific costs of failure mechanisms involve costs of vessels, equipment and materials, which can vary significantly. It is chosen not to take this into account. [23]

- The parts of the structure of the SFT to be considered for the reliability study are the cables, tunnel tubes, the end joints, connection joints and the foundation.

- For robustness, spatial variability of wave load, tether failure and leakage will be considered.

1.4.2. Approach

For a probabilistic analysis, multiple methods or programs can be used. These different tools are schematized in Figure 1.2.
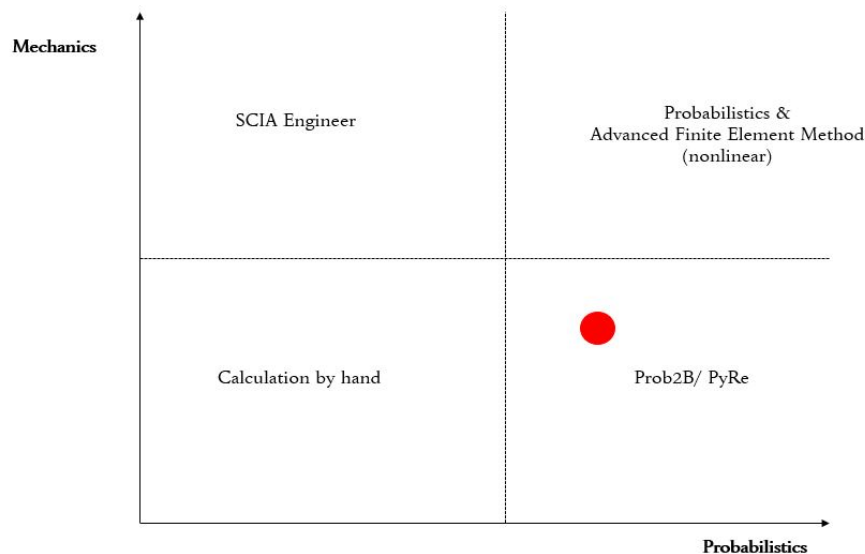
Figure 1.2: Bottom-left: analytical methods, based on basic theory, Top-right: numerical methods, based on more complex models

These methods and their applications will be explained in more detail in Chapter 2. The red dot in Figure 1.2 shows the level of probabilistics and mechanics applied to this research. It can be seen that the level of probability is relatively high compared to the level of mechanics. In this research, the generic probabilistic toolbox Prob2B will be used. This was developed by the department "Built Environment and Geosciences" of The Netherlands Organization for Applied Scientific Research (TNO) [10]. Within Prob2B seven reliability calculation methods are available. Furthermore, the PyRe (Python Reliability) module from Python will be used, which has four reliability methods available. The necessary methods for this research are available in both Python and Prob2B.

1.5. Research outline

Following this introduction, Chapter 2 "Literature review" will consist of the theoretical background. Fundamentals in probabilistic design are explained: probability of failure, target reliability, parameter distributions, time dependence, failure, availability and survival. Subsequently, reliability methods (level I until level IV) are discussed. Thereafter, a reliability assessment of other civil structures will be performed, to create an overview of failure mechanisms and suitable target reliabilities.

In Chapter 3 "Case study", a reference case of an SFT in Norway will be analyzed and the loading types will be explained. Next, Chapter 4 "Framework for reliability analysis" will elaborate on the methodology. The procedure is discussed, failure mechanisms are assessed and the input parameters are described. Furthermore, multiple system-properties are assessed to select a suitable target reliability for the SFT. Subsequently, Chapter 5 "Full probabilistic design" uses the most important failure mechanisms to perform calculations. Limit state functions will be formulated and a first-order reliability method (FORM) and a Monte Carlo (MC) simulation will be performed to calculate the reliability and to determine the most important parameters. In Chapter 6 "Derivation of partial safety factors", partial factors will be calculated based on the FORM analysis. These factors will be compared to Eurocode.

In Chapter 7 "Robustness analysis", the robustness will be assessed and improvements will be suggested. Subsequently, in Chapter 8 "Conclusion, Discussion & Recommendations", final conclusions will be drawn and topics for discussion will be presented. Lastly, a recommendation for further research will be given.
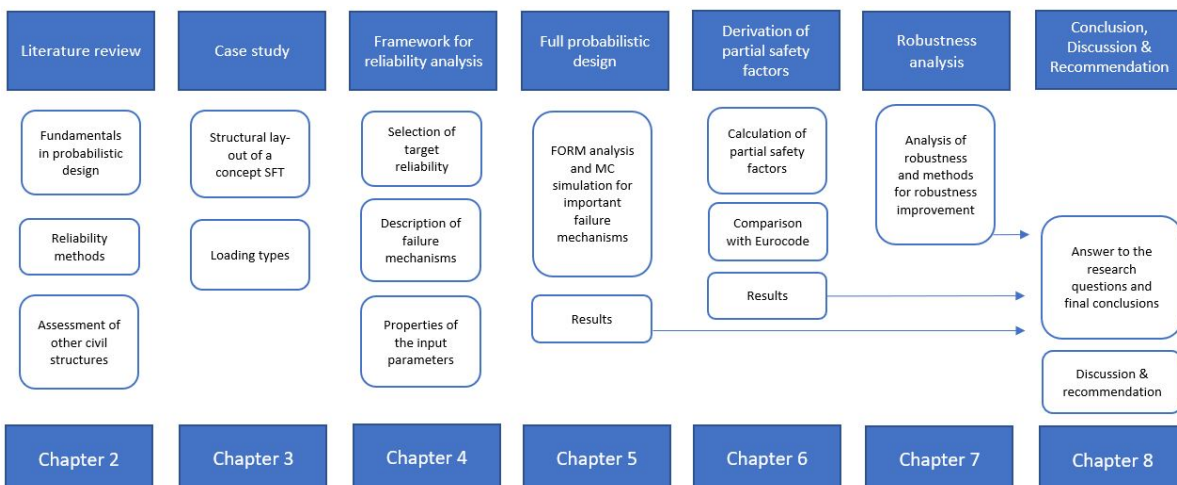
Figure 1.3: The structure of this research

2

Literature review

2.1. Fundamentals

2.1.1. Failure probability and safety levels

The probability of failure can be set as a value between 0 (structure will not fail) and 1 (structure will fail). For many civil structures, maximum allowable failure probabilities are determined in guidelines and standards [23]. In order to calculate the actual failure probability of a certain mechanism, a limit state function has to be formulated.[1]

$$Z = R - S \tag{2.1}$$

where: Z = the limit state function
R = the resistance
S = the load effect

The probability density functions of the resistance (R) and load (S) can be seen in Figure 2.1. For any given sample, a probability density function gives a relative likelihood that the value of the random variable would equal that sample. More about the distributions of Z, R and S will be explained in Chapter 2.1.2. Furthermore, Equation 2.1 leads to a distribution of the Z-value, which can be seen in Figure 2.2. When $Z < 0$, the structure no longer fulfills its performance requirements.
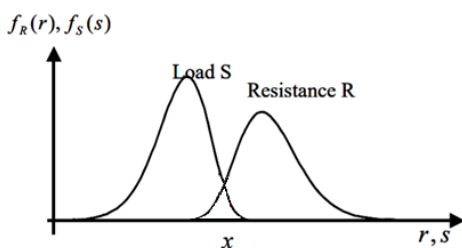
Figure 2.1: Probability density functions of R and S [18]
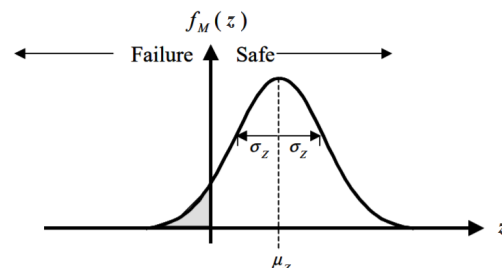
Figure 2.2: Probability density function for the limit state function Z [18]

The probability for a healthy person to die as a result of an accident in daily life is about 10^{-4} per year in developed countries, which means 1 of the 10.000 persons a year [23]. It is certainly not accepted that the probability to become a victim of structural failure is larger than the probability to die because of an accident. An appropriate requirement for the individual risk for structures would be a value between 10^{-5} and 10^{-6} [47].

---

[1]Model uncertainty should be added to both resistance (R) and loading (S) as well, because mathematical models are not fully correct. These factors can be found in Appendix A.

To determine the desired safety level, the following parameters should be taken into account [46]:

- the consequence class for the structure

- the characteristic loads

- the design rules and material properties

- the material factors, load factors and the combination factors

Eurocode EN1990 formulated three consequence classes (CC) for constructions. The class CC1 indicates a low consequence structure, which is the case for e.g. storage and places where people do not normally enter. CC2 is for smaller buildings with medium impact, and CC3 applies to large public buildings and bridges which have a large impact [13]. The characteristic load values, the design rules, the material properties, the load factors and material factors will be further described in Chapter 2.2.

2.1.2. Distributions

Variables which are uncertain to some extend are called stochasts. Stochastic variables are described by their distribution, mean value (μ), standard deviation (σ) or variation coefficient ($V = \sigma^2$). The standard deviation determines the magnitude of the spread of values around its mean. The normal distribution occurs naturally in many situations. The values of a normal distribution are distributed according to Figure 2.3. This type of distribution is also called a 'bell curve'.
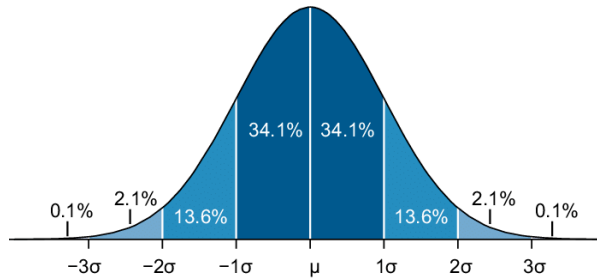
Figure 2.3: Normal distribution [62]

The probability density function of the normal distribution can be written as follows:

$$f(x) = \frac{1}{\sigma\sqrt{2 \cdot \pi}} \cdot \exp\left(-\frac{1}{2} \cdot \left(\frac{x - \mu}{\sigma}\right)^2\right) \tag{2.2}$$

where: $\mu =$ the mean value
         $\sigma =$ the standard deviation

When the joint probability density functions (f_x) are known, the probability of failure (P_f) can be calculated according to:

$$P_f = \int_{g(X)<0} f_x(x)dx \tag{2.3}$$

The resistance (R) tends to be a lognormal distribution, because this is often a product of variables, and negative resistances are hardly possible. A lognormal distribution is a distribution of a random variable whose logarithm is normally distributed. The values used to derive a lognormal distribution are normally distributed. Values are positively skewed and the distribution is asymmetric. For a lognormal distribution, the probability density function can be found as follows:

$$f(x) = \frac{1}{x\sigma\sqrt{2 \cdot \pi}} \cdot \exp{-\frac{(\ln(x) - \mu)^2}{2\sigma^2}} \tag{2.4}$$

Where:

$$\delta = \frac{\sigma}{\mu} \qquad\qquad \zeta = \sqrt{\ln{1 + \delta^2}} \qquad\qquad \lambda = \ln\mu - \frac{\zeta^2}{2} \tag{2.5}$$

Current velocity and the traffic load could be implemented as Gumbel distributions, because these are extreme value distributions. The following formulas hold:

$$f(y) = \alpha \cdot \exp\left[-\alpha(x - u) - \exp -\alpha(x - u)\right] \tag{2.6}$$

Where:

$$\mu = u + \frac{\gamma}{\alpha} = u + \frac{0.5772}{\alpha} \qquad\qquad \sigma = \frac{\pi}{\alpha \cdot \sqrt{6}} = \frac{1.282}{\alpha} \tag{2.7}$$
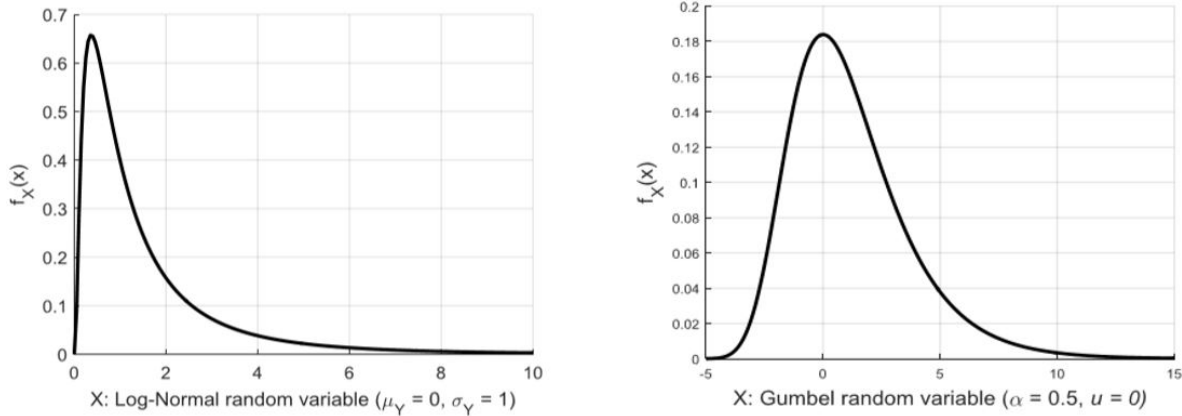
Figure 2.4: Lognormal distribution (left) and Gumbel distribution (right) [25]

A Gumbel or lognormal distributed variable cannot be added up to a normal distributed variable. In Appendix E, this property is explained. All variables need to be transformed to normal distributions in order to add them up. [25]

2.1.3. Target reliability

A target value needs to be defined, following from an acceptable level of risk. The question *"How safe is safe enough?"* needs to be raised when setting the reliability target for a structure. The consequence classes mentioned in Chapter 2.1.1 correspond to reliability classes (RC). Subsequently, these classes are related to target reliability indices (Figure 2.5). According to Eurocode EN1990 [13], values are given for two reference periods, i.e. 1 year and 50 years. They are primarily intended to be used in design of new structures.

Reliability Class	Minimum values for β	
	1 year reference period	50 years reference period
RC3	5,2	4,3
RC2	4,7	3,8
RC1	4,2	3,3

Figure 2.5: Reliability classes and recommended minimum value for the reliability index β [13]

Target reliability indices were mainly developed for buildings and bridges [38]. The reliability index (β) can be defined as the distance between the mean value of Z, μ_Z, and the failure line $Z = 0$. For normally distributed variables, the formula can be written in the following form:

$$\beta = \frac{\mu_Z}{\sigma_Z} \tag{2.8}$$

If β increases, the failure probability decreases and the reliability or safety increases. However, for a system that has a nonlinear limit state function, Formula 2.8 cannot be used to calculate the β. The formula for β can also be written as:

$$\beta_t = -\Phi^{-1}(P_{f;t}) \tag{2.9}$$

Where Φ^{-1} is the inverse normal distribution. The relationship between β and P_f is given in Figure 2.6.

P_f	10^{-1}	10^{-2}	10^{-3}	10^{-4}	10^{-5}	10^{-6}	10^{-7}
β	1,28	2,32	3,09	3,72	4,27	4,75	5,20

Figure 2.6: Relation between reliability index β and probability of failure P_f [13]
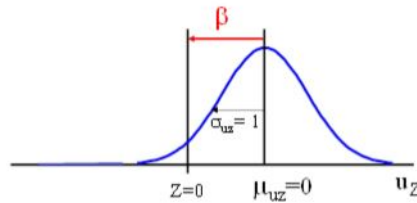
Figure 2.7: Definition of reliability index β [25]

The target failure probabilities should be chosen based on the consequence and nature of failure, the economic losses, the social inconvenience, the influence on the environment and the required costs and effort to reduce the probability of failure [23]. Since the value for the target reliability is based on many factors, it is complicated to determine this for a new structure.

2.1.4. Time dependence
Target reliability indices are always related to a reference period of, for example, one year or fifty years. This formula is used to transform annual into lifetime probabilities of failure:

$$P_{f;t_{ref}} = 1 - (1 - P_{f;t_1})^{n_{ref}} \tag{2.10}$$

where: $P_{f;t_{ref}}$ = the probability of failure in the interval $[0, t_{ref}]$ [-]
$\quad\quad\quad P_{f;t_1}$ = the probability of failure in the interval $[0, t_1]$ [-]
$\quad\quad\quad n_{ref}$ = the number of years in the reference period t_{ref} [-]
$\quad\quad\quad t_1$ = the reference period of one year [$year$]

This equation is valid only if reliability problems are largely time-variant [38]. In Figure 2.8, the probability of failure for both time-independent and time-dependent mechanisms can be seen.
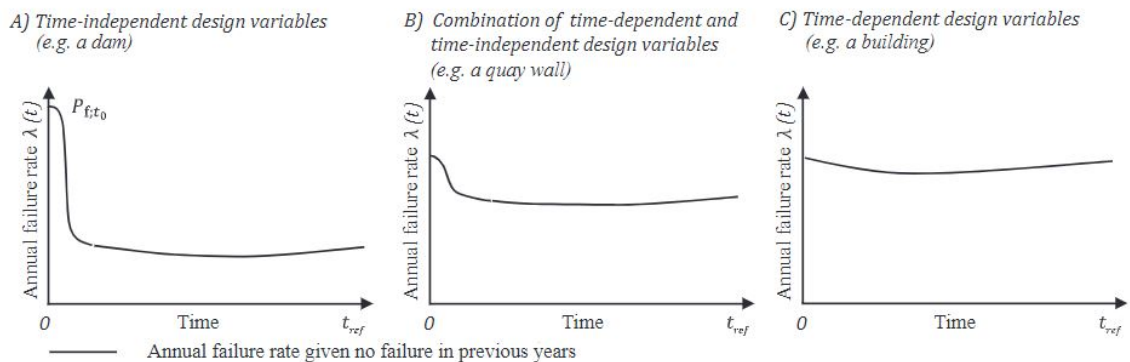
Figure 2.8: Bathtub curves for annual failure rate in time [38]

For a dam (Figure 2.8, A), when the structure has not failed during the first year, the probability of failure will be very low for the following years. For a building subjected to wind load (Figure 2.8, C), the survival of one year does not mean that it will survive the next year. This is because wind load is dependent on time. A maximum can occur in any year.

An SFT is subjected to a combination of time-dependent and time-independent design variables (Figure 2.8, B). Their values will be determined in the following chapters.

2.1.5. Individual and group risk

Uncertainty and risk are central features for constructions. Risk is defined as the consequence of a certain event multiplied by the probability of occurrence. This value can be used to compare multiple risks. The individual criterion or group risk criterion can be governing. For individual risk, the probability that a person dies can be formulated as follows:

$$P_{IR} = P_d = P_f P_{d|f} \text{ [per year]} \tag{2.11}$$

Where $P_{d|f}$ is the probability that someone dies when the failure occurs. The fatality rates given collapse can be found in Eurocode. The P_d should be smaller than 10^{-5}, so the necessary failure probability can be calculated. Individual risk can be voluntary as well as involuntary. On the contrary to group risk, which is mostly involuntary. For example, the number of people that would die in one flood event.

Group risk concerns the frequency of a fatal event, irrespective of any one individual. Risk analysis and management need to consider a number of factors that are not typical for individual risks. The following formula can be applied to calculate the group risk (P_{GR}) of one single building:

$$P_{GR} \leq AN^{-\alpha} \text{ [per year]} \tag{2.12}$$

Where N is the expected number of casualties, and A and α are constants. Recommended values for A and α are 0.01 and 2 respectively [47]. Group risk is usually represented as an F-N curve, according to Figure 2.9. The expected annual frequency (F) is plotted against the number of casualties (N).
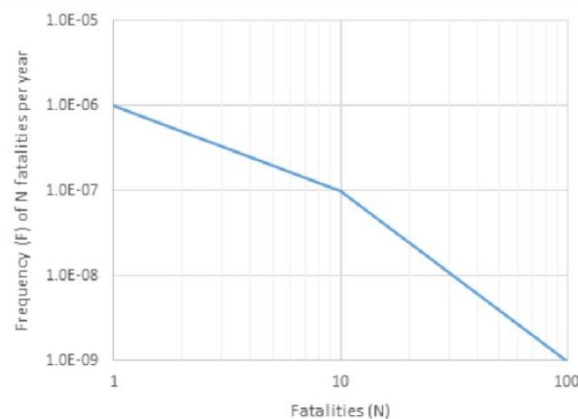
Figure 2.9: F-N curve for group risk [2]

The residence time of an individual in/on/under a structure is an important criterion. For a building, the residence time can be large, which makes the individual criterion is important. However, for a bridge, the residence time is relatively short, and the group risk criterion is governing [44]. For an SFT, which in this respect is comparable to a bridge, the group risk criterion will also be governing.

2.1.6. Failure

Failure can either be seen as technical failure - of a system or a component - or as social failure. Social failure means that the tunnel does not meet the user's requirements. This can result in an unusable tunnel. Technical failure can for example be due to flooding or collapse of the tube [50]. Systems can be subdivided in serial and parallel systems. A serial system is considered to have failed if any of the components fails. A parallel system will only fail when all of the components fail. Thus, a parallel system would be preferred.

System failure is usually the most serious consequence associated with failure of a structure. Therefore, it is necessary to assess the probability of system failure following an initial component failure. The component reliability requirements should depend upon the system's characteristics [23].

The ultimate limit state (ULS) defines the state when the ultimate bearing capacity of the structure is reached. The serviceability limit state (SLS) defines the limit of functionality of the structure, "fitness-for-use". It takes into account deflections, vibrations, crack widths, factors of safety, accelerations, etc. The structure is not comfortable or usable anymore if the SLS is reached.

A distinction can be made between irreversible and reversible serviceability limit states. Irreversible means that consequences of actions exceeding the specified service requirements remain after the actions are removed. For reversible limit states, this is not the case. Thus, irreversible limit states are of more importance. Furthermore, a Progressive Limit State (PLS) can be formulated. This is designed to preserve human lives in the event of certain loads or load combinations at a very low probability of occurrence. Mostly defined as 10^{-4} per year. Lastly, a Fatigue Limit State (FLS) can also be determined, to account for the fact that some materials lose strength due to repeated loading [1].

All these limit states can be applied to SFTs. The ULS means complete failure of the structural system of the SFT. The SLS means that the SFT can no longer be used.

2.1.7. Availability

According to Rijkswaterstaat [36], tunnels in The Netherlands need to be available for 98% of the time. This means that traffic needs to be able to go through the tunnel 8585 hours per year. The other 2% of the time, the tunnel may be closed for repairs (planned or unplanned maintenance) or may be congested due to an accident. This standard does not take into account external factors, like externally caused accidents and natural disasters. The availability of an SFT depends mostly on the location. Extreme seismic events could negatively influence the availability, as well as hydrodynamic actions (for instance the waves induced by large ships navigating at the water surface level above the tunnel). The required availability also depends on the amount of traffic and importance of the road. An SFT will probably be connected to the main road network of its area, so this could be comparable to the tunnel standards from Rijkswaterstaat. [36]

2.1.8. Survival

The tunnel needs to allow for sufficient space for escape routes. If damage to the structure is so critical that it might lead to total collapse, the water inflow rate should be limited, so that people have time for safe evacuation. In case of traffic accidents and car fires, the SFT will have to meet normal design criteria used for rock or immersed road tunnels. These criteria include emergency stops, emergency exits, smoke ventilation, emergency lights, traffic monitoring, regulation, and more. A second tunnel or a compartment of the tunnel should serve as evacuation tunnel. This route needs to have a separate ventilation and light system, and should allow for ambulances to enter. In the case of twin tubes, evacuation could be possible from one tube to the other. [42]

2.2. Reliability methods

Mathematically, the structural reliability is the probability that a system does not reach a defined limit state under a given reference period. The methods to calculate the structural reliability can be divided into five groups from Level IV (most advanced) to Level 0 (most simple):

- Level IV methods (risk-based): The costs of failure have to be calculated. The associated risk is used as a measure of the reliability. Uncertainty, costs and benefits are taken into account to compare different designs on an economic basis.

- Level III methods (non-linearized): Joint distribution functions are used to model the uncertain parameters. The probability of failure can be calculated by numerical integration.

- Level II methods (approximation): Mean values and standard deviations are defined for the uncertain parameters. Correlation coefficients are also specified.

- Level I methods (semi-probabilistic): The uncertain parameters are modelled by characteristic values for load and resistance, and partial coefficients (γ 's) are applied. This method is used in design practice.

- Level 0 methods: Deterministic calculations (parameters have a set value, not a range).

It is decided not to apply a level IV analysis in this research, because this method requires knowledge of costs. It is hard to derive the economical value and also to predict them for the future. Subsequently, a level 0, I, II and III will be used when considered necessary. These methods will be explained in the following sub sections.

2.2.1. Level IV analysis

A Level IV analysis is also known as the full-risk based approach. Here, the consequences given failure and the safety costs are considered in the design. The formula is given as follows:

$$E[C_{tot}(p_c)] = C_C(p_c) + E[H] \cdot P_f(p_c) \tag{2.13}$$

where: $C_c(p_c)$ = the costs of safety
p_c = the decision variable / parameter
$E[H]$ = the expected consequences given that the failure occurs
$P_f(p_c)$ = the probability of failure

These parameters are difficult to determine, which makes it hard to apply this method. In most cases, calculations are done up to a Level III analysis. [4]

2.2.2. Level III analysis

For a level III analysis, the probability of failure P_f is calculated exactly, using analytical formulations, numerical integration and Monte Carlo simulations. The Monte Carlo method uses the possibility of drawing random numbers between zero and one, called a uniform probability density function. Because many samples need to be generated, this simulation cannot be executed by hand.

Theoretically, an infinite number of simulations will result in an exact probability of failure. However, the time and power of computers is limited. An appropriate amount of simulations n are required to reach an acceptable level of accuracy. The probability of failure from the Crude Monte Carlo method can be written as:

$$P_f = \frac{N_f}{N} \tag{2.14}$$

where: N = the total number of samples
N_f = the subset of N which results in failure

The number of samples should be large enough to get sufficiently accurate results. This can be formulated as [11]:

$$N > 400(\frac{1}{P_f} - 1) \tag{2.15}$$

2.2.3. Level II analysis

In a level II analysis, the joint probability density function is simplified and the limit state function is linearized, usually with a technique called the first-order reliability method (FORM). In this method, the limit state function is linearized in the so-called design point, the most probable of all combinations (R,S) for which failure occurs, i.e. the point on the limit state $Z = 0$, with the highest probability density. This point can be defined according to the following formula [55]:

$$S_d = \mu(S) - \alpha_S \cdot \beta \cdot \sigma(S)$$
$$R_d = \mu(R) - \alpha_R \cdot \beta \cdot \sigma(R)$$

(2.16)

where: S_d, R_d = the design points for S and R
$\mu(S), \mu(R)$ = the mean values for S and R
α_S, α_R = the sensitivity factors, which depend on $\sigma(S)$ and $\sigma(R)$
β = the reliability index
$\sigma(S), \sigma(R)$ = the standard deviations of S and R

The value of β can be found by calculating the shortest distance from the origin to the limit state surface in standard normal space. A transformation to the standard normal space is done by subtracting the mean value, so that the mean becomes zero, and by dividing by the standard deviation.

In the graphical representation of Figure 2.10, the α-values can be found. The α-values indicate the relative importance of the parameter [23]. An example calculation of α-values with FORM can be found in Appendix B.
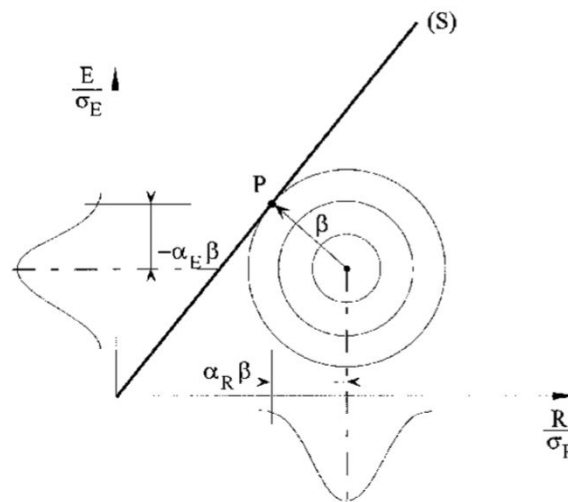
Figure 2.10: Graphical representation of α- and β-values [13]

Thus, in a stardard normal space, the β-value is defined in the standard normal space as distance from the origin of the coordinate system to the $Z = 0$ line.

The FORM method is based on the first-order Taylor series approximation of a limit state function. For the Second Order Reliability Method (SORM), an extra element is added to the Taylor series. For a large β-value, the results of FORM and SORM do not differ much [10].
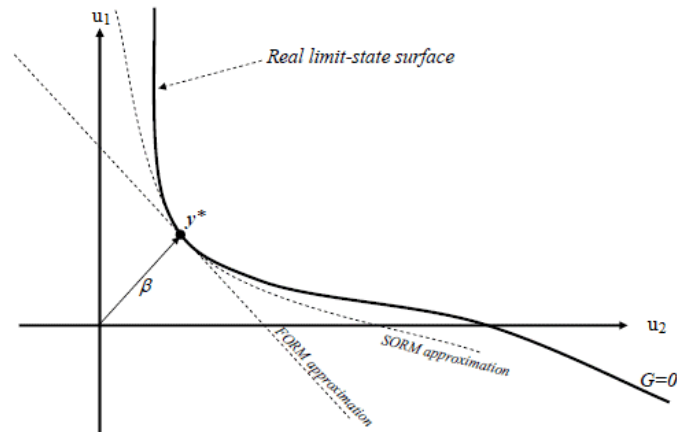
Figure 2.11: Linearization in design point according to FORM and SORM [22]

2.2.4. Level I analysis

The level I analysis, also called the partial factor method or semi-probabilistic method, has to satisfy the following equation:

$$\frac{R_k}{\gamma_R} - S_k \cdot \gamma_S > 0 \tag{2.17}$$

where: R_k, S_k = the characteristic value of respectively the resistance and load
γ_R, γ_S = the partial safety factors

For example, R_k can be defined as a value that has a probability of non-exceedance of 5 %. The characteristic value of the resistance (R_k) is divided by a factor γ_R, which results in the design value for the resistance (R_d). The same goes for the load: S_k is multiplied by a factor γ_S, resulting in the design value of the load S_d. A graphical representation of this can be seen in Figure 2.12.
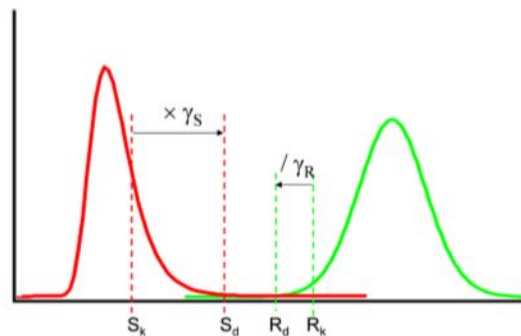
Figure 2.12: A probability density function with the load (in red) and resistance (in green) [25]

Load Resistance Factor Method

Load factors should be material-independent and material factors should be load-independent, in order for the partial method to be applied [55]. For conventional structures, such as bridges and buildings, partial factors are formulated in the Eurocodes. The values of partial factors are based on level II calculations [25]. Examples of partial resistance factors are 1.15 for steel (γ_s) and 1.5 for concrete (γ_c). Partial load factors can be found in Appendix A. Factors are formulated for the strength and equilibrium conditions, for ULS and SLS. According to Eurocode EN1990 [13], a multiplication factor k_{FI} is applicable to partial factors of unfavourable actions. This k_{FI} is equal to 1.1 for reliability class RC3, 1.0 for the reliability class RC2 and 0.9 for reliability class RC1.

For each critical load case, the design values of the effects of actions need to be determined by combining the values of actions that are considered to occur simultaneously. In Eurocode EN1990 [13],

the following combinations of actions for permanent or temporary design situations are formulated, of which the least favourable of the two expressions should be used.

$$E_d = E\left(\sum_{j\geq1}\gamma_{G,j}G_{k,j}\text{"+"}\gamma_P P\text{"+"}\gamma_{Q,1}\Psi_{0,1}Q_{k,1}\text{"+"}\sum_{i\geq1}\gamma_{Q,i}\Psi_{0,i}Q_{k,i}\right) \tag{2.18a}$$

$$E_d = E\left(\sum_{j\geq1}\xi_j\gamma_{G,j}G_{k,j}\text{"+"}\gamma_P P\text{"+"}\gamma_{Q,1}\Psi_{0,1}Q_{k,1}\text{"+"}\sum_{i\geq1}\gamma_{Q,i}\Psi_{0,i}Q_{k,i}\right) \tag{2.18b}$$

where: "+" = means "to be complied with"
$\sum$ = means "the combined effect of"
ξ = a reduction factor for unfavorable permanent actions G
G = permanent actions
P = pretension
Q = variable actions

Considering normally distributed variables, the characteristic value can be computed as follows [25]:

$$X_{k,inf} = \mu_X - 1.64 \cdot \sigma_X \tag{2.19}$$

$$X_{k,sup} = \mu_X + 1.64 \cdot \sigma_X \tag{2.20}$$

Where $X_{k,inf}$ can be applied for favorable loads, and $X_{k,sup}$ for unfavorable loads. In order to come from characteristic values to design values, partial factors are used.

$$R_d = \frac{R_k}{\gamma_R}; \ S_d = S_k \cdot \gamma_S \tag{2.21}$$

Characteristic values

According to Eurocode EN1990, the characteristic value of the resistance (R) can be taken as the 5 % quantile of the lognormal distribution. The characteristic value for a permanent load (G) is the 50 % quantile of the normal distribution. For the annual maximum of the variable load (Q), the characteristic value is the 98 % quantile of the 1-year Gumbel distribution. These properties can be found in Figure 6.2.

Variable	Distribution type	Mean	Coefficient of variation	Characteristic value
G	Normal distribution	1,00	0,10	50 %
Q_1, Q_2	Gumbel distribution	1,00	0,40	98 %
R	Lognormal distribution	1,00	0,05	5 %
X_R	Lognormal distribution	1,00	0,03	50 %

Figure 2.13: Probabilistic models for basic random variables [23]

2.3. Reliability assessment of other civil structures

In this section, the target reliabilities and failure mechanisms of other civil structures will be discussed. The similarities between these structures and SFTs will be highlighted. The final goal is to find an acceptable target reliability for an SFT. These β-values can be defined on element level as well as on system level.

2.3.1. Geotechnical structures

In geotechnical design, the predominant sources of uncertainty are the soil properties and the calculation model uncertainty. For geotechnical structures, the loading during construction will be their maximum exposure. Most geotechnical structures have multiple failure modes. For example, a gravity retaining wall has at least three failure modes: horizontal sliding along the base of the wall, overturning

or rotation about the toe of the wall, and bearing capacity failure of the soil beneath the wall. These failure modes tend to physically interact, because the load or capacity for different failure modes can be correlated. On the one hand, self-weight of a gravity retaining wall is the major source of capacity against sliding and overturning, but on the other hand, it is also a major source of load for the bearing capacity failure mode.

A pile foundation is a system of piles, consisting of several pile groups with a few individual piles. Reliability analysis of the pile system requires the consideration of the reliability of the individual piles, the pile group effects, and the system effects arising from pile superstructure interactions. The reliability of a pile group can be significantly larger than that of single piles. The calculated β-value of single piles is between 1.4 and 3.1. Recommended target β-values are between 2.0 and 2.5 for single driven piles and between 2.5 and 3.0 for single drilled shafts.

The probability of failure associated with the "most likely" failure mode identified by FORM only provides a lower bound for the system probability of failure. In contrast to a pile foundation where the sliding surface is mostly restricted to the interface between soil and pile, the trajectory of a slip surface in a soil mass is coupled to the specific realization of a random field and can only be determined through finite element analysis or comparable numerical methods. Many geotechnical structures form failure mechanisms in the surrounding soil mass in the ULS (e.g. slopes, tunnels, deep excavations). Each potential slip surface in the soil mass is a failure mode. This class of system reliability problems is complex, because of the coupling between mechanics and spatial variability. From Annex D of ISO2394, it follows that the target β-value for bearing capacity should be 3.5. For shallow foundations, the β should be between 2.8 and 3.5. Furthermore, it was shown that the probability of failure of foundations should be between 10^{-3} and 10^{-4}, which corresponds to values of β between 3.1 and 3.7. In the design of superstructures, a target reliability of $\beta = 3.5$ is often used. [63]

2.3.2. Flood defences
Dikes, embankments, breakwaters, sluices and locks have multiple failure mechanisms. For reliability calculations on flood defences, the flood defence system is normally subdivided into flood defence sections. These defence sections are characterized by one cross-section with details of geometry, revetment, soil properties and more. Each cross-section can fail in multiple ways, and a limit state equation is used to define each failure mechanism.

A program called PC-ring is developed for advanced reliability analyses of flood defence systems. This program takes the principal dike failure modes into account for all elements of a system and also considers the correlations between failures of the elements. The four most common failure mechanisms are:

- Overtopping/ overflow

- Instability of the inside slope

- Uplift/ piping

- Attack of the revetment on the outside slope

Only the most representative sections of the system's probability of failure should be modelled, in order to limit the time of data gathering. Calculations at the level of the probability of failure of a single element can be done through numerical integration, FORM, SORM, crude Monte Carlo and Directional Sampling [43]. In the research of Roubous et al (2018), target reliability indices for quay walls were investigated. In quay wall design, the dominant stochastic variables are largely time-independent. Examples of these variables are the retaining height, soil strength and material properties [38].

The Water Act defines safety standards for flood defenses. For the Dutch flood defense system, the target reliability is defined by the exceedance probabilities of the hydraulic loading conditions. In other words, these are maximum allowable probabilities of flooding. They range from $1/100$ per year to $1/100.000$ per year, which equals a target value of $\beta = 1.3$-4.3 for the system [39]. Furthermore, a flood defense requires a design life of 50 years (for dikes) or 100 to 200 years for hard structures [17].

2.3.3. Buildings

Buildings can fail due to a weak foundation, bad material quality, or by applying a heavier load than expected. Most failures actually occur during the construction phase. "Sparsely occupied" buildings fall into CC2, and for "densely occupied" buildings CC3 is used. In the Dutch Building Decree safety criteria for human lives have been formulated and quantified in target level for individual risk [6]. In the Dutch Code for existing structures, NEN 8700, the limit value for the individual risk (maximum acceptable probability that a person dies in one year as result of a collapsing structure) has been taken as 10^{-5} [47].

In principle, buildings are designed to resist normal loads such as loads due to self-weight, occupancy, climate and seismic effects. However, since the failure of the Ronan Point apartment block by an accidental gas explosion in London in 1968, the phenomena of abnormal loading and progressive collapse are considered in engineering practice as well [21]. For buildings, progressive collapse is an important phenomenon. A review of multistory building failures during construction showed that punching shear failure is a critical mode of failure which often leads to progressive collapse.

2.3.4. Bridges

In The Netherlands, bridges in highways have to satisfy the requirements of CC3, so they require a reliability of $\beta = 4.3$ for new bridges, $\beta = 3.8$ for repair and $\beta = 3.3$ for unfit for use. Bridges in less important roads have to satisfy the criteria of CC2, which are stated as a $\beta = 3.8$ for new bridges, $\beta = 3.3$ for repair and $\beta = 2.5$ for unfit for use. This holds for a reference period equal to the design working life of 100 years [46]. The ratio of dead weight and permanent load versus traffic load is an important factor in the reassessment of a bridge [45].

For concrete bridges, EN 1992-2 is available and for steel bridges, there is EN1993-2. A bridge can suffer from fatigue and deterioration over time. Failures of 500 bridges in the United States between 1989 and 2000 were studied. The most frequent causes of bridge failures were attributed to floods and collisions [57].

In Figure 2.14, the reliability profile for a reinforced concrete bridge is shown. The deterioration rate is defined as α. A β-value of 4.6 is used as target. For non-maintained bridges, different states are defined in Figure 2.15. State 5 means extremely good, 4 means very good, 3 means good, 2 means acceptable and 1 is non-acceptable [48].
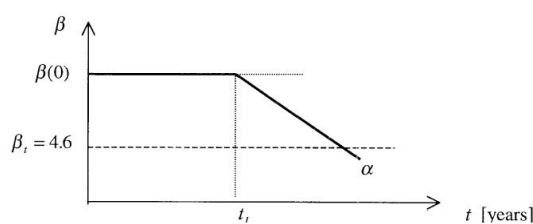
Figure 2.14: Reliability profile of reinforced concrete bridge [48]   Figure 2.15: Reliability profile without maintenance [48]
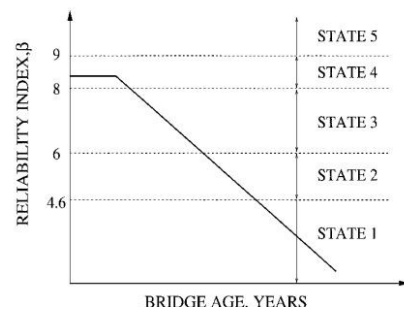
2.3.5. Bored tunnels

For the construction of a bored tunnel, a tunnel boring machine is used to excavate the soil or rock, and to place the circular tunnel elements. The construction stage is challenging, and therefore should be considered. Bored tunnels fall into CC3, which means a β-value of 4.3 for a reference period of 50 years. Mostly, they are designed for 100 years.

The initial stress in the soil and the stiffness of the construction joints are of great importance. Ultimate limit states are drilling front instability (active collapse, passive collapse or blow out), collapse of the lining (globally or locally) and flotation of the tunnel tube. Serviceability limit states are large

displacements and deformations (globally and locally), leakage, crack formation and damage to the surroundings. [54]

The probability of failure of the tunnel is a function of the local probability of failure:

$$P(F_{tunnel}) = \frac{L}{\delta L} \cdot P(F_{local}) \tag{2.22}$$

where: L = the length of the tunnel [m]
         δL = the length over which failure is strongly correlated

The length of δL depends on correlation lengths, scatter and the influence of stochastic variables. [50]

2.3.6. Immersed tunnels
The construction method of an SFT will be similar to that of an immersed tunnel. An immersed tunnel consists of prefabricated elements, constructed in a dry dock. In order to connect the elements, water is pumped out of the space between the installed bulkheads. A rubber seal is installed at the end of an element and is compressed by water pressure on the free end of the new element, which causes the inter-modular joint to close. In particular, research has been conducted to analyse the failure of joints and occurring of leakage. Geotechnical failure, like soil liquefaction, groundwater migration and settlements, can lead to cracks and leakage. For the Marmaray tunnel, a minimum design life of 100 years was required. At a depth of 58 m, this tunnel was under exposure of the highest saline water pressure that was ever experienced in the history of immersed tunnels. Turkish standards were used for concrete design and crack-control. [19]

According to Baber and Lunniss [28], safety factors against uplift are important. An immersed tunnel is designed as gravity structure and uses only its self-weight to resist the uplift. For a temporary condition, a safety factor of 1.10 could be used. For a permanent condition, a factor of 1.15 could be applied [28]. Furthermore, other safety factors used for immersed tunnels can be found in Appendix A.3.

2.3.7. Offshore platforms
Due to the ocean environment and the explosion risk associated with hydrocarbons, safety is an enormous challenge for offshore structures. Global failure modes of an offshore platform are capsizing, structural failure and positioning system failure [33]. Normally the initial event leads to flooding, and thereby capsizing of the platform. ISO 19900 contains the standards and codes for offshore structures, including limit states, and ISO 19901-7 is dedicated to mooring systems. There are different types of foating platforms: ship-shaped units, spars, semi-submersibles, and Tension-Leg Platforms (TLPs). The tension legs of TLPs can be used for a comparison with the tether foundation of the SFT. These tension legs are vulnerable to failure due to extreme tensions. A Von-Mises failure criterion can be applied to define the failure of the tethers against maximum tension. The minimum tension occurs when tethers slack due to loss of tension. The parameters taken into account for the reliability analysis are pretension, thickness, set down, tide and surge, response uncertainty factor, yield strength, Young's modulus, foundation translational and rotational mispositioning [41].

Even in low wind or weak current, all waves have to be considered for the design of a TLP. This may lead to a small offset or, more critically, a minimum tendon tension. For other types of floating platforms, the minimum mooring line tension is not a critical design issue [8]. The minimum breaking strength is applied as the characteristic strength for mooring components. A tension limit should be expressed as a percentage of its minimum breaking strength (MBS) after reductions for corrosion and wear. These limits apply only to properly maintained moorings and systems in which the connecting components have an MBS greater than or equal to that of the mooring lines.

Failure can also occur due to fatigue and corrosion, which are both gradual phenomena. Fatigue lead to catastrophic accidents with mobile units around 1980. After this, more research into fatigue loading was performed. Corrosion affects both ULS and FLS. It is prevented by using corrosion protection and a thickness allowance [32].

2.4. Spatial variability

The length of a breakwater or dike can be a few hundreds of meters. The loads, e.g. wave load, can be variable along the length of the structure. Floating bridges and breakwaters have lengths which are often much larger than the incident wavelength. For coastal areas and lakes, there are three global stochastic variables: water level, wind velocity and wind direction. For loads on rivers, variables are river discharge, duration of a high discharge, wind velocity, wind direction, water level at the river mouth and duration of the storm surge [43].

The longer the structure, the higher the chance to experience either a weak spot or an extreme load. For a dike, this means that the probability of failure increases with the length of the dike. This could also be the case for an SFT. The underlying reason for this is a lack of full correlation between the different resistance and load parameters due to spatial variability. The implication for the design of long structures is that the reliability requirements to a cross-section need to be stricter than for the whole reach [53]. Thus, a higher target reliability needs to be applied to a cross-section.

The two main factors determining the magnitude of this length effect are:

- The spatial variance in resistance properties or loading: for a wide distribution around the mean value of a parameter, the length effect will be larger

- The spatial correlation: for a smaller correlation, the length effect will be larger

For load-dominated failure mechanisms, the probability of failure of a whole dike reach is close to the probability of failure for a cross-section. On the other hand, resistance-dominated failure mechanisms can have a significant length effect, up to a ratio of hundred between the probability for a whole dike reach and the probability for a cross-section. The length effect is largest for geotechnical failure mechanisms such as macro instability and piping. Wave loads on dikes are strongly dependent on the wind direction and orientation within the reach. At one location, failure could occur due to wind from the west, and at the other location, failure could occur due to wind from the east. This results in a higher probability of failure for the entire reach, than for one of the individual locations. [17]

2.5. Conclusion

An important part of this chapter concerned the theory on reliability analysis and probabilistic design. This is the starting point for answering the research questions which were formulated in Chapter 1. First, sub-questions $1a$, $1b$ and $1c$ about the literature review will be answered. Consequently, main research question 1 will be answered.

1a. What does failure, availability and survival mean in the case of SFTs?
The probability for a healthy person to die as a result of an accident in daily life is about 10^{-4} per year in developed countries. The individual risk (IR) should be smaller than 10^{-5} per year. It is necessary to assess the probability of a system to meet these requirements. Failure can either be social or technical, of which technical failure can result in loss of lives. Multiple limit states can be formulated for the SFT, of which the ULS is of most importance. This state is reached when the capacity of the structure is exceeded. Failure of a subsystem, for example the tethers, can lead to complete failure of the structure. The same occurs for failure of the tube, joint or foundation. The availability for the SFT should be 98 %. This means that, during this period, traffic is able to travel through the tube without hindrance. In case of traffic accidents and car fires, the SFT will have to meet normal design criteria used for rock or immersed road tunnels. Safety routes need a separate ventilation- and light system. For the SFT system with twin tubes, evacuation can take place from one tube to the other tube.

1b. What are target reliabilities for geotechnical- and hydraulic structures, buildings and bridges?
For geotechnical structures, piles, foundations and superstructures have been investigated. For single driven piles, recommended target β-values are between 2.0 and 2.5 and for single drilled shafts this is between 2.5 and 3.0. The target β for bearing capacity should be 3.5. For shallow foundations, the β should be between 2.8 and 3.5. The β of foundations should correspond to values of β between 3.1 and 3.7. In the design of superstructures, a target reliability of β = 3.5 is often used. For hydraulic

structures, the target reliability is defined by the exceedance probabilities of the hydraulic loading conditions. They range from a maximum allowable probability of $1/100$ per year to $1/100.000$ per year. The Building Decree focuses on failure of one component, instead of the entire defense system. For flood defences, a new defense requires a design life of 50 years (for dikes) or 100 to 200 years for hard structures. Buildings can fall into CC2, $\beta = 3.8$ ("sparsely occupied" buildings), or into CC3, $\beta = 4.3$ ("densely occupied" buildings). The same holds for bridges. Bridges in highways have to satisfy the requirements belonging to CC3, so a $\beta = 4.3$ for new bridges, $\beta = 3.8$ for repair and $\beta = 3.3$ for unfit for use. Bridges in less important roads are in CC 2 and have to satisfy $\beta = 3.8$ for new bridges, $\beta = 3.3$ for repair and $\beta = 2.5$ for unfit for use. The β-values for the different structures are summarized in Table 2.1.

Parameter	Target reliability index [2]	Source
Geotechnical structures		
Single driven piles	2-2.5	Zhang et al. [63]
Single drilled shafts	2.5-3.0	Zhang et al. [63]
Bearing capacity soil	3.5	ISO2394, Annex D [23]
Shallow foundations	2.8-3.5	Zhang et al. [63]
Other foundations	3.1-3.7	Zhang et al. [63]
Hydraulic structures		
Flood defenses	1.3-4.3	Schweckendiek et al. [39]
Bridges and buildings		
Bridges in highways	4.3 (new), 3.8 (repair)	Steenbergen et al. [46]
Bridges in less important road	3.8 (new), 3.3 (repair)	Steenbergen et al. [46]
Sparsely occupied buildings	3.8	Dutch Building Decree [6]
Densely occupied buildings	4.3	Dutch Building Decree [6]

Table 2.1: Reliability indices of other structures

1c. What is the effect of the spatial variability on the design of flood defences?
When considering the length, an SFT can be compared to a dike. The longer the structure, the higher the probability of finding either an extreme load or a weak spot. The following parameters can be investigated:

- The spatial variability in the subsoil: The higher the spatial variability in the subsoil, the higher the length effect. However, the influence of the soil on the SFT structure cannot be quantified yet. The SFT is only in contact with the soil through tethers at specific locations, and these locations can be investigated beforehand. Nevertheless, uncertainty of the soil will remain.

- The material properties: The SFT consists mainly of concrete and steel. The length effect of these materials will be quantifiable. Furthermore, the joints can be investigated. Many joints may increase the probability of one leaking joint.

- The loads on the structure: The wave load on the SFT can differ over the length of the tube. Most loads are however permanent loads, and these will not have a large influence on the length effect. The variability of waves will be discussed in Chapter 7.

---

[2]The reference periods for the β-values depend on the type of structure. Usually, this is 1 year for flood defenses and 50 years for buildings and bridges

<div style="text-align: right; font-size: 4em;">3</div>

Case study

The case study used in this research is the Bjørnafjorden-crossing in Norway. For this crossing, an SFT was recently designed and calculated by a Norwegian research group [35]. Risks and uncertainties were shortly addressed in their study, and general partial factors from Eurocode were applied. However, the reliability of the system was not discussed. The aim of this chapter is to investigate the design for the Bjørnafjorden-crossing, and to use its properties as a basis of the reliability analysis.

3.1. General

3.1.1. Immersed tubes

The tube segments of the tunnel were taken as approximately 200 m, which means 27 tunnel elements are necessary to reach the total length of 5500 m. Two types of circular cross-sections are used, which can be seen in Figure 3.1: T9.5 (A) and T12.5 (B), for respectively a road with a width of 9.5 m and 12.5 m. Emergency lay-by's (B) are required every 250 m, so for this reason the T12.5 is applied [35]. The lay-by itself is 30 m and has a transition zone of 30 m on each side. A circular cross-section has been chosen, as this induces only compressive stresses and no bending in the cross-sectional plane.

Figure 3.1: Two tube profiles: T9.5 (left) and T12.5 (right) [35]

Figure 3.2: Two tubes and framework [35]

The ballast compartments have a total area of 13.5 m^2 and 26.7 m^2. The SFT facilitates traffic on two lanes in each direction. Besides cars, bikers and pedestrians will also be able to cross the tunnel. The tubes are connected with a framework of horizontal crossbars and diagonals, shown in Figure 3.2. The horizontal bracing consists of four diagonals with an inclination of $40°$. A cross beam is constructed every 200 m. The concrete design is based on concrete of grade B55 (C45/55) according to Eurocode 2. The maximum aggregate size of the concrete is 20 mm.

The only constraint for the vertical profile is the requirement for a minimum ship clearance, which is set to 20 m relative to low astronomical tide (LAT). This is considered to be well below the reach of ship keels, so that a direct hitting from surface vessels is not possible. The impact of wave loads, generated by wind, is considerably reduced from 20 m to 30 m water depth. Submarines entering the training basin in the Bjørnafjord should be able to navigate over the SFT in submerged position. For the hori-

zontal profile, bathymetry, geological conditions, rock tunnel constrains, bridge structural performance, construction aspects and costs were investigated. [35]

3.1.2. Tethers

The tethers are steel tubes of steel grade S235 and have a cross-sectional area of 0.129 m^2. The steel class and cross-sectional area are the same for all tethers, because of constructibility. The tether is just resistible to tension and cannot sustain compression. Along the length of the SFT, there are 26 moorings. Each mooring contains four tethers. The lengths differ along the length of the crossing. The tethers are installed at depths varying from -120 m to -550 m, which means that the tethers have a length of 90 m to 520 m. The tethers are connected on the outside of the cross-section, according to the configuration in Figure 3.3.
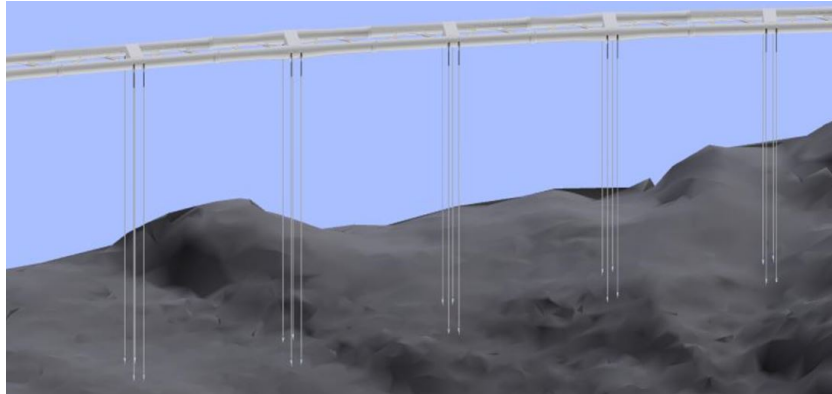
Figure 3.3: The configuration of the tethers for the Bjørnafjorden [35]

The foundation for the tethers is not the same at every location of the crossing, because of different soil properties and depths. Several types of foundations have been considered: gravity foundations, piled foundations, rock bolts, suction caisson anchors and deep-water anchors. In this case, drilled and grouted rock anchors were chosen for all tethers. Gravity foundations were more costly because of large dimensions and a large amount of solid ballast material required. For locations with moraine, clay or mixed deposits above the bedrock, a casing is made through the layers and the rock anchor is drilled and grouted to the bedrock. Thus, the tethers in the Bjørnafjorden report are grouted and straight.

3.1.3. Reinforcement

The tunnel elements will be post-tensioned in both longitudinal and transverse direction. A relatively high level of prestress is required in the longitudinal direction, because a large compressive stress is necessary to compensate the tensile stresses caused by the bending moment. Strands from steel type Y1860-S7 are applied. The main reinforcing steel is of class B500-NC. Bars with diameter 12, 16, 20, 25 or 32 mm, bundles of one, two or three bars and center distance of 1000, 500, 200 or 150 mm may be applied. The outer and inner cover and amount of bars are not specified. Shear reinforcement is chosen as reinforcement with diameter 8, 12 or 16 mm, with center distance of 500, 200 or 150 mm in each direction. [35]

3.1.4. Construction joints

Joints have multiple tasks. They ensure the waterproofing, allow for limited relative displacements, and guarantee the equilibrium of the structure. The flexible construction joints in use for immersed tunnels are not optimal to use for SFTs, because SFTs are subjected to significant displacements and rotations in the longitudinal bending planes. Rigid inter-modular joints and terminal joints would be the most feasible solution, allowing for axial displacements due to thermal variations and tri-axial rotations. The inter-modular joints designed for the SFT prototype of Qiandao Lake in China can be seen as bolted connections. The steel joint consists of two ring end plates, each of them belonging to one of the adjacent modules. The flanges are connected by means of high strength steel bolts. The bolted

flanges are placed at the internal concrete and steel layers. The water tightness of the connection is guaranteed by a rubber ring crushed between the modules. The end joint design is very challenging, because it is situated between the stiff land bored tunnel and the submerged tunnel part. Both parts are subjected to different loads. Therefore a transition structure is needed. [29]

3.2. Loading

3.2.1. General

The load on the submerged floating tunnel can be divided into permanent load, variable load and accidental load. In this chapter, the content of the permanent and variable loads will further explained. The accidental loads are not included. The permanent load includes the downward forces (self-weight of the tubes, asphalt, installations) and the upward forcing (buoyancy). The variable load includes traffic load, wave-current load, temperature load, marine growth, water absorption, shrinkage, creep and vortex induced vibrations. The stability of the SFT depends on the balance between dead load, moving load, buoyancy and anchoring force [61]. The weights of concrete and seawater will be defined as unit weights, γ_c and γ_w.

$$\gamma_c = \frac{\rho_c \cdot g}{10^3} \qquad\qquad \gamma_w = \frac{\rho_w \cdot g}{10^3} \qquad\qquad (3.1)$$

where: γ_c, γ_w = the unit weight of concrete and water respectively $[kN/m^3]$
ρ_c, ρ_w = the density of concrete and water respectively $[kg/m^3]$
g = the gravitational acceleration $[m/s^2]$

3.2.2. Permanent loading

Downward loading
The distributed load due to the concrete tube will be calculated according to:

$$q_c = A_c \cdot 1.1 \cdot \gamma_c = \left(\frac{1}{4} \cdot \pi \cdot D^2 - \frac{1}{4} \cdot \pi \cdot d^2 \right) \cdot 1.1 \cdot \gamma_c \qquad\qquad (3.2)$$

where: q_c = the distributed load due to the weight of the concrete tube $[kN/m]$
A_c = the area of the concrete tube cross-section $[m^2]$
γ_c = the unit weight of concrete $[kN/m^3]$
D = the outer diameter of the tube $[m]$
d = the inner diameter of the tube $[m]$

The concrete area of the tube is multiplied by a factor of 1.1, because concrete walls are constructed inside the tube as well. The unit weight of reinforced concrete was taken as 26.5 kN/m^3 in the Bjørnafjorden report. This was stated to be the greatest occurring weight. This high value can be due to heavy aggregates and the availability of materials in Norway. Normal concrete has a density around 24 kN/m^3 and reinforced concrete has a density around 25 kN/m^3. Furthermore, not only the self-weight of the concrete tubes contributes to the permanent downward loading, also the equipment, asphalt and ballast need to be added. Equipment consists of electrical installations, power supply, lighting, ventilation and a drainage system.

Hydrostatic pressure
The buoyancy force is the result of the pressure difference between the top and bottom of the structure. The hydrostatic pressure depends on the water depth and density of the water. The water levels have been measured at the location.

Return period [years]	Highest water level [m]	Lowest water level [m]
10	+1.27	-1.12
100	+1.42	-1.22

Table 3.1: Highest and lowest water levels for given return periods (from MSL) [35]

The hydrostatic force can be calculated as:

$$F_{p,hor} = \int_{h_t}^{h_b} \rho_w \cdot g \cdot y \, dy \cdot A = \frac{1}{2} \cdot \rho_w \cdot g \cdot (h_b^2 - h_t^2) \cdot A \tag{3.3}$$

where: $F_{p,hor}$ = the hydrostatic force $[N]$
        h_b = the height of the bottom of the structure $[m]$
        h_t = the height of the top of the structure $[m]$
        ρ_w = the density of water $[kg/m^3]$

Buoyancy force
The resulting upward force is called the gross buoyancy load. This does not depend on the depth, but only on the submerged area and the density of the water. The values for the unit weight of seawater are set as follows [35]:

$$\gamma_{w,max} = 10.084 \; kN/m^3 \qquad \gamma_{w,mean} = 10.035 \; kN/m^3 \qquad \gamma_{w,min} = 9.987 \; kN/m^3 \tag{3.4}$$

The distributed buoyancy load can be formulated as:

$$q_b = A_s \cdot \gamma_w = \pi \cdot R^2 \cdot \gamma_w \tag{3.5}$$

where: q_b = the distributed load due to buoyancy force $[kN/m]$
        A_s = the submerged area of the object $[m^2]$
        γ_w = the unit weight of water $[kN/m^3]$
        R = the radius of the tube $[m]$

3.2.3. Traffic load

Traffic loading acts in the vertical direction as well, but is a quasi-static variable load. First, the loading model from Eurocode EN1991-2 will be used to calculate the traffic load. [14] The traffic lane has a width of 9.5 m, which can be divided in three parts of 3 m: two driving lanes and one service lane. In the lay-by element, an extra lane of 3 m is added.

Lane	Width $[m]$	Distributed area load $[kN/m^2]$	Equivalent line load $[kN/m]$
Lane 1	3	5.4	16.2
Lane 2	3	2.5	7.5
Lane 3	3	2.5	7.5
Remaining area	0.5	2.5	1.25
Bicycle lane	4	2	8
Sum			**40.5**

Table 3.2: Traffic loading per tube [35]

In order to determine the maximum traffic load, the maximum vehicle weight and the density of vehicles during a traffic jam can be investigated. The maximum weight of trucks allowed in the EU is 50.000 kg [51]. A case is considered, where all three lanes are fully loaded with small trucks. In between the trucks, there is a space of 1 m taken into account. This results in a load of about 100 kN/m.

$$q_{t,max} = \frac{F_{truck,max} \cdot n_{lanes}}{L_{truck,min} + 1} \tag{3.6}$$

where: $q_{t,max}$ = the maximum traffic load $[kN/m]$
        $F_{truck,max}$ = the maximum force due to trucks $[kN]$
        n_{lanes} = the amount of traffic lanes [-]
        $L_{truck,min}$ = the minimum length of a truck $[m]$

However, this has a very low probability of occurrence, because only small trucks have to be in the same tunnel element, all small trucks need to be fully loaded and there has to be a traffic jam.
In order to take this into account in the calculation, a large standard deviation can be used.

3.2.4. Hydrodynamic forces

Hydrodynamic forces can be fluctuating (caused by waves) or constant (caused by steady currents) and will result in a dynamic load pattern on the SFT. Drag, lift and inertia forces are of interest. Drag force is a force parallel to the direction of flow, and lift force occurs perpendicular to the flow. The inertia force is caused by the pressure gradient in accelerating flow. It is equal to the product of the mass of water displaced by the cylinder and the acceleration in undisturbed flow [26]. Waves and currents should not be computed separately, but their velocities should be added. Otherwise, the influence of drag force will be underestimated. For the inertia force, only the wave speed needs to be taken into account, not the current speed, because currents do not contribute to inertia force.

Currents

A current can be generated by wind or by the tide. The current was found to be strongest in the middle of the fjord. The current velocity for a 100 year return period is 0.54 m/s [35]. The drag force and lift force can be calculated according to the following empirical formulas:

$$F_{c,x} = \frac{1}{2} \cdot \rho_w \cdot u^2 \cdot (C_D + C_D') \cdot A \tag{3.7}$$

$$F_{c,y} = \frac{1}{2} \cdot \rho_w \cdot u^2 \cdot (C_L + C_L') \cdot A \tag{3.8}$$

where: $F_{c,x}, F_{c,y}$ = the forcing due to the current in horizontal and vertical direction respectively [N]
        p_w = the density of the water [kg/m^3]
        C_D = the static drag coefficient [-]
        C_D' = the dynamic drag coefficient [-]
        C_L = the static lift coefficient [-]
        C_L' = the dynamic lift coefficient [-]
        A = the area facing the flow [m^2]
        u = the flow velocity [m/s]

The drag coefficient depends on the shape and structure of the object and can be measured in a wind tunnel. It can also be derived from the relationship between the Reynolds number and drag force. [52]

$$Re = \frac{u \cdot D}{v} \tag{3.9}$$

where: Re = the Reynolds number [-]
       u = the flow velocity [m/s]
       D = the characteristic dimension [m]
       v = the kinematic viscosity, which is 10^{-6} [m^2/s]

The lift coefficient increases as the inclination angle increases, and reaches a maximum around an angle of 45°. The accompanying drag coefficient is in that case 1.0 [52]. The lift force is zero for a straight approaching flow. Cylinders have a drag coefficient around 1 for a Reynolds number between 10^2 and 10^5. For a higher Reynolds number, so more turbulent flow, the drag coefficient is somewhat smaller. The dynamic coefficients (C_L' and C_D'), indicating turbulence, will not be quantified and added to the equation. Turbulence is taken into account by using a certain deviation for the wave-current load.

Waves

Waves are characterized by an oscillating motion of the water particles. Two types exist: wind waves and internal waves. Internal waves are caused by differences in temperature, salinity, or concentration of suspended sediment. For oscillating flow, the Morison equation could be applied. This leads to a more elaborate equation than Equation 3.7 and 3.8, because inertia force is also added. The Morrison force can be either dominated by drag force or inertia force.

$$F_{w,x,y} = \underbrace{\left(\rho_w \cdot C_m \cdot V \cdot \dot{u}_{x,y} \right)}_{\text{Inertia force}} + \underbrace{\left(\frac{1}{2} \cdot \rho_w \cdot C_d \cdot A \cdot u_{x,y} \left| u_{x,y} \right| \right)}_{\text{Drag force}} \tag{3.10}$$

where: $F_{w,x}, F_{w,y}$ = the Morrison force, due to waves in horizontal and vertical direction respectively [N]
$\dot{u}_x, \dot{u}_y$ = the flow acceleration [m/s^2]
C_m = the inertia coefficient, $1 + C_a$ [-]
C_a = the added mass coefficient [-]
V = the volume of the body [m^3]

For wind waves at sea, the Norwegian Public Roads Administration (NPRA) specified a significant wave height $H_{s,wind,100y}$ = 3.0 m with a period range of 4 < T_p < 6 s, corresponding to a perpendicular angle of attack. The significant wave height is the average of the highest $1/3$ of the waves. It is assumed that these characteristics are constant along the length of the tunnel.

Waves generates by wind storms propagate to other areas, where they occur not associated to local wind. Those waves are called swell waves. For swell waves, the significant wave height is $H_{s,swell,100y}$ = 0.3 m with a period range of 12 < T_p < 16 s. In Figure 3.4, it can be seen that the influence of the wind waves becomes very small at larger depth. The swell waves, on the other hand, still have 50% of their value at a depth of 30 m.
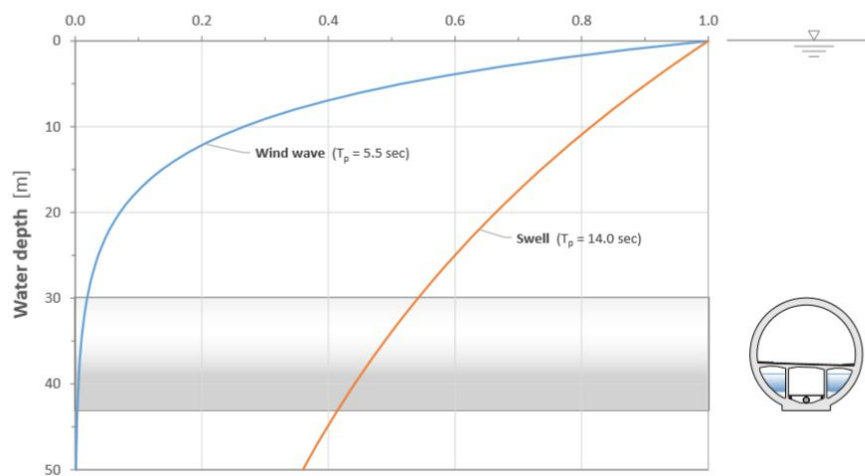
Figure 3.4: Influence of wind and swell waves relative to the depth [35]

The Bjørnafjorden-crossing has a depth up to 500 m, which means that deep water conditions hold. According to linear wave theory, Equations 3.11 and 3.12 can be used to compute the particle velocity.
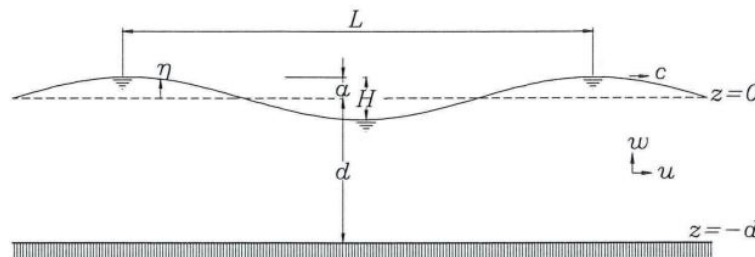
Figure 3.5: Sinusoidal wave shape [52]

$$u_x = \frac{\pi H}{T} \cdot e^{\frac{2\pi}{L}z} \cdot \cos\theta; \ u_y = \frac{\pi H}{T} \cdot e^{\frac{2\pi}{L}z} \cdot \sin\theta \qquad (3.11)$$

$$\theta = \omega t - kx; \ k = \frac{2\pi}{L}; \ \omega = \frac{2\pi}{T}; \ L = \frac{gT^2}{2\pi} \qquad (3.12)$$

where: u_x = the horizontal velocity $[m/s]$
$\quad\quad\quad\ u_y$ = the vertical velocity $[m/s]$
$\quad\quad\quad\ H$ = the wave height $[m]$
$\quad\quad\quad\ T$ = the wave period $[s]$
$\quad\quad\quad\ z$ = the coordinate of the depth relative to the water surface $[m]$
$\quad\quad\quad\ \omega$ = the angular frequency $[rad/s]$
$\quad\quad\quad\ \theta$ = the combination of the angular frequency and wave number $[rad]$
$\quad\quad\quad\ k$ = the wave number $[rad/m]$
$\quad\quad\quad\ L$ = the wave length $[m]$

For w_x, the maximum θ of 0 was used, and for w_y the value 0.5π was used. The maximum particle velocity during the swell wave, 30 m below water level, resulted in $w_x = w_y = 0.036$ m/s. This is significantly smaller than the current velocity. Since this is significantly smaller than the current velocity, the wave load will not be calculated separately.

3.2.5. Other variable loads

For the tether variant, the tidal loads are negligible, because their impact depth is small. Only currents need to be taken into account as horizontal forcing to to the water. Furthermore, variable self-weight (marine growth and water absorption), temperature loading, shrinkage, creep and vortex-inducted vibrations need to be considered.

Marine growth

Marine growth affects hydrodynamic loading, because of increased mass and drag force. Several types of marine growth may be found on a submerged member after a certain time. Their influence depends on water depth, water temperature, season and ocean current. There are generally three types: hard growth, soft growth and long flapping weed. Hard growth can be defined as mussels, oysters and tubeworms. Seaweeds, soft corals, anemones, sponges, hydroids and algae can be seen as soft growth. Long flapping weed is kelp, which is similar to soft growth organisms, but its size is much larger. [27]

Water depth $[m]$	Thickness $[mm]$	Submerged mass $[kN/m^2]$
+0.5 to -12	150	0.468
> 12	75	0.234

Table 3.3: Thickness of marine growth from NORSOK [34]

The water depth refers to mean water level. The load due to marine growth is also dependent on time. Right after the installation of the tunnel, its value will be zero. After a certain time, the layer will grow up until 75 mm [34]. This gives a distributed load of approximately 10 kN/m.

Water absorption

Water penetrates into unsaturated concrete. The tube is built in a construction dock, and when the tube is submerged, water penetrates the outer shell. The effective porosity and the sorptivity are important parameters for water absorption. However, this is a debatable factor in literature. It will not be taken into account in the next chapters.

Temperature loading

Since the temperature of sea water is lower than the temperature at the production site, the section will have tensile forces after installation. Temperature load influences the buoyancy of the structure. Furthermore, the differences between the inside and outside of the tube will cause distortions to the tunnel structure that result in bending moments and shear forces in the structural members. It is important to regulate the inside temperature to prevent these distortions. To account for this, a larger standard deviation can be taken for the buoyancy force. [28]

Shrinkage and creep
Shrinkage and creep cause volume changes of concrete. Volume change is one of the most detrimental properties of concrete. It affects the durability and long-term strength, by causing restraint forces. This should thus not be too large. Axial loads from post-tensioning and external water pressure are relevant creep loads. However, compared to other loading types, the influence of creep and shrinkage is negligible. [35]

Vortex-Induced Vibrations
The tethers are subject to forces with periodical irregularities, which induces motions interacting with an external fluid flow. Wind tunnel tests have been performed to confirm the response model for vortex induced vibrations (VIV) [12]. According to Morison's formula, the buoyancy (F_l) caused by VIV is defined as follows [64]:

$$F_l = \frac{1}{2} \cdot \rho_w \cdot C_L \cdot D \cdot v^2 \cdot \cos \omega_s t \tag{3.13}$$

$$\omega_s = \frac{2 \cdot \pi \cdot St}{D} \qquad\qquad st = \frac{f_v \cdot D}{V} \tag{3.14}$$

where: F_l = the lift or buoyancy per unit length of an SFT tube [N]
   D = the diameter of an SFT tube [m]
   v = the current velocity [m/s]
   C_L = the buoyancy coefficient [-]
   ω_s = the angular frequency of vortex-incited vibration [rad/s]
   ρ_w = the density of the water [kg/m^3]
   t = the time [s]
   St = the Stouhal number [-]
   f_v = the vortex shedding frequency [$1/s$]
   V = the velocity of the incoming flow [m/s]

The vibrations can be limited by choosing reasonable structure parameters, by installing damping devices or by using an additional disturbing flow device. The percentage of VIV will be compared to the forcing due to waves and current, to determine if the VIV needs to be taken into account. [61]

Accidental loads
A certain probability of failure for accidental loads will be taken into account, to be able to calculate the probability of failure of the entire system. The accidental loads will not be calculated in detail. There are many types of accidents that can occur. However, they have a low frequency of occurrence.

3.3. Summary
The design made for the Bjørnafjorden in Norway is taken as reference case for this research. The structure contains two identical concrete tubes with steel reinforcement. Between the two tubes, there are crossbeams and diagonals. The diameter of the tube is not the same along its length, because there are emergency lanes every 250 m. The tube elements are 200 m, and the total length of the SFT is approximately 5400 m. The tube is stabilized by steel tethers attached to the seabed with drilled and grouted rock anchors. In the following chapters, a single tube will be investigated.

Several loading types were defined, e.g. the permanent downward loads, the buoyancy force, the traffic loading and the wave-current loading. The hydrostatic load needs to be considered for the axial loading. The vortex-induced vibrations, temperature loading and creep and shrinkage turned out to be negligible. For the accidental loads, a probability of failure can be assumed to be able to determine the failure probability of the entire system. The accidental loads will not be further explained.

4

Framework for reliability analysis

In this chapter, a framework for the reliability analysis will be described. In order to perform a reliability analysis, a full probabilistic design should be made. The procedure for this will be explained. A suitable β-value and important failure mechanisms will be selected. Next, the input parameters for the analysis will be described. The experience gained from the other structures (Chapter 2.3) can only partly be used, since the SFTs differ from common civil structures. In general, SFTs have [3]:

- Different relevant limit states;

- Different magnitude of consequences and costs involved with failure of relevant limit states;

- Different accuracy of the models that predict the structural response;

- Different load scenarios.

An overview of the loading situation can be seen in Figure 4.1. A single tube structure will be investigated.
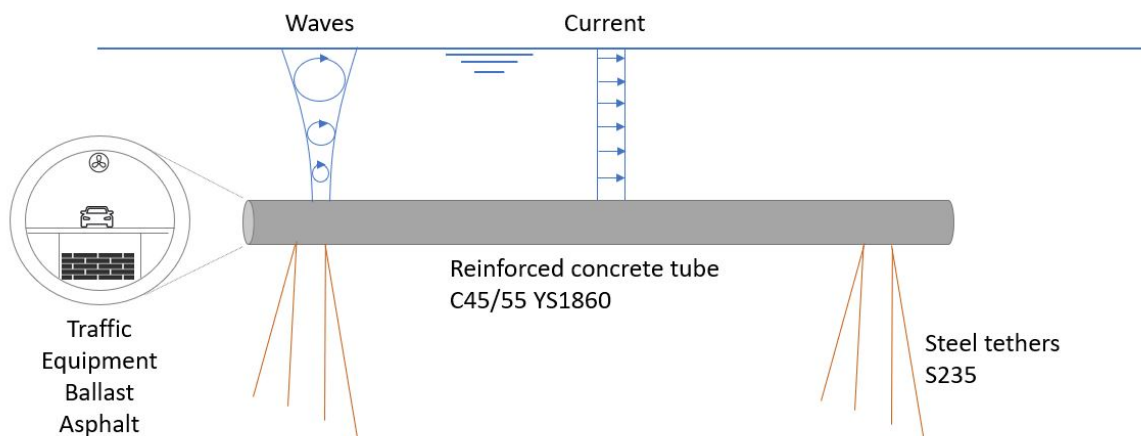
Figure 4.1: Simple model of an SFT with load cases, side-view

4.1. Procedure

In order to assess the system, a target β-value needs to be selected. Next, input parameters need to be defined by their mean-values and standard deviations. Consequently, limit state functions can be formulated. A FORM analysis and MC simulation can be performed, based on these distributions and limit state functions. FORM is a fast method, but also has disadvantages. Sometimes there is no convergence, or the result is inaccurate if the Z-function is curved, or a local minimum can be found instead of a global minimum. For this reason, a MC simulation is performed simultaneously. The MC simulation is used to confirm the β-value. This results in a full probabilistic design. Python and Prob2B are used simultaneously to check the validity of both methods. The following steps are performed:
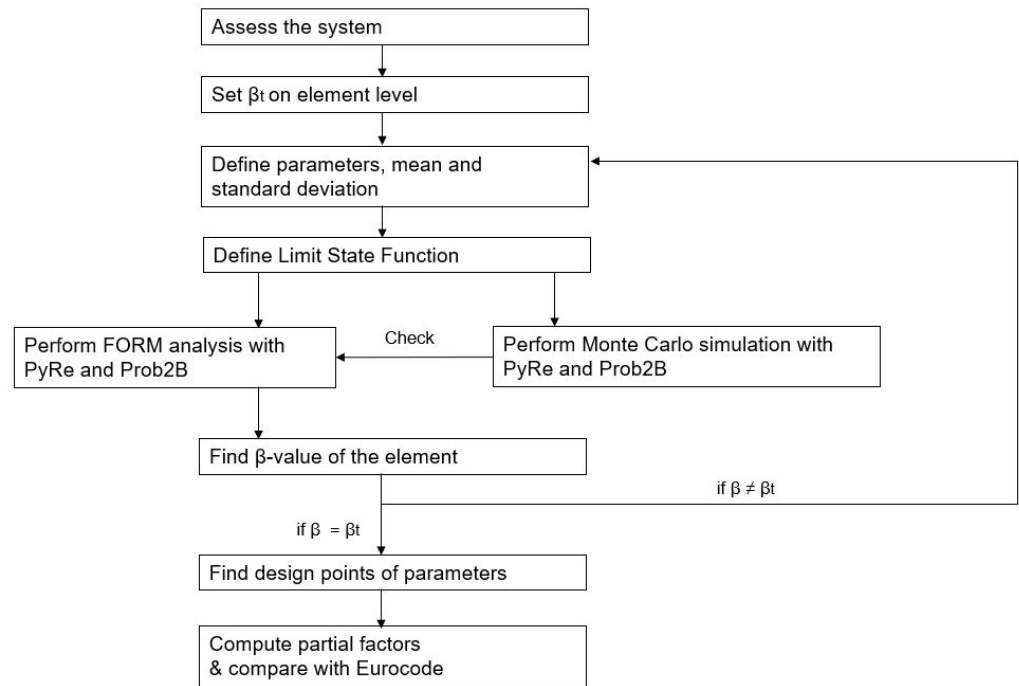
Figure 4.2: Flowchart to compute partial factors

The factors resulting from the full probabilistic model will be compared with the general partial factors from Eurocode. These general partial factors can be found in Appendix A.

4.2. Selection of target reliability

The target reliability index, β, can be defined on system- or element level. It is important to investigate how the elements relate to the system. A fault tree will be made to visualise the interaction between events and conditions. Different failure mechanisms will be described and length effects are addressed. Furthermore, the design life of the structure has to be taken into account, and should be compared to the reference period of the β-values. Individual risk and group risk will be discussed as well. Ultimately, a conclusion will be drawn about the target β-value for this research.

4.2.1. Element versus system

First, a fault tree of an SFT can be presented as in Figure 4.3. This tree is based on all structural elements of the SFT. The failure mechanisms are all ultimate limit states (ULS) [1]. Design errors, execution errors and inspection errors are not included in the fault tree. Failure of the SFT can also mean that the structure is not going to be used, because of fear or because of comfort. This is not included in the fault tree either.
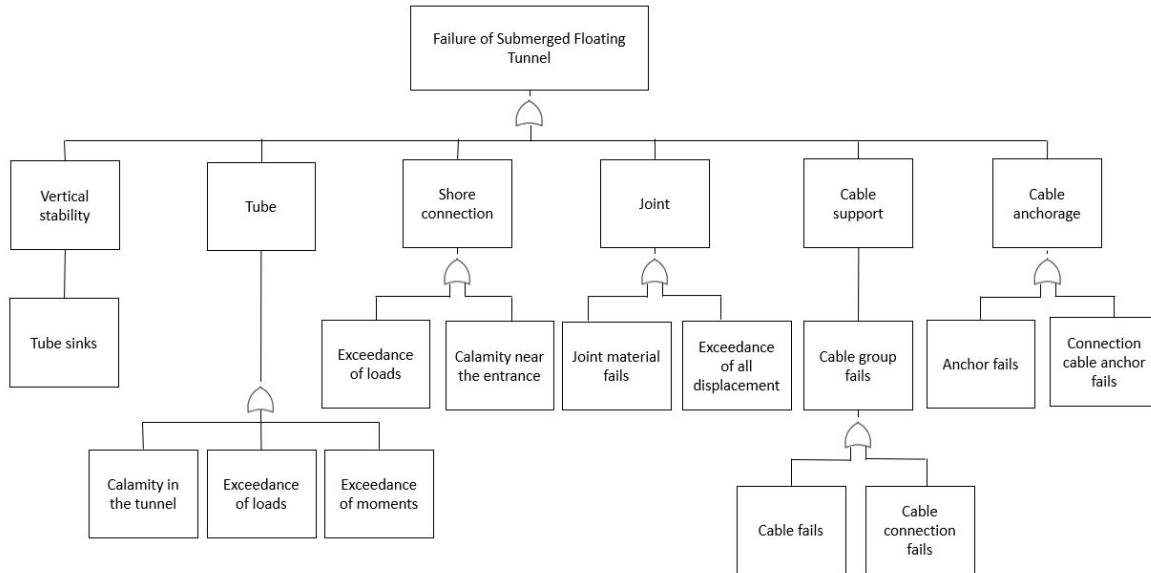
Figure 4.3: Fault tree adjusted from Ahrens and Gursoy, 1997 [1]

In the system, OR-gates can be found. This means that the structure will fail if one of the elements fails. The following formula can be used to determine the probability of failure in case of an OR-gate:

$$P(\text{A or B}) = P(A \cup B) = P(A) + P(B) - P(A \cap B) \tag{4.1}$$

For an OR-gate, the following statements can be made:

$$
\begin{array}{ll}
\text{mutually exclusive:} & \sum P_i \\[2mm]
\text{independent:} & 1 - \prod(1 - P_i) \\[2mm]
\text{fully dependent:} & \max P_i
\end{array}
$$

Second, a simplified fault tree is made to make a clear division between failure of the tube, failure of tethers and accidental loads. A section of an SFT consists of a cross-section and an element of limited length. Its parameters will be further described in Chapter 5. This section can be investigated based on β-values of the individual failure mechanisms. The mechanisms in Figure 4.4 are assumed to be uncorrelated, thus $P(A \cap B) = 0$. However, in reality, correlation effects will be present. This means that the actual probability of failure of the section will be lower, and thus the β-value will be higher. A correlation has to be large to be of significant influence. As a starting point, the β's for the individual failure mechanisms are set to 3.8. Failure due to accidental loads is set to 4.3, however this is out of scope of this research.
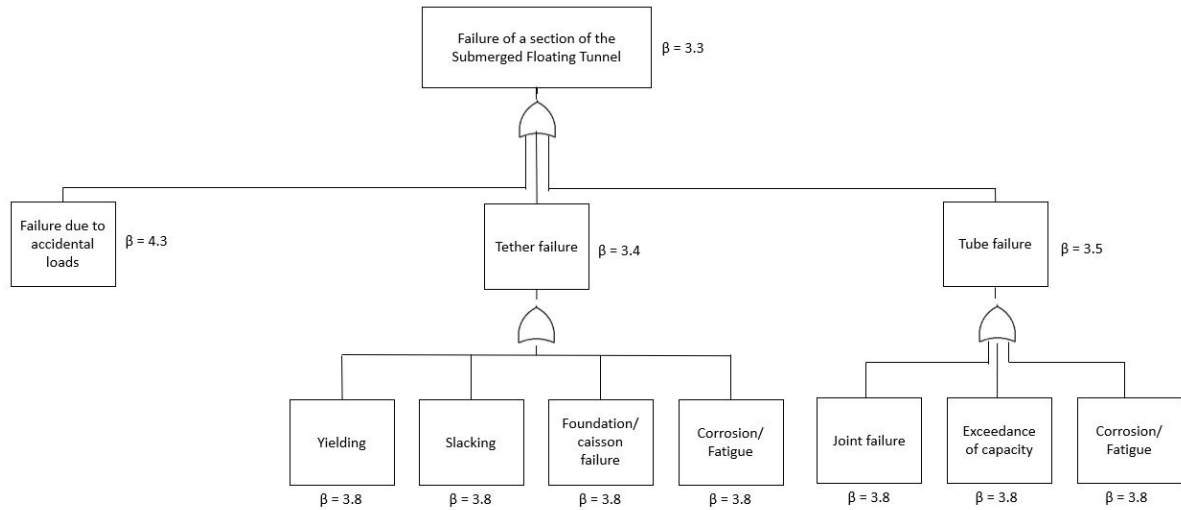
Figure 4.4: Simplified fault tree, β-values based on the assumption of independent variables

The failure mechanisms sum up to a β-value of 3.3 for failure of the section. This falls into CC1, which is relatively low. A larger β-value of the section can be reached by increasing the β-value of the elements. This is demonstrated in Figure 4.5. Now, a β-value of 3.8 is reached for the section.
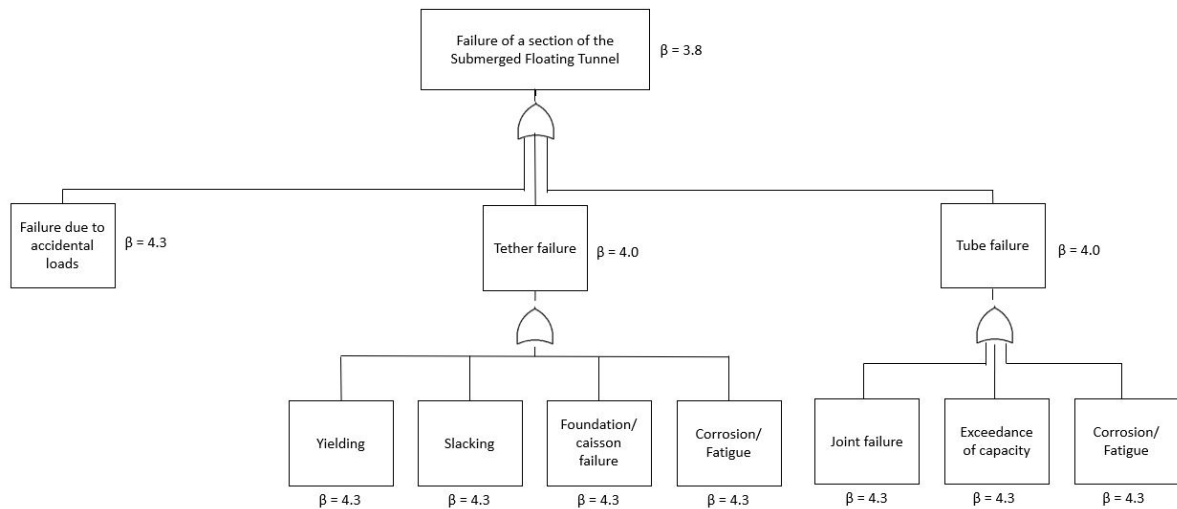
Figure 4.5: Simplified fault tree, β-values based on the assumption of independent variables

It is important to check whether the reliability on system level (β_{system}) is also sufficient. For the entire system, the fault tree of Figure 4.6 can be constructed. The SFT will consist of multiple individual sections. The failures of the individual sections can be classified between independent and fully dependent. When the system is fully dependent, the probability of failure of the system will be the same as an individual section. When independent failure of multiple sections could occur, the probability of failure would be very large, and a target β-value for the system would never be met.
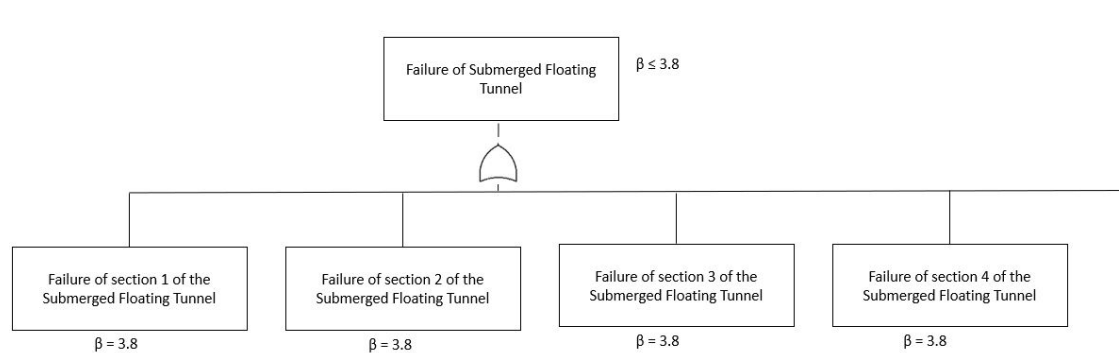
Figure 4.6: Fault tree for the entire SFT system

4.2.2. Length effect

When all elements in the fault tree can fail individually, the total probability of failure of the system is large. This is called the length effect of the system. The spatial variability of material properties, loading parameters and correlations influence the length effect. Those properties are described in Chapter 2.4.

For a wide distribution around the mean value of a parameter, the length effect will be larger. The SFT consists mainly of concrete and steel. The concrete and steel density have a small spread compared to the variable loads. Thus, the length effect of these materials will be quantifiable.

For this research, the length effects and probability of consequential system failure are considered small. Thus, it will be safe to apply β-values on element-level.

4.2.3. Reference period versus lifetime

The β-value is defined for a certain reference period. In Eurocode, β-values are available for a reference period of 1 year and a reference period of 50 years.

The lifetime of a structure depends on the type and use of the structure. A new defense requires a design life of 50 years for dikes or 100 to 200 years for hard structures [17]. In most cases, a structure has a lifetime of more than 1 year, however reference periods of 1 year can still be applied. It is more accurate to use a reference period of 1 year. However, it is also more complex, since every individual year needs to be considered. A lifetime of 100 years is not compatible with Eurocode, because β-values for reference periods of 100 years are not formulated. In this research, a lifetime of 50 years of the SFT is chosen, in order to be compatible with the β-values for a reference period of 50 years. Consequently, the Gumbel distributions for the variable loads have to be scaled up to 50 years as well. This method can be found in Chapter 2.1.4.

4.2.4. Group risk versus individual risk

An appropriate requirement for the individual risk for structures would be a value between 10^{-5} and 10^{-6} per year [47]. The individual risk criterion does not depend on the number of fatalities. However, the group risk does depend on the number of fatalities. It shows a decreasing quadratic relationship between acceptable failure probability and the amount of fatalities [25]. For 100 fatalities, the acceptable failure probability for group risk would be 10^{-9} per year. This is should be similar to the acceptable probability of failure of the system. However, this would mean that a β_{system} of around 5 is necessary.

4.2.5. Conclusion

The first main research question about the target reliability for SFTs can be answered: *1. Which target reliability should be applied to SFTs?*. In the previous sections, multiple properties of the system were considered. Since general partial factors from Eurocode are determined on a β-value of 3.8, a β-value of 3.8 for a reference period of 50 years should be chosen for the individual failure mechanisms. For the individual and group risk, 3.8 cannot be met. The length effect is assumed to be small. However,

if this would increase due to a change in design, the value of the β_{system} would decrease. This should be taken into account and handled cautiously.

For future research, it can be recommended to use a β-value of 4.3, to reach a β_{system} of 3.8. This could be seen in Figure 4.5. Furthermore, since the structure would more likely have a lifetime of 100 years, a reference period of 50 years is not compatible. This issue is not addressed in Eurocode and will not be further addressed in this research.

4.3. Selection of failure mechanisms

The failure mechanisms encountered in the fault trees of Chapter 4.2 are further analysed. The goal is to select the most important failure mechanisms for the reliability analysis.

4.3.1. Failure of the tether

The tethers are unable to withstand compressive axial force. They are presumably made of several segments connected through joints which allow free rotations, in order to enormously reduce the stresses induced by hydrodynamic transverse loading [29]. The equilibrium of the structure must be maintained when the SFT is subject to all unfavorable loading cases. There are two possible motions of the tethers:
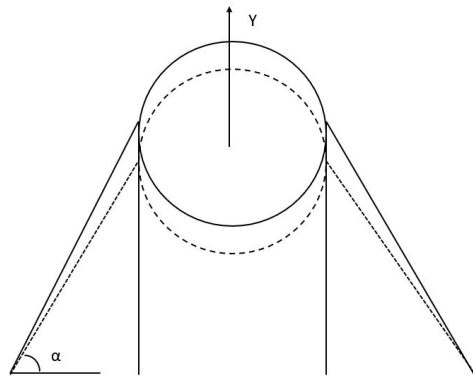
Figure 4.7: Motion due to vertical forcing
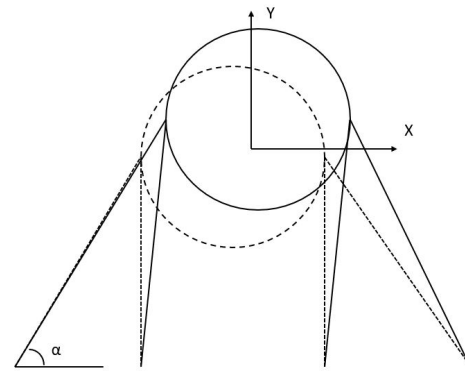
Figure 4.8: Motion due to horizontal and vertical forcing

Due to this configuration with four tethers, rotation of the tube will not occur. Figure 4.7 demonstrates movement purely caused by vertical motion. This motion can be directed either upwards or downwards. Figure 4.8 shows movement due to horizontal as well as vertical motion. It should be noted that the angle of the inclined tethers (α) is not the same for both cases.

Yielding of the tether

When the stress in the cross-section reaches the yield point, the material begins to deform plastically. The yield point is the point where nonlinear (elastic and plastic) deformation begins. The steel tether could start to yield when the buoyancy force increases or the downward force decreases. The tube can loose weight by erosion, temporary replacements, shortage of ballasting, or when the tube deforms due to waves. The yield strength of steel and the cross-sectional area determine the strength of the tether. The vertical forces acting on the tether are the self-weight and other permanent forces, the buoyancy force, and the variable loads (traffic load and lift force). For this study, not all tethers need to be investigated separately because equal properties are assumed.

Slackening of the tether

Due to marine accumulation, extra ballasting, or leakage, slackening can occur. Loosening of the anchorages can also occur due to waves, and often lasts for one to two seconds during each wave run. Slack means that there is no tension in the cable anymore, and the stiffness is zero. As a result of slackening, snap forces occur, which can lead to structural failure of the system. The most dominant structural parameters influencing the yield-slack transition are the BWR, the tether angle and the submergence depth. [35]

Foundation failure
Predicting the capacity of the foundation under uplift loading is important for the design of a foundation. Soil investigations at large depth can be challenging and can have a large scatter. Strength and stiffness deviations to the design assumptions can cause unexpected settlements. Furthermore, liquefaction can occur.

Tethers can be anchored to the seabed with caissons. However, if the caisson is placed on the bottom of the sea, the soil below it might fail due to the weight. On the other hand, the caisson needs to be heavier than the moving rocks on the seabed to stay at its place. To prevent horizontal sliding of a gravity-based foundation, the maximum horizontal platform force should not exceed the shear capacity of the foundation. For a tension pile, as well as for a gravity-base foundation, an important soil property is the undrained shear strength. [37]

4.3.2. Tube failure
The tube can fail in longitudinal direction because of exposure to large forces, resulting in large moments. Concrete cannot sustain tension, so the cross-section should remain in compression.
The tube can also fail in transverse direction. This could occur due to compression (Figure 4.9) or due to shear force (Figure 4.10). These mechanisms will be explained in more detail in the next section.
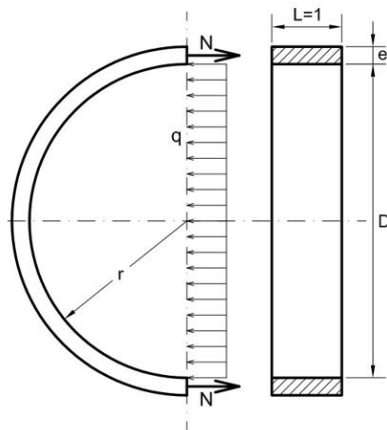
Figure 4.9: Compressive force due to hydrostatic pressure   Figure 4.10: Shear force due to force in tethers
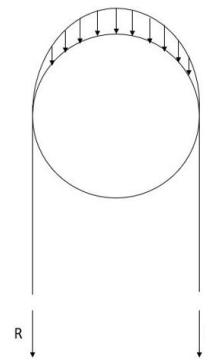
Exceedance of capacity
This can be divided into failure in longitudinal direction and failure in transverse direction. In the transverse direction, the tube is exposed to an all-round hydrostatic pressure and to a point load due to the attachment points of the tethers. The tube can fail due to compression or shear. The compression criterion will not be governing. This is explained in Appendix C. For the shear force (point load due to tethers), calculations need to be performed. If the shear force cannot be taken by the concrete, shear reinforcement is necessary. In the longitudinal direction, the tube can deform due to tidal differences (rising tide, falling tide, rotary tide) or excitation due to waves or currents. Furthermore, sea level rise and extreme water levels can cause larger hydrostatic loads on the cross-section, which increases cross-sectional forces and moments. When the deformation is too large, this leads to a loss of stability, which will lead to failure in longitudinal direction.

Leakage
A pinhole in a steel weld or a construction imperfection of a concrete seal cannot always be encountered, since the outside surface area of the tube has a significant size. There are three potential leakage routes for water to enter the tunnel: through the concrete in the roof, wall or floor (1), through the expansion joints (2) or through the closure joints or final joints (3). Leakage through a joint is called local damage. The impact of this damage depends on the size of the crack opening, status of the joints and the pumping system capacity. In the research of Baravalle and Köhler [3], the reversible concrete tube

water tightness was studied for a cross-section of an SFT. Temperature variation, water level variation and shrinkage and creep in concrete were not taken into account. The reinforcement was centered at a certain distance from the center of the cross-section as simplification.

Leakage results in an increase in downward forces, which decreases the buoyancy-weight ratio and leads to sinking of the tube. The all-round pressure of the tube does not function favorable anymore, since there is also water inside the tube.

4.3.3. Fatigue and corrosion

Fatigue and corrosion have to be taken into account for both tether and tube. Dynamic load on the tethers will have a fatigue effect. Tidal action is a change of current twice a day, which will be an fatigue load during the lifetime. Extreme fatigue will cause failure of the subsystem. Depending on the subsystem this might cause progressive collapse of the tethers, or it could only cause local damage which can be repaired in time. The horizontal forcing causes a change in stress in the tethers, which should be checked with the amount of load cycles according to the Wohler diagram.
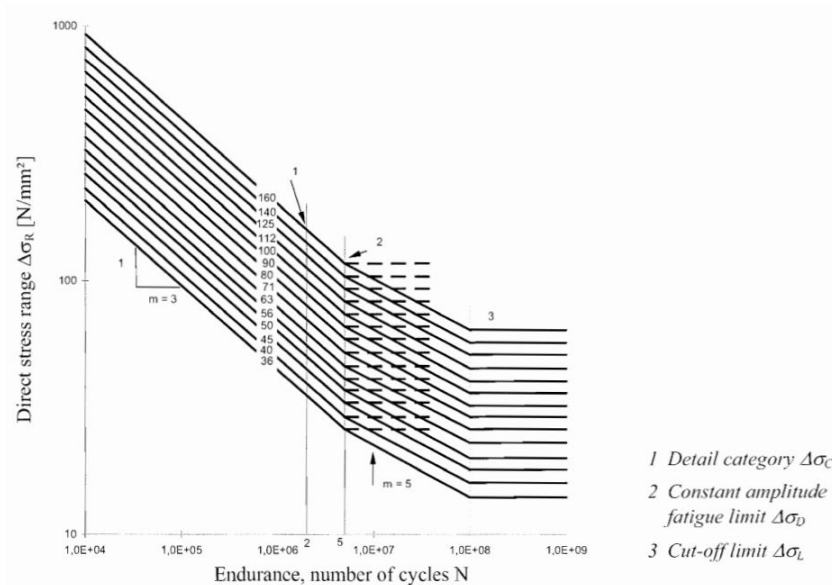
Figure 4.11: Fatigue diagram of Eurocode EN1993 [16]

When the increment in stress is less than the limit stress in the diagram, the amount of cycles can be infinite. This was checked for the impact of the current loading on the tube. For a current velocity of 1.5 m/s, this resulted in a stress increment of $\Delta\sigma_R = 1.2 \cdot 10^{-2} N/mm^2$. This value lies below the fatigue limit, which can be seen in Figure 4.11.

Although the tethers are attached far below sea level where the concentration of oxygen needed for the corrosion process is low, the tethers will corrode slowly. In Norway, the SFT will be placed in a marine corrosive environment, so the materials of tube and anchor will corrode more easily. Reduction of the tether cross-section will influence the stiffness and strength of the tether. Ultimately, the tether might fail and break. Because all tethers are situated in the same environment, the corrosion process for each tether will be similar. Besides, for the tube of the SFT, corrosion can occur both on the inside and outside due to leakage.

4.3.4. Conclusion

In the previous chapter, different failure mechanisms where explained. From these mechanisms, the following four cases are chosen to investigate in depth:

- Failure of the tethers

    - Yielding
    - Slackening

- Failure of the tube

    - Failure of the tube in longitudinal direction
    - Shear failure of the tube in transverse direction

These four mechanisms are chosen, because they are expected to have the largest influence on the system. Within the scope and planning of this study, it has been assumed that the additional failure mechanisms of corrosion, fatigue, geotechnical failure and accidental failure are not governing due to their complexity and expected research time needed. For geotechnical failure extensive research into the geolocation should be performed.

Compression in transverse direction was first assumed to be an important failure mechanism as well. However, it is proven that the compressive stress is small compared to the concrete resistance. The proof of this can be found in Appendix C.

4.4. Input parameters

In Chapter 3.2 permanent loads and variable loads were described. The loads can be displayed in time, according to Figure 4.12. The APT-distribution is the instantaneous distribution. The max-distribution is the extreme value distribution. [25]
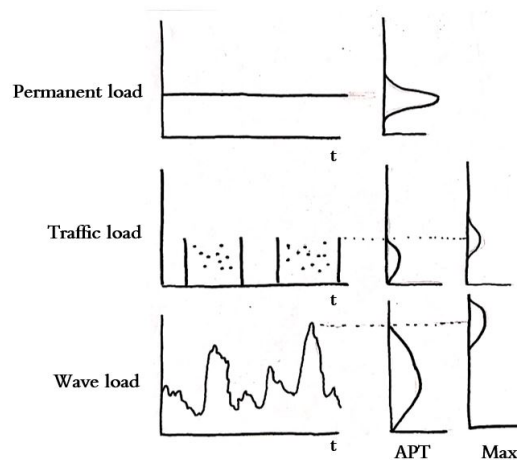
Figure 4.12: Time dependency of loading types

In this section, the distributions of the materials and loads will be further explained. Permanent loads can be divided into loading by steel, concrete, water and other materials in or around the tube. Variable loads are traffic load and current load.

4.4.1. Steel

For the steel tethers of steel quality S235, the distribution for the yield strength can be seen in Figure 4.13.
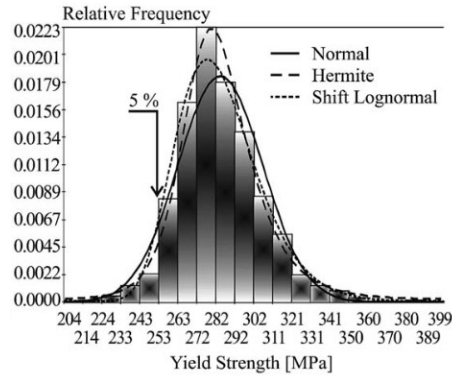
Figure 4.13: Statistic characteristics of yield strength of S235 steel [31]

A mean value of 284 N/mm^2 can be assumed, with a coefficient of variation of 0.07. [24] This gives a standard deviation of about 20 N/mm^2. The prestressing steel reinforcement in the concrete tube will be of class Y1860, which means a yield strength of 1860 MPa. The initial presstressing, which can be used for the calculation of the longitudinal capacity, can be taken around 1050 N/mm^2. The distribution of the yield strength of steel will be taken as lognormal distribution.

4.4.2. Concrete

The following formulas hold for the concrete compressive strength:

$$f_{cd} = \frac{\alpha_{cc} \cdot f_{ck}}{\gamma_c f} \tag{4.2}$$

$$f_{cm} = f_{ck} + 8 \tag{4.3}$$

where: f_{cd} = the design value of the compressive strength [N/mm^2]
f_{ck} = the characteristic value of the compressive strength [N/mm^2]
f_{cm} = the mean value of the compressive strength [N/mm^2]
α_{cc} = the coefficient taking account of long term and unfavorable effects [-]
$\gamma_c f$ = the partial safety factor of concrete, which is 1.5 [-]

The partial safety factor γ_{cf} is 1.1 for the mean strength and 1.5 for the characteristic strength of the concrete. The compressive strength of concrete B55 (C45/55) is $f_{ck} = 45N/mm^2$. Thus, the mean value of the compressive strength is 53 N/mm^2. The design value depends on α_{cc}, which is 1.0 for new structures, which gives a value of $f_{cd} = 30N/mm^2$.

The unit weight of concrete varies between 22 kN/m^3 and 25 kN/m^3. The average weight of reinforcement steel is 7850 kg/m^3. The standard deviation depends on the ratio between concrete and reinforcement.

The shear capacity of concrete depends on the type of cross-section and on the reinforcement layout. The following formulas can be found in Eurocode 2 [15]:

$$V_{Rd,c} = C_{Rd,c} \cdot k \cdot (100 \cdot \rho_l \cdot f_{ck})^{\frac{1}{3}} \cdot b \cdot d + 0.15 \cdot \sigma_{cp} \cdot b_w \cdot d \tag{4.4}$$

$$\sigma_{cp} = \frac{N_{Ed}}{A_c} \qquad\qquad k = 1 + \sqrt{\frac{200}{d}} \tag{4.5}$$

where: $V_{Rd,c}$ = the design value of the shear resistance $[N]$
$C_{rd,c}$ = a nationally determined parameter = $0.18/\gamma_c$ $[-]$
k = a form factor, nationally determined $[-]$
ρ_l = the reinforcement ratio $[-]$
f_{ck} = the characteristic compressive strength of concrete $[N/mm^2]$
b_w = the smallest width of the cross-section in the tensile area $[mm]$
d = the effective depth of the cross-section $[mm]$
σ_{cp} = the stress due to axial force in the cross-section $[N/mm^2]$

The tube will be assumed fully prestressed, without shear reinforcement. All shear will be taken by the concrete. The value for $V_{Rd,c}$ has an uncertainty of about 20 %, because this is an empirical formula with several uncertain coefficients. This is included in the model uncertainty. More of this can be found in Chapter 5.5.1.

4.4.3. Water
The buoyancy and the hydrostatic pressure depend on the density of the water. The density is influenced by salinity of the water and by temperature. At the mouth of a river or stream, the tide causes mixing of salt- and freshwater and thus affects the salinity. Near the fjords, tide does not have a large influence. The mean value should be around 10.035 kN/m^2, and the standard deviation can be taken as 0.4 kN/m^2. A normal distribution can be used.

4.4.4. Other permanent loads
The tube dimensions are important for the self-weight, but also for the buoyancy force. The diameter and thickness of the tube has a standard deviation of about 2.5 %. There will be a deviation in the mean values of the dimensions, due to placement and manufacturing errors.

Ballast, asphalt, equipment and structural elements also influence the self-weight. Different ballast materials are used, with the following densities: rock (aggregate); 20 kN/m^3, olivine; 24 kN/m^3, iron ore; 38 kN/m^3. Solid ballast as well as water ballast needs to be taken into account. For asphalt, equipment and structural elements, a coefficient of variation of 0.1 can be applied. [24]

Marine growth can also play a role. For the marine growth, a deviation of 20 % can be taken into account, because this load is very uncertain.

4.4.5. Variable loads
Wave-current load
For the Bjørnafjorden, the current velocity for a 100 year return period was stated as 0.54 m/s. Measured current velocities usually range from 0.01 to 0.20 m/s. However, in the Strait of Gibraltar and in the Equatorial Atlantic, near-bottom currents with maximum velocities of up to 3 m/s were recorded [40]. Current velocity can thus have a large spread. Furthermore, for the Bjørnafjorden, the particle velocity due to waves was found as 0.036 m/s. According to measurements, a wind speed of about 100 km/h results in a wind wave with an average height of 14 m and a period of 14 s, and wave length of 200 m. At a depth of -30 m, which will be the depth of the SFT, this wind speed would result in a maximum particle velocity of 1.7 m/s [20]. For this research, a combined wave-current velocity will be taken into account with a standard deviation of 10 %. In Figure 4.14, the probability density for a 1-year and 50-year distribution of wave-current load is shown. The formula for the load can be defined as follows:

$$F_{wave-current} = \frac{1}{2} \cdot \frac{\gamma_w}{g} \cdot C_D \cdot u_c^2 \cdot D \cdot L + \frac{1}{2} \cdot \frac{\gamma_w}{g} \cdot C_L \cdot u_c^2 \cdot D \cdot L \tag{4.6}$$

where: $F_{wave-current}$ = the load due to waves and current $[kN]$
u_c = the combined flow velocity for waves and current $[m/s]$
γ_w = the unit weight of water $[kN/m^3]$

Traffic load

The deviation of traffic load is large, because a traffic jam with fully loaded trucks results in a large loading compared to an empty tunnel. A deviation of 15 % is taken into account for this load. In Figure 4.15, the probability density for a 1-year and 50-year distribution of traffic load can be seen.
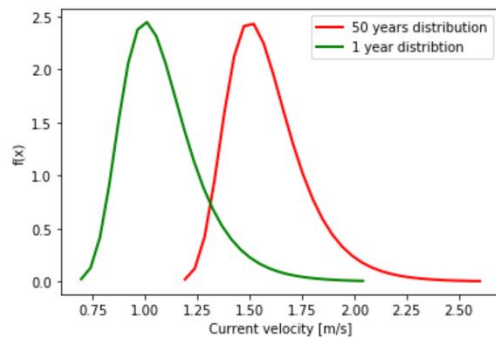
Figure 4.14: The probability density functions for the 1-year and 50-year distribution of wave-current velocity u_c
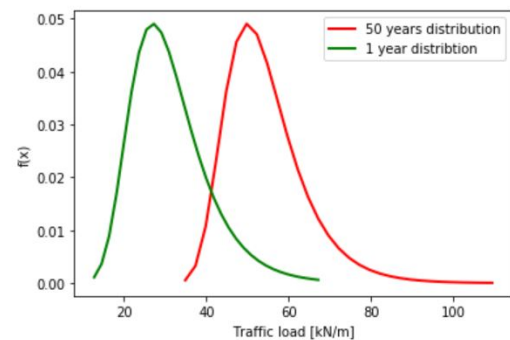
Figure 4.15: The probability density functions for the 1-year and 50-year distribution of traffic load q_t

4.5. Summary

The first main research question was answered in Chapter 4.2.5. It was concluded that a target reliability of 3.8 should be applied to the SFT, for consistency with Eurocode. Based on this chapter, sub questions $2a$, $2b$ and $2c$ can be answered as well.

2a. Which properties should be taken into account to determine the target reliability?

In order to determine a suitable target reliability, the length effect, dependency, lifetime, individual risk and group risk have to be assessed.

2b. How does failure of one component relate to system failure?

In the fault trees of Chapter 4.2.1, components were described. These components add up to form a system with probabilities of failure. When the mechanisms would be fully dependent, the probability of the system would be equal to the probability of one component. In this case, the system has a lower reliability than a component, because failures are independent. Between mechanisms, OR-gates are placed. When one element fails, this would lead to system failure.

2c. Which failure mechanisms should be considered to assess the reliability?

The mechanisms from Chapter 4.3.4 should be taken into account. These mechanisms are yielding, slackening, failure of the tube in longitudinal direction and shear failure of the tube in transverse direction. It has been assumed within the scope and planning of this study that the additional failure mechanisms of corrosion, fatigue, geotechnical failure and accidental failure are not governing, due to their complexity and expected research time needed. For geotechnical failure extensive research into the geolocation should be performed.

5

Full probabilistic design

The goal of this chapter is to develop a simplified parametric design of an SFT that satisfies a β-value of 3.8 for the individual failure mechanisms. In this way, the design points according to FORM and Eurocode are comparable, because Eurocode is based on a β-value of 3.8 as well.

A standard SFT element will be defined in section 5.1. Subsequently, all relevant failure mechanisms will be discussed. The limit state functions will be formulated, and a FORM calculation and MC simulation will be performed with Prob2B and Python. When the FORM analysis and MC simulation give approximately the same output for the same mechanism, the FORM analysis can be used for the α-values and the design points. The following steps are performed with Python and Prob2B:

Python, PyRe module	Prob2B
• Define variables • Define limit state function Z • Define distribution types • Execute FORM analysis • Get the failure probability and β-value • Get α-vales and design points • Execute MC simulation • Get the failure probability and β-value • Compare output with Prob2B • Draw a 3D probability density plot of the resistance and the load	• Define variables and distribution types • Define limit state function Z • Execute FORM analysis • Get the failure probability and β-value • Get α-vales and design points • Execute MC simulation • Get the failure probability and β-value • Compare output with Python module

Table 5.1: Program structure diagram for Python and Prob2B

The Python module and Prob2B will give approximately the same α-values and design points. They have been used simultaneously in order to validate the output.

5.1. Element description

For this calculation, one span of 150 m length is taken as starting point. This element has a diameter of 15 m and a thickness of 0.85 m. This element is attached to the bottom of the sea with four tethers on each end: two straight tethers and two inclined tethers. All four tethers are made of the same steel grade, S235. In total, a tube of 5400 m will consist of 36 elements and 140 steel tethers. The tube of the SFT is assumed to be monolite, and will be post-tensioned. The parameters for this element are summarized in Table 5.2. Their mean value, standard deviation and coefficient of variation are given. These parameters will be applied to all of the limit states functions.
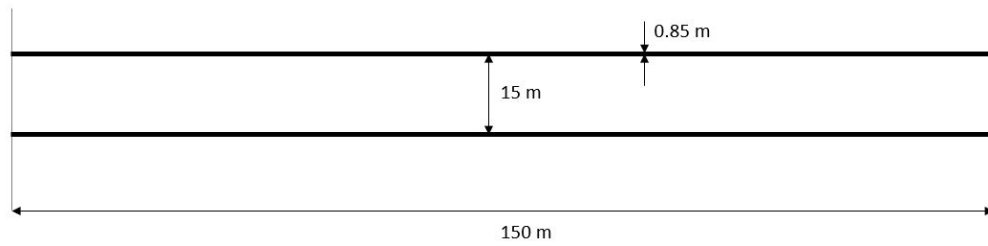
Figure 5.1: Side view of one element of the SFT

Parameter	Distr. [1]	Mean	St.dev.	CV	Source
Cross-section tether (A_t) [m^2]	NORM	0.67	0.017	0.025	Case study [35]
Yield strength S235 (f_y) [N/mm^2]	LOG	285	20	0.07	Melcher et al. [31]
Diameter of the tube (D) [m]	NORM	15.0	0.375	0.025	Case study [35]
Thickness of the tube (t) [m]	NORM	0.85	0.021	0.025	Case study [35]
Length of the tube (L_{tube}) [m]	DET	150	-	-	Case study [35]
Gravitational acceleration (g) [m/s^2]	DET	9.81	-	-	Expert knowledge
Unit weight of concrete (γ_c) [kN/m^3]	NORM	24.5	1.7	0.07	Eurocode 2 [15]
Unit weight of water (γ_w) [kN/m^3]	NORM	10.035	0.4	0.04	Case study [35]
Drag coefficient (C_D) [-]	LOG	0.7	0.2	0.3	Probabilistic Model Code [24]
Lift coefficient (C_L) [-]	LOG	0.1	0.02	0.2	Probabilistic Model Code [24]
Wave-current velocity for 50 years (u_c) [m/s]	GUM	1.5	0.15	0.1	Case study [35]
Structural weight of asphalt ($q_{asphalt}$) [kN/m]	NORM	28	2.8	0.1	Case study [35]
Weight of permanent equipment ($q_{equipment}$) [kN/m]	NORM	10	1	0.1	Case study [35]
Weight of average solid ballast ($q_{ballast}$) [kN/m]	NORM	100	10	0.1	Case study [35]
Traffic load for 50 years ($q_{traffic}$) [kN/m]	GUM	50	7.5	0.15	Eurocode 1991-2 [14]
Marine load (q_{marine}) [kN/m]	NORM	10	2	0.2	Case study [35]
Area of strands (A_{strand}) [mm^2]	DET	150	-	-	Tensa BV [7]
Initial strength of prestressing Y1860 (f_s) [N/mm^2]	LOG	1300	90	0.07	Melcher et al. [31]
Concrete compressive strength C45/55 (f_c) [N/mm^2]	LOG	53	8	0.15	Eurocode 2 [15]
Model uncertainty for shear capacity θ_1 [-]	LOG	1	0.2	0.2	Expert judgement [15]
Model uncertainty for resistance θ_R [-]	LOG	1	0.05	0.05	Probabilistic Model Code [24]
Model uncertainty for load effects θ_S [-]	LOG	1	0.05	0.05	Probabilistic Model Code [24]
Model uncertainty for the capacity of the cross-section $\theta_{\sigma R}$ [-]	LOG	1	0.05	0.05	Probabilistic Model Code [24]
Model uncertainty for stresses in the cross-section $\theta_{\sigma S}$ [-]	LOG	1	0.05	0.05	Probabilistic Model Code [24]

Table 5.2: Input parameters for reliability analysis

---

[1]NORM= Normal distribution, LOG= Lognormal distribution, GUM= Gumbel distribution, DET= Deterministic value

5.2. Failure mechanism "Yielding of the tethers"

5.2.1. Limit State Function

The tube is attached to the bottom of the sea with four tethers per mooring. The tethers should always be under tension, otherwise the tube is unstable. However, the tension forces should not be too large, because that would cause the tethers to yield. Due to horizontal actions, e.g. wave force, tethers can yield on one side of the tube while they slack on the other side. Due to upward forcing, e.g. buoyancy force or lift force, all tethers have the possibility to yield. These mechanisms could be seen in Figure 4.7. In this analysis, all four tethers will be considered as equally loaded and equally prone to yield. The forces are described as forces in the plane of the tether.

The tension force in the tether is maintained my multiple forces described in Chapter 3.2. Resistance against yielding depends on the material of the tethers (the cross-section of the tethers, $A_{tethers}$, and yield strength of steel, f_y), as well as on the permanent downward acting forces (the self-weight of the tube, the weight of asphalt, ballast, equipment and marine load). Upward forces act as unfavorable loading, and increase the tension force in the tether. This is caused by buoyancy force (F_B), lift force and drag force ($F_{wave-current}$). Both the models for resistance and load contain uncertainty, because the used mathematical models are not a full representation of reality. This is included in model factors for uncertainty (θ_R and θ_S).

When considering a period of 50 years, traffic load should be taken into account because there will certainly be traffic in that period. However, the governing situation for yielding is when the variable downward load ($F_{traffic}$) is zero. For this reason, the traffic load is not included in the limit state function. The resulting reliability is thus an underestimation of the real reliability. The limit state for yielding can be expressed as follows:

$$Z = \theta_R \cdot F_{resistance,steel} - \theta_S \cdot (F_{buoyancy} + F_{wave-current} - F_{concrete} -$$
$$F_{ballast} - F_{asphalt} - F_{equipment} - F_{marine}) \quad (5.1)$$

Subsequently, the elaborated version of the limit state function can be presented as:

$$Z = \theta_R \cdot f_y \cdot 10^3 \cdot A_t \cdot n_{tethers} - \theta_S \cdot \left(\frac{1}{4} \cdot \pi \cdot D^2 \cdot \gamma_w \cdot L + \frac{1}{2} \cdot \frac{\gamma_w}{g} \cdot C_L \cdot u_c^2 \cdot D \cdot L + \right.$$
$$\frac{1}{2} \cdot \frac{\gamma_w}{g} \cdot C_D \cdot u_c^2 \cdot D \cdot L - \left(\frac{1}{4} \cdot \pi \cdot D^2 - \frac{1}{4} \cdot \pi \cdot (D - 2 \cdot t)^2 \right) \cdot \gamma_c \cdot L \cdot 1.1 -$$
$$\left. q_{ballast} \cdot L - q_{asphalt} \cdot L - q_{equipment} \cdot L - q_{marine} \cdot L \right) \quad (5.2)$$

5.2.2. Reliability

According to Python and Prob2B, the β-value for these parameters is 3.8 for a period of 50 years. This failure mechanism is almost only based on permanent loads (buoyancy force and self-weight), which have large volumes. The influence of the variable lift force and drag force is very small compared to the self-weight. Because traffic load is not taken into account, the β-value is an underestimation of the real β-value. Wave-current force is the only forcing in this equation which is time dependent. The 50-year maximum distribution of this loading type is taken into account.

The joint probability density function can be drawn for the main variables, the resistance (R) and the strength (S), to investigate the values with the largest probability to occur and to find the failure point. The R and S consist of different parameters, as stated in the limit state function. The area under this failure line is equal to the failure probability. In Figure 5.2, the area in front of the $Z = 0$ line should be considered. In this area, the load is larger than the resistance, which means failure.
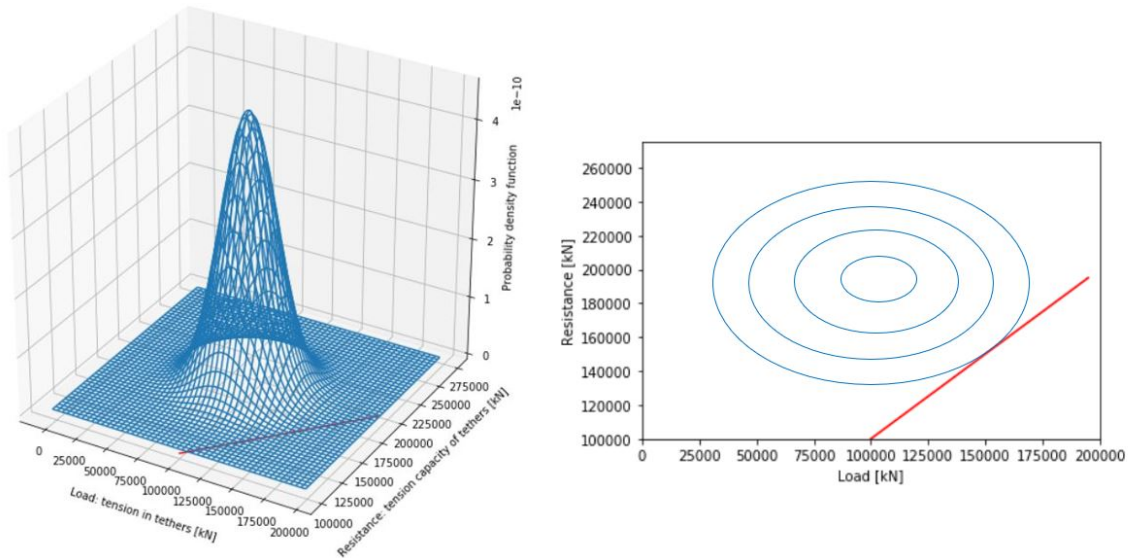
Figure 5.2: Joint probability density functions (left) and 2D plot (right), with failure line in red

In a 2D plot, the failure point is the point where the line $Z = 0$ and the contour plot intersect. From this, the design points and α-values can be read. This theory can be found in Appendix B.

Dominant parameters of this failure mechanism are the yield strength of steel, the density of water and the density of concrete. This followed from the α-values from the FORM-analysis, which can be found in Chapter 5.6. The α-values of the water density and concrete density can be plotted next to the wave-current velocity, to compare the influence of both variables. The α-values of the wave-current velocity are negligible compared to the these other loads. Even when a COV of 0.5 for the wave-current velocity is reached, the α-value does not come near the α-value of the concrete and water density.
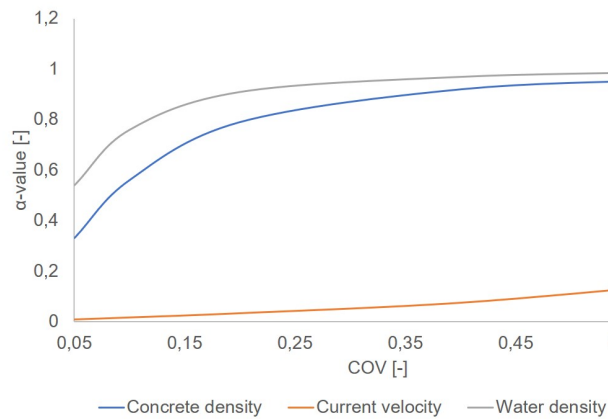
Figure 5.3: The α-values plotted against the COV

5.3. Failure mechanism "Slackening of the tethers"

5.3.1. Limit State Function

In order to prevent slack, an equilibrium should be maintained between upward and downward forces. The tether should never be exposed to a compressive force, because this will cause the tethers to "hang" and the tube to sink. This will take place when the destabilizing forces are larger than the stabilizing forces, i.e. the downward forces are larger than the upward forces. For this criterion, EN1990 gives the following formula for static equilibrium [13]:

$$E_{d,dst} \leq E_{d,stb} \tag{5.3}$$

where: $E_{d,dst}$ = the destabilizing load [kN]
$E_{d,stb}$ = the stabilizing load [kN]

In the governing situation for slackening, lift force acts as a downward force. The accompanying drag force has no vertical component, so this force is not included in the formulation. Both the models for resisting forces and load contain uncertainty, because the used mathematical models are not a full representation of reality. This is included in model factors for uncertainty (θ_R and θ_S).

$$Z = \theta_R \cdot F_{buoyancy} + \theta_S \cdot \left(-F_{wave-current} - F_{concrete} - \right.$$

$$\left. F_{ballast} - F_{asphalt} - F_{equipment} - F_{traffic} - F_{marine} \right) \tag{5.4}$$

This formula can be elaborated into:

$$Z = \theta_R \cdot \frac{1}{4} \cdot \pi \cdot D^2 \cdot \gamma_w \cdot L + \theta_S \cdot \left(-\frac{1}{2} \cdot \frac{\gamma_w}{g} \cdot C_L \cdot u_c^2 \cdot D \cdot L - \left(\frac{1}{4} \cdot \pi \cdot D^2 - \frac{1}{4} \cdot \pi \cdot (D - 2 \cdot t)^2 \right) \cdot \gamma_c \cdot L \cdot 1.1 \right.$$

$$\left. - q_{ballast} \cdot L - q_{asphalt} \cdot L - q_{equipment} \cdot L - q_{traffic} \cdot L - q_{marine} \cdot L \right) \tag{5.5}$$

5.3.2. Reliability

Both wave-current load and traffic load are time dependent loads, which means that the Turkstra rule had to be applied. For one load the extreme value is taken, and this is combined with the instantaneous value of the other load [25]. The instantaneous value has a lower mean value than the extreme value, but the standard deviation remains the same.

Combination	u_c	q_t
Combination 1	$1.5 \, m/s$	$27 \, kN/m$
Combination 2	$1 \, m/s$	$50 \, kN/m$

Table 5.3: Combinations of input values for time dependent loads, wave-current and traffic, respectively

For both combinations, the output of Python and Prob2B resulted in a β-value of approximately 3.8 for a period of 50 years. The β-value for combination 1 was slightly higher. In Figure 5.4, the joint probability density function is drawn for the resistance (R) and the load effect (S).
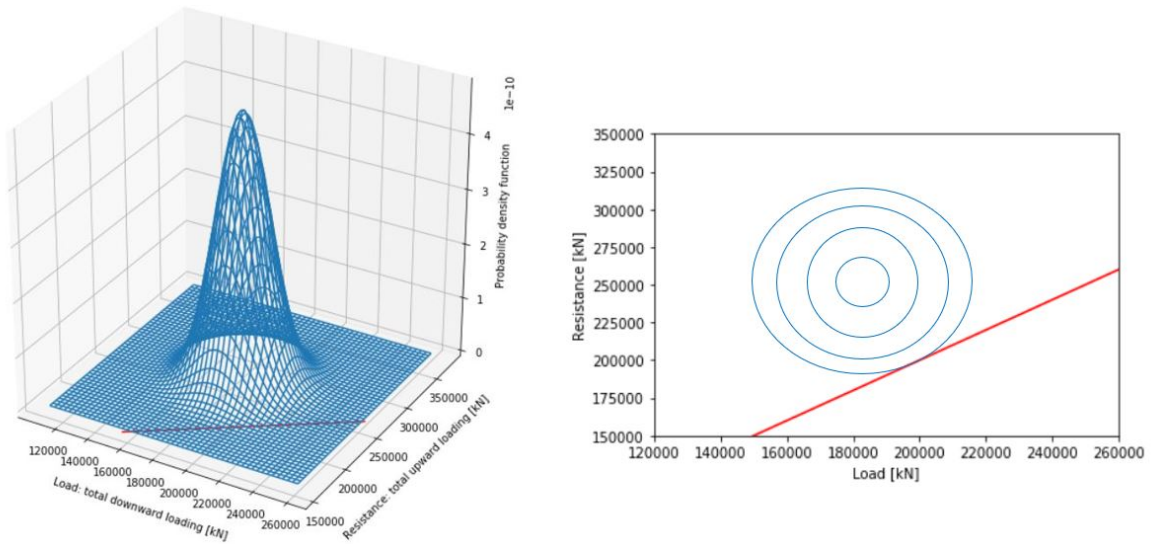
Figure 5.4: Joint probability density functions (left) and 2D plot (right), with failure line in red

When the thickness increases and the diameter remains 15 m, the buoyancy force does not change. A larger thickness makes the structure more susceptible to tether slack. This can be seen in Figure 5.5. On the other hand, when the outer diameter is increased without changing the thickness, the buoyancy force increases more than the self-weight, which makes the structure less susceptible to tether slack. This can be seen in Figure 5.6.
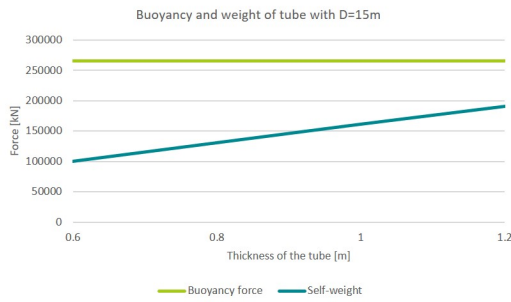
Figure 5.5: Buoyancy and weight for differing tube thickness
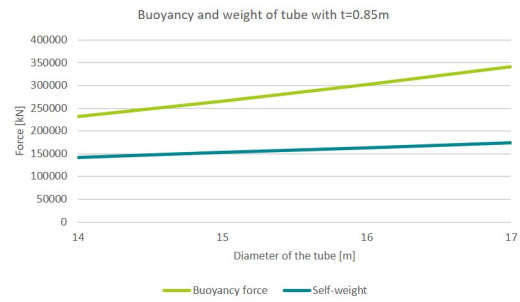
Figure 5.6: Buoyancy and weight for differing tube diameter

The dominating parameters of this failure mechanism are the the density of water and the density of concrete. This followed from the α-values from the FORM-analysis, which can be found in Chapter 5.6. The α-values of the wave-current velocity and traffic load are negligible compared to the concrete- and water density. The same holds as for yielding, which could be seen in Figure 5.20.

5.4. Failure mechanism "Longitudinal failure of the tube"

5.4.1. Beam model

The concrete tube can be modelled as a beam on supports. Concrete can consist partly of prestressing steel and partly of normal reinforcement. When the cross-section is partly prestressed, cracks are allowed to a certain extend. For this concrete beam, full prestressing is assumed, which means that there is no tension allowed in the cross-section, and crack widths will not be calculated.
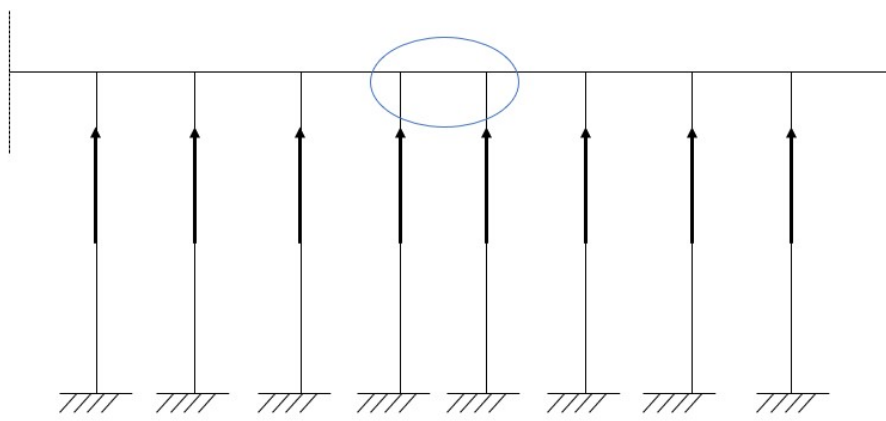
Figure 5.7: Simple model of submerged floating tunnel with tethers, side-view

A section in between tethers can be modelled as a fully clamped beam subjected to a distributed load according to the structural schedule of Figure 5.8. The maximum bending moment in longitudinal direction can be found at the supports, where the tethers are attached to the tube.
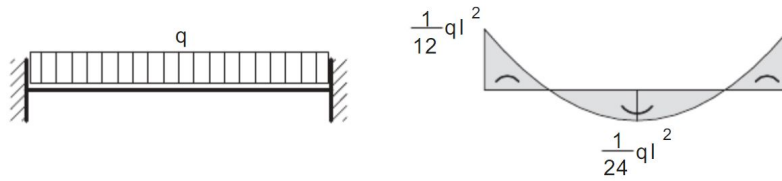
Figure 5.8: Moment diagram of a clamped beam with a distributed load [58]

$$M_{max,extern} = \frac{1}{12} \cdot q_{total} \cdot L^2 \qquad (5.6)$$

where: M_{Ed} = the applied bending moment $[kNm]$
       q = the total distributed force $[kN/m^2]$
       L = the length of the tube element $[m]$

From Chapter 5.2.1, the distributed force (q_{total}) could be written as:

$$q_{total} = \frac{1}{4} \cdot \pi \cdot D^2 \cdot \gamma_w \cdot L + \frac{1}{2} \cdot \frac{\gamma_w}{g} \cdot C_L \cdot u_c^2 \cdot D \cdot L +$$

$$\frac{1}{2} \cdot \frac{\gamma_w}{g} \cdot C_D \cdot u_c^2 \cdot D \cdot L - \left(\frac{1}{4} \cdot \pi \cdot D^2 - \frac{1}{4} \cdot \pi \cdot (D - 2 \cdot t)^2 \right) \cdot \gamma_c \cdot L \cdot 1.1 -$$

$$q_{ballast} \cdot L - q_{asphalt} \cdot L - q_{equipment} \cdot L - q_{marine} \cdot L \qquad (5.7)$$

Furthermore, the normal force in the prestressing steel has to be calculated. This depends on the area of the steel and the properties of Y1860S7 steel. The amount and the area of the strands is taken from

a technical report of Tensacciai [7]. The eccentric prestessing cables cause an internal moment, which also needs to be taken into account.

$$N_p = f_s \cdot A_p \cdot 10^3 \tag{5.8}$$

$$A_p = n_{tendons} \cdot n_{strands} \cdot A_{strand} \tag{5.9}$$

where: N_p = the normal force in the steel due to prestressing $[kN]$
            f_s = the average tension in the prestressing $[MPa]$
            A_p = the area of prestressing $[mm^2]$
            $n_{tendons}$ = the amount of tendons in the cross-section: $60(centric), 20(eccentric)$ [-]
            $n_{strands}$ = the amount of strands in the cross-section: 37 [-]
            A_{strand} = the area of one strand: $150mm^2$

The cross-section of the tube can be seen in Figure 5.9. Normal reinforcement is displayed as green dots and eccentric reinforcement as red dots.
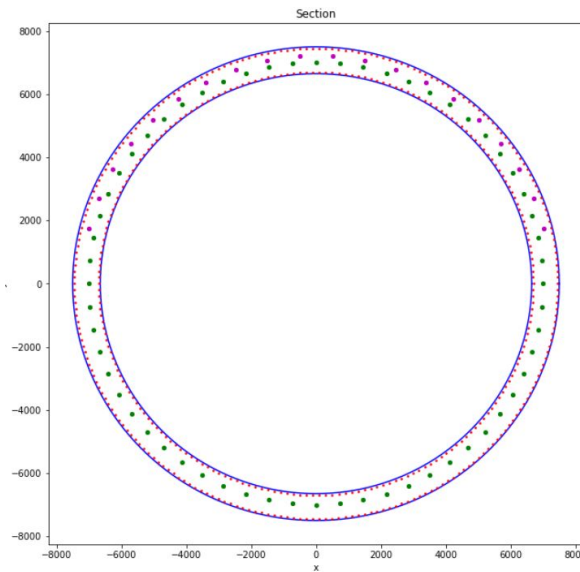
Figure 5.9: Cross-section of concrete tube with reinforcement

Besides prestressing, normal force is also imposed by hydrostatic pressure. This depends on the density of water, the depth of the tube below water level and on its dimensions. The following formula follows:

$$N_{extern} = \gamma_w \cdot d \cdot A \tag{5.10}$$

where: N_{extern} = the normal force due to hydrostatic pressure $[kN]$
            γ_w = The unit weight of water $[kN/m^3]$
            d = the depth of the center of the tube $[m]$
            A = the submerged area of the tube $[m]$

The center of the tunnel is assumed to be at a depth of 40 m below the water surface.

5.4.2. Limit State Function

The point along the cross-section with the largest bending moment needs to be further investigated. For this point, two cases need to be investigated:

- The elastic moment with zero tension in cross-section [lower limit]

- The plastic moment capacity [upper limit]

For an elastic stress state, all stress distributions are considered to be linear. In Figure 5.11, the stress distribution at the attachment point of the tethers is shown.
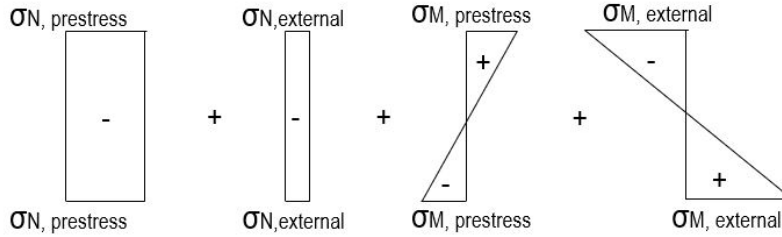
Figure 5.10: Linear stress distributions of the four components

The stress at the bottom of the cross-section can be calculated according to the formula below.

$$\sigma_{c,total} = -\frac{N_{extern}}{A_c} - \frac{N_p}{A_c} - \frac{N_p \cdot e}{W} + \frac{M_{extern}}{W} \tag{5.11}$$

$$W = \frac{\pi \cdot (D^4 - d^4)}{32 \cdot D} \tag{5.12}$$

where: $\sigma_{c,total}$ = the total stress in the cross section $[kN/m^2]$
M_{extern} = the applied bending moment $[kNm]$
N_{extern} = the normal force due to hydrostatic pressure $[kN]$
W = the section modulus $[m^3]$
N_p = the normal force due to prestressing $[kN]$
A_c = the concrete area of the tube $[m^2]$
e = the assumed eccentricity of the post-tensioning = $\frac{1}{3} \cdot D$ $[m]$
D = the outer diameter $[m]$
d = the inner diameter $[m]$

It is assumed that the resulting compressive stress in the concrete cross-section is within the acceptable limit. The cross-section should not be subjected to tensile stresses, so Equation 5.13 should be satisfied. This limit state will result in the lower limit for the β-value. Both the models for resistance and load contain uncertainty, because the used mathematical models are not a full representation of reality. This is included in model factors for uncertainty ($\theta_{\sigma R}$ and $\theta_{\sigma S}$).

$$Z = \theta_{\sigma R} \cdot \left(\frac{N_p}{A_c} + \frac{N_p \cdot e}{W} \right) - \theta_{\sigma S} \cdot \left(\frac{N_{extern}}{A_c} + \frac{M_{extern}}{W} \right) \tag{5.13}$$

In reality, a larger external moment can be applied to the cross-section before it fails in terms of cracking and transmitting the load. The cross-section does not have to be fully in compression when evaluated purely for the ULS of cross sectional failure. A part can be in tension. The structure will definitely fail when the moment exceeds the plastic moment capacity. In this case, the stress distribution is not linear, so Figure 5.11 is not valid anymore. For the maximum plastic moment capacity, it can be assumed that 1/3 of the cross-section is yielding with an inner arm of 0.8 times the diameter. [15]

$$M_{plastic,max} = \frac{1}{3} \cdot A \cdot f_{yd} \cdot 0.8 \cdot D \tag{5.14}$$

The plastic moment at this point is:
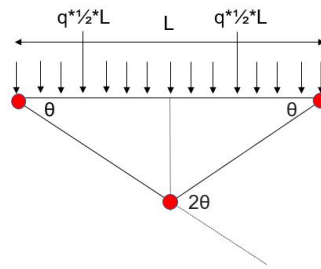
Figure 5.11: Element with three plastic hinges

$$M_{plastic} \cdot \theta + M_{plastic} \cdot 2\theta + M_{plastic} \cdot \theta = 2 \cdot \left(q \cdot \frac{1}{2} \cdot L \cdot \frac{1}{4} \cdot L \cdot \theta \right) \tag{5.15}$$

This results in:

$$M_{plastic} = \frac{1}{16} \cdot q_{total} \cdot L^2 \tag{5.16}$$

The following limit state will cause the upper limit:

$$Z = M_{plastic,max} - M_{plastic} \tag{5.17}$$

5.4.3. Reliability
For the elastic calculation, with no tension in the cross-section, the β-value resulted in 3.8 for a period of 50 years. For the second limit state, for the plastic moment capacity with the same structural parameters and the same loads, the β-value resulted in 6.7. This means that there is space for optimization if you would allow tension in the cross-section. The joint probability density function is drawn for the first limit state, and the $Z = 0$ line is illustrated. For a β-value of 6.7, the $Z = 0$ line would cover a much smaller surface or even be not visible.
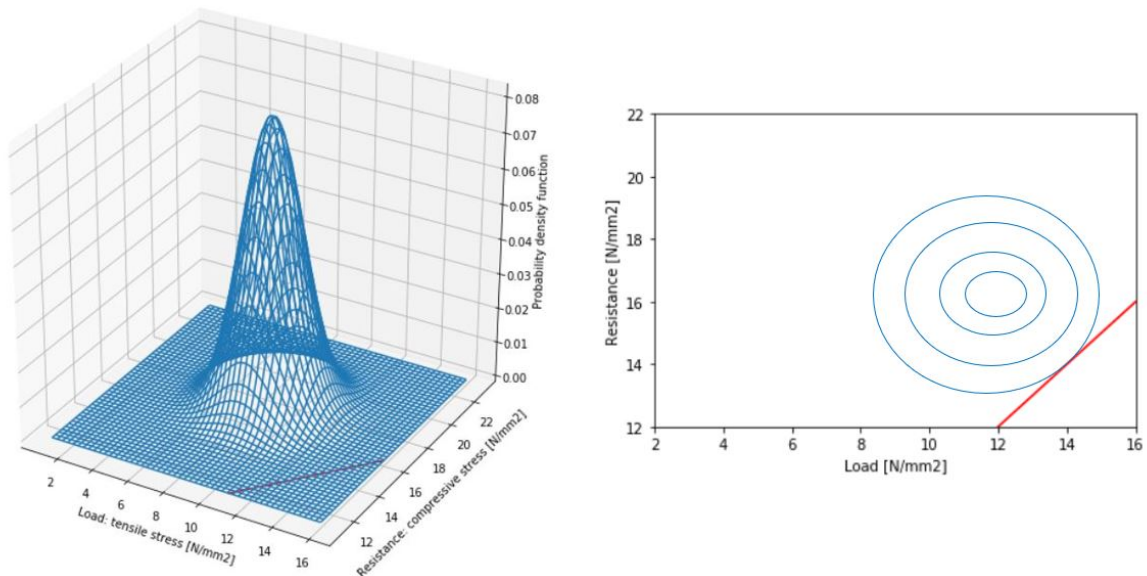
Figure 5.12: Joint probability density functions (left) and 2D plot (right), with failure line in red

The dominating parameters of this failure mechanism are the prestressing of the steel, the density of water and the density of concrete. This followed from the α-values from the FORM-analysis, which can be found in Chapter 5.6. The α-values of the wave-current velocity are negligible compared to the concrete- and water density. The same holds as for yielding, which can be seen in Figure 5.20.

5.5. Failure mechanism "Shear failure of the tube"

5.5.1. Ring model

The tension force in the vertical tethers acts over top half of the perimeter of the tube, which introduces a compressive force on the tube. This is displayed in Figure 5.13. Due to a horizontal forcing, the inclined tethers will also be activated. When a wave-current forcing is imposed, the tether on the side of the incoming wave or current is subjected to extra tension, and the tether on the opposite side is subjected to more compression. Thus, the occurrence of a wave or current makes the tethers downstream prone to slack. However, because of a low horizontal forcing compared to vertical forcing, the situation with vertical forcing on the tube is discussed only.
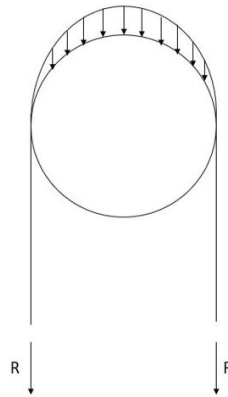
Figure 5.13: Forces in ring due to vertical tether tension force

Subsequently, the tube can be modelled as a beam on two supports, subjected to a distributed load.
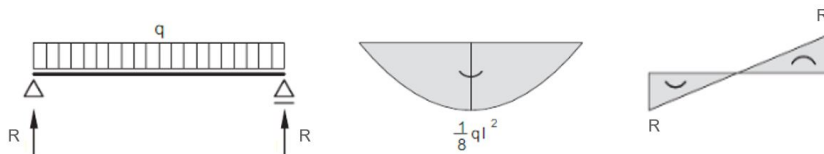
Figure 5.14: Moment- and shear force-diagram of a simply supported beam with a distributed load [58]

The shear force is largest closest to the point of application of the tethers. From the equilibrium situation, $2 \cdot R = q \cdot L$ needs to be valid. From this, the following formula follows for the maximum shear force:

$$V_{Ed} = \frac{1}{2} \cdot q_{total} \cdot L \tag{5.18}$$

5.5.2. Limit state function
In Eurocode 2, formulas for the verification of shear resistance can be found [15]. In case there is no shear reinforcement, all load will be taken by the concrete. The formula can be rewritten in order to get mean values:

$$V_{Rm,c} = C_{Rm,c} \cdot k \cdot (100 \cdot \rho_l \cdot f_{cm})^{\frac{1}{3}} \cdot b \cdot d + 0.15 \cdot \sigma_{cp} \cdot b \cdot d \qquad (5.19)$$

where: $V_{Rm,c}$ = the mean value of the resistance [N]

k = a form factor [-]: $1 + \sqrt{\frac{200}{d}} \leq 2.0$

ρ_l = the reinforcement ratio [-]: $A_{sl}/(b_w \cdot d) \leq 0.02$

A_{sl} = the area of the tensile reinforcement [mm^2]

σ_{cp} = the stress in the concrete: $N_{Ed}/A_c < 0.2 f_{cd}$ [N/mm^2]

N_{Ed} = the axial force in the cross-section due to loading or prestressing [N]

A_c = the area of the concrete cross-section [mm^2]

b_w = the smallest width in the tensile area [mm]

d = the effective depth of the cross-section [mm]

The axial force is computed in the same way as for the longitudinal failure mechanism, in order to calculate the stress in the concrete.

$$N_{Ed} = f_s \cdot A_p \qquad (5.20)$$

The recommended value for the factor $C_{Rd,c}$ is $\frac{0.18}{\gamma_c}$, which gives a design value of $\frac{0.8}{1.5} = 0.12$. The mean value can be taken as 0.15. The effective depth d of the concrete tube can be taken as the tube thickness. The width (b_w) is equal to the length of half a tube:

$$b_w = \frac{1}{2} \cdot \pi \cdot D \qquad (5.21)$$

Furthermore, the formula for the shear resistance is an empirical formula. It is based on calculations of a shear beam, to which certain factors (e.g. k and $C_{Rm,c}$) apply. The applicability to another type of structure is quite uncertain. For this reason, a 20 %-deviation is taken into account in the model uncertainty of the resistance θ_1. The following limit state can be formulated for shear failure:

$$Z = \theta_1 \cdot V_{Rm,c} - \theta_S \cdot V_{Ed} \qquad (5.22)$$

5.5.3. Reliability
This calculation resulted in a β-value of 5. This means that the probability that the tether forces cause shear failure is significantly lower ($P_f = 1 \cdot 10^{-7}$) than the probabilities of failure for the other mechanisms ($P_f = 7 \cdot 10^{-5}$). The aim was a β-value near 3.8. To reach this, the amount of reinforcement or the element length can be decreased. However, this will result in insufficient reliability for the longitudinal failure capacity. This means that the longitudinal failure is governing over the shear failure. The dominating parameters of this failure mechanism are the model uncertainty for the resistance, the initial strength of the prestressing, the density of water and the density of concrete. This followed from the α-values from the FORM-analysis, and can be found in Chapter 5.6. Finally, the failure line $Z = 0$ will not be displayed in a 2D or 3D plot, because the probability of failure is almost zero.

5.6. Conclusion
The resulting β-values from the four failure mechanisms can be found in Table 5.4. The β-value for yielding is a slight underestimation of the real β-value. This is caused by two factors: the traffic load was not taken into account (1) and the wave-current force was only taken as unfavorable loading (2). The β-value for slackening resulted in 3.8, which is also a slight underestimation, since the lift force was only taken as unfavorable loading. The β for longitudinal failure turned out to have a value between 3.8 and 6.7. The β-value of shear failure could be tuned near 3.8 by changing the intermediate distance of the tethers. However, it is better to have longitudinal failure first, since this is a ductile mechanism. Considering shear failure has a β-value of 5, the partial factors for this mechanism will not be calibrated. The general partial factors from Eurocode are calibrated on a β-value of 3.8.

Parameter	Yielding	Slackening	Longitudinal failure	Shear failure
β	3.8	3.8	3.8 - 6.7	5

Table 5.4: Summary of β-values of the failure mechanisms

All α-values that followed from the FORM-analysis can be found in Table 5.5. The most dominant parameters can be seen in bold. It has been proven that the α-value does not only depend on the coefficient of variation, but also on the absolute value of the mean of the parameter. The permanent parameters turned out to be dominant, because their relative contribution to the total load is large.

The influence of the variable loads, traffic load and wave-current load, is small. For an increase in standard deviation of the traffic load, the α-value of the traffic load does increase. However, it has to increase by an unrealistic amount to increase the α-value significantly.

The model uncertainties also have a notable α-value. This means that it would be favorable to improve the accuracy of the model. The model uncertainty influences the entire loading or resistance.

Parameter	α-values			
	Yielding	Slackening	Longitudinal failure	Shear failure
f_y	**0.42**	0	0	0
A_t	0.15	0	0	0
γ_w	**-0.46**	**0.41**	**-0.51**	-0.30
D	**-0.45**	0.27	-0.33	-0.39
C_D	0	0	0	0
C_L	0	0	0	0
u_c	0	0	0	0
t	0.13	-0.18	0.14	0
γ_c	**0.43**	**-0.50**	**0.44**	0.29
L	0	0	0	0
$q_{ballast}$	0	0	0	0
$q_{asphalt}$	0	0	0	0
$q_{equipment}$	0	0	0	0
$q_{traffic}$	0	0	0	0
q_{marine}	0	0	0	0
A_{strand}	0	0	0	0
f_s	0	0	**0.45**	0.26
f_c	0	0	0	0
θ_1	0	0	0	**0.75**
$\theta_{\sigma R}$	0	0	0.32	0
$\theta_{\sigma S}$	0	0	-0.32	0
θ_R	0.29	**0.48**	0	0
θ_S	-0.29	**-0.48**	0	-0.19
Rel. index	**3.8**	**3.8**	**3.8**	**5**

Table 5.5: The resulting α-factors from FORM analysis with dominant parameters in bold

General
Certain loading types and certain dimensions are applied to this SFT element. Conclusions were derived from this specific case, but some conclusions can also be made general. For a different case assuming similar uncertainties, in order to result in a β-value of 3.8, the ratio between self-weight and loading needs to be approximately the same. For increasing dimensions, and thus increasing self-weight, the loading will increase simultaneously. In this case, the division of α-values is expected to be the same. For the dimensions of the tube, boundaries can be set. The driving lanes need to fit in, so a minimal diameter would be around $10\ m$. Around a diameter of $20\ m$, the necessary amount of reinforcement and the amount of tethers becomes uneconomical. For the reinforcement to fit in the tube and to guarantee a certain amount of cover, a minimal tube thickness can be set. A safe domain

for the diameter and thickness can be defined by varying their parameters in the limit state functions. The rest of the parameters will still have the same mean value. According to the yielding criterion, a maximum diameter of 18 m could be applied. According to slackening, a minimum diameter of 11 m could be applied. Naturally, these limits are based on one case study, and should not be taken too strictly. However, they can serve as a basis for design.
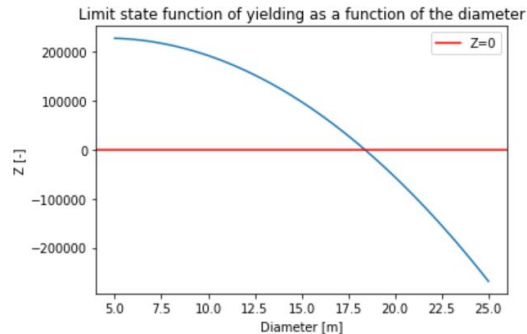
Figure 5.15: Upper limit for the diameter: D < 18 m
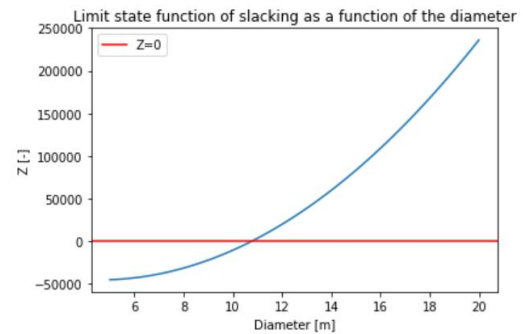
Figure 5.16: Lower limit for the diameter: D > 11 m

According to the yielding criterion, a minimal thickness of 0.3 m should be applied. However, the necessary area for reinforcement is not taken into account. This would increase the lower limit of the thickness. According to the slackening criterion, a maximum thickness of 1.35 m should be applied. Here, the same holds as for the diameter requirements: the values are based on one case study and cannot be taken too strictly.
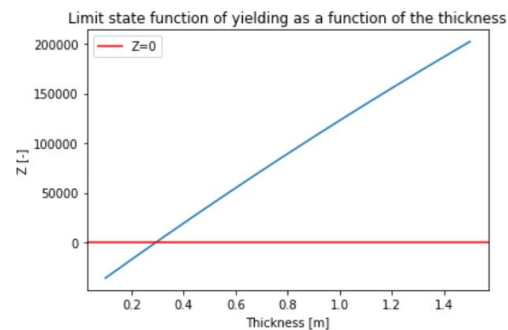
Figure 5.17: Lower limit for the thickness: t > 0.3 m
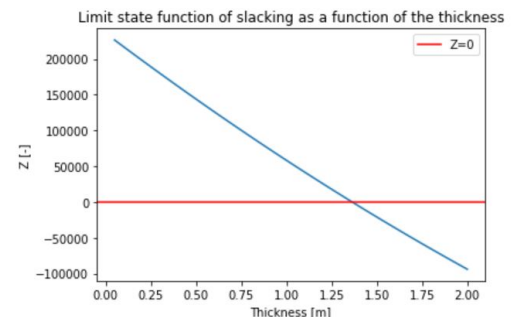
Figure 5.18: Upper limit for the thickness: t < 1.35 m

Finally, sub questions $3a$ and $3b$ about the full probabilistic design can be answered. These answers can be found below.

3a. Which parameters are dominant?
For the failure mechanism of tether yielding, the yield strength, water density and concrete density have the largest influence on the reliability. For the failure mechanism of tether slackening, the water density, concrete density and the model uncertainties have the largest α-values. For longitudinal failure, the water density, concrete density and initial prestressing are the most important parameters. For shear failure, the water density, diameter and initial prestressing are the most important. Since the β-value for shear failure is not close to 3.8, the α-values will not be used in comparison. The α-values of different parameters can be plotted for a changing coefficient of variation (COV):
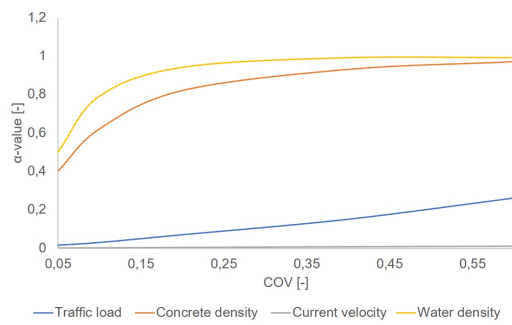
Figure 5.19: The α-values for different parameters for slackening
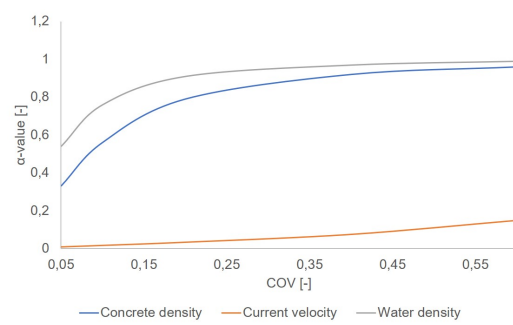
Figure 5.20: The α-values for different parameters for yielding

3b. How can the required reliability level be met?
The reliability of yielding can be increased by using a higher quality steel or by applying more tethers. For the reliability of the longitudinal failure mechanism, the resistance of the system can be increased by increasing the amount of reinforcement. However, for tether slackening, no resistance parameter can be changed without influencing another mechanism in this model. Slackening is the only mechanism of which all parameters influence another mechanism. This means that this criterion should first be checked, before adapting the resistance parameters of the other mechanisms. The reliability can be improved by decreasing the amount of ballast or changing the dimensions. A decrease in thickness or an increase in diameter causes the β-value for slackening to increase, however, this negatively affects yielding and longitudinal failure. To increase the overall reliability, the element length can be decreased. This means that less loading is subjected to the same amount of tethers. Furthermore, the reduction in length causes a reduction of the bending moment in the longitudinal direction of the tube.

<div style="text-align: right">6</div>

Derivation of partial safety factors

6.1. General

A level I method makes use of partial factors to ensure the reliability of a structure. Partial factors can be calculated numerically with a reliability analysis. A more elaborate explanation on the partial factor method can be found in Chapter 2.2.4. The reliability model will be based on the results of the Level II and III method from Chapter 5.

In this chapter, the reliability model outcomes will be compared to Eurocode. It should be kept in mind that the Eurocode factors are not calibrated to analyze SFTs. The steps for this comparison are shown in the program structure diagram of Table 6.1.

Reliability model procedure	Eurocode procedure [1]
- Find α-values through FORM-analysis - Choose parameters with α-values above 0.1 as stochasts, and the rest of the values as deterministic parameters - Find the design points of the stochasts - Find characteristic values according to Eurocode - Divide parameters in favorable load, unfavorable load and variable load - Calculate partial factor by using the design value and the characteristic value - Compare partial factor with Eurocode	- Divide parameters in favorable load, unfavorable load and variable load - Find matching partial factors according to Eurocode - Compare partial factor with reliability model

Table 6.1: Program structure diagram for reliability model and Eurocode

---

[1]Assuming applicability of the set of general factors to SFTs

In order to determine the partial factors (γ_R and γ_S) the design values and characteristic values are needed. The probabilistic distributions of the resistance and strength are shown in Figure 6.1.

$$\gamma_R = \frac{R_k}{R_d} \; ; \; \gamma_S = \frac{S_d}{S_k} \tag{6.1}$$
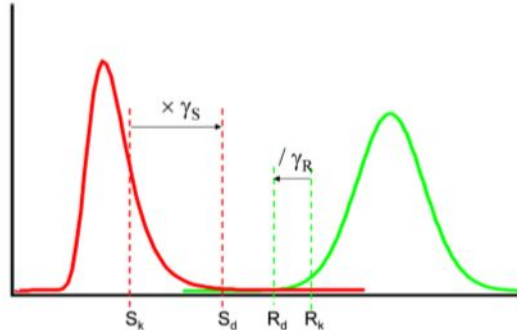
Figure 6.1: A probability density function with the load (in red) and resistance (in green) [25]

For both FORM and Eurocode, the same characteristic values are used. Table 6.2 will be used to find the characteristic value.

Variable	Distribution type	Mean	Coefficient of variation	Characteristic value
G	Normal distribution	1,00	0,10	50 %
Q_1, Q_2	Gumbel distribution	1,00	0,40	98 %
R	Lognormal distribution	1,00	0,05	5 %
X_R	Lognormal distribution	1,00	0,03	50 %

Figure 6.2: Probabilistic models for basic random variables [23]

6.1.1. FORM analysis
The design value is a direct output from the FORM-analysis of Prob2B and Python, so this can directly be used for calculating the partial factor. The failure mechanisms were all tuned to a β-value of 3.8 for a reference period of 50 years. From Chapter 5, the most important parameters followed. The parameters with a significant influence, an α-value larger than 0.1, can be found in Table 6.2.

Parameter	α -values		
	Yielding	Slackening	Longitudinal failure
f_y	0.42	0	0
γ_w	-0.46	0.41	-0.52
D	-0.45	0.27	-0.34
t	0.13	-0.18	0.14
γ_c	0.43	-0.50	0.44
f_s	0	0	0.46
θ_R	0.29	0.48	0
θ_S	-0.29	-0.48	0
$\theta_{\sigma R}$	0	0	0.32
$\theta_{\sigma S}$	0	0	-0.32

Table 6.2: The dominant parameters and α-values from FORM analysis

The two time-dependent parameters, i.e. the traffic load (q_t) and wave-current velocity (u_c), had an α-value near zero.

6.1.2. Eurocode

According to Eurocode, loading types have to be divided in favorable-, unfavorable- and variable loads. One partial factor is stated for one loading type. Furthermore, Eurocode distinguishes in types of calculations. For a strength calculation, the STR-conditions can be used. For an equilibrium calculation, the EQU-conditions can be used. These factors can also be found in Appendix A. The factors according to the STR-conditions are defined as follows:

$$\gamma_f = 1; \; \gamma_u = 1.35; \; \gamma_V = 1.5; \; \gamma_v = 1.5 \cdot 0.7 \tag{6.2}$$

The partial factors for the EQU-conditions are:

$$\gamma_f = 0.9; \gamma_u = 1.1; \gamma_V = 1.5; \gamma_v = 1.5 \cdot 0.7 \tag{6.3}$$

where: γ_f = partial factor for favorable loading [-]
γ_u = partial factor for unfavorable loading [-]
γ_V = partial factor for most important variable load [-]
γ_v = partial factor for other variable loads [-]

For the resistance, general partial factors can be found in Eurocode. For example, the partial material factor for the strength of steel (γ_{steel}) is 1.15.

In Eurocode, assumed coefficients of variation, standard α-values and β-values are used to calculate the design value. These design values lead to the partial factors from Equation 6.2. A calculation to check this principle can be found in Appendix F.

In order to be able to apply the standard α-values, which result in the general partial factors, the following equation needs to be satisfied:

$$0.16 < \frac{\sigma_S}{\sigma_R} < 7.6 \tag{6.4}$$

For all of the reliability models in the next sections, this criterion should be checked.

6.2. Failure mechanism "Yielding of the tethers"

The STR-conditions from Eurocode would apply to this mechanism. The partial factors from the STR-conditions will be compared to the calculated partial factors.

6.2.1. Analysis

From the α-values of the FORM calculation, it was found that the yield strength, water density, concrete density, diameter, thickness and model uncertainties have a significant α-value. Thus, these seven most important parameters will be used for the analysis. These parameters can be found in the following resistance or loading parts:

- Resistance/ Material strength: f_y, θ_R

$$R = \theta_R \cdot f_y \cdot 10^3 \cdot A_t \cdot n_{tethers} \tag{6.5}$$

- Favorable permanent/ Self-weight of the tube: γ_c, D, t, θ_S

$$S_1 = \theta_S \cdot \left(\left(\frac{1}{4} \cdot \pi \cdot D^2 - \frac{1}{4} \cdot \pi \cdot (D - 2 \cdot t_c)^2 \right) \cdot \gamma_c \cdot L \cdot 1.1 + q_{ballast} \cdot L + \right.$$

$$\left. q_{asphalt} \cdot L + q_{equipment} \cdot L + q_{marine} \cdot L \right) \tag{6.6}$$

- Unfavorable permanent load/ Buoyancy force γ_w, D, θ_S

$$S_2 = \theta_S \cdot \frac{1}{4} \cdot \pi \cdot D^2 \cdot \gamma_w \cdot L \tag{6.7}$$

- Variable load/ Wave-current force: γ_w, D, θ_S

$$S_3 = \theta_S \cdot \left(\frac{1}{2} \cdot \frac{\gamma_w}{g} \cdot C_L \cdot D \cdot u_c^2 \cdot L + \frac{1}{2} \cdot \frac{\gamma_w}{g} \cdot C_D \cdot D \cdot u_c^2 \cdot L \right) \tag{6.8}$$

The formulation for the limit state function can be described as follows:

$$Z = R - (-S_1 + S_2 + S_3) \tag{6.9}$$

6.2.2. Results

In order to test the effects of variables a series of model calculations is performed. Model 3 is most similar to the earlier used model that resulted in β-value of 3.8. In model 1 and 2 several parameters are given a deterministic value. They lead to a higher β-value. This makes a comparison with Eurocode invalid. For this reason, the results of Model 1 and 2 are displayed in gray. What is meant to be demonstrated is the effect on the α-values of the individual parameters.

In Model 1, only the yield strength, water density and concrete density are taken as variable parameters. The rest of the parameters are implemented as deterministic values. In Model 2, the diameter and thickness are added. In Model 3, also the model uncertainties are added. In model 1, 2 and 3A, it is assumed that D and t are fully uncorrelated. In model 3B, it is assumed that D and t are correlated. This can also be seen in Table 6.3. Furthermore, Equation 6.4 is fulfilled for for Model 3A and 3B. This makes partial factors from these models comparable to the general partial factors from Eurocode.

Model	Stochasts	Deterministic values	D and t correlated?
Model 1	f_y, γ_w, γ_c	$A_t, D, t, L, C_D, C_L, u_c, q_{as}, q_{bal}, q_t, q_m, \theta_R, \theta_S$	No
Model 2	$f_y, \gamma_w, \gamma_c, D, t$	$A_t, L, C_D, C_L, u_c, q_{as}, q_{bal}, q_t, q_m, \theta_R, \theta_S$	No
Model 3A	$f_y, \gamma_w, \gamma_c, D, t, \theta_R, \theta_S$	$A_t, L, C_D, C_L, u_c, q_{as}, q_{bal}, q_t, q_m$	No
Model 3B	$f_y, \gamma_w, \gamma_c, D, t, \theta_R, \theta_S$	$A_t, L, C_D, C_L, u_c, q_{as}, q_{bal}, q_t, q_m$	Yes

Table 6.3: Stochasts and deterministic values per model

The partial factors, according to these four models, are stated in Table 6.4.

Parameter	Eurocode STR	Factor from Model 1:	Factor from Model 2:	Factor from Model 3A:	Factor from Model 3B:
Material strength	1.15	1.14	1.04	1.07	1.11
Favorable permanent loads	1	0.85	0.9	0.98	1.0
Unfavorable permanent loads	1.35	1.1	1.21	1.23	1.22
Unfavorable variable load	1.5	1.1	1.15	1.18	1.18
β-value	3.8	4.9	4.3	3.8	3.9

Table 6.4: Comparison of partial factors from Eurocode with the models

For Model 1, unfavorable permanent load and variable load both depend on the water density. Thus, the same factors follow. All partial factors from Model 1 until 3B are lower than the partial factors from Eurocode. The factor of the diameter (D) has a quadratic influence on the buoyancy force, so this causes the increase in partial factor of unfavorable permanent load from Model 1 to Model 2. In Model 3, the material resistance does not only depend on yield strength, but also on the model uncertainty. This causes the increase of the material strength from Model 2 to Model 3 (A and B). When correlation between D and t increased, the β-value also increased (from 3.8 to 3.9). The corresponding α-values can be found in the table below.

Reliability model	α-values						
	f_y	γ_w	γ_c	D	t	θ_R	θ_S
1	0.67	-0.53	0.53	-	-	-	-
2	0.49	-0.51	0.47	-0.51	-0.14	-	-
3A	0.42	-0.47	0.44	-0.46	0.13	0.30	-0.30
3B	0.50	-0.48	0.47	-0.04	-0.34	0.32	-0.29

Table 6.5: The α-values of different models for yielding

For the correlated case, the α-values of D and t have the same sign. Thus, if the design point of the diameter is larger than 15, the design point for the thickness is larger than 0.85. The design values for these parameters can be found in the table below.

Parameter	Mean value	Characteristic value	Uncorrelated Design values	Correlated Design values
f_y $[N/mm^2]$	285	252	249	245
γ_c $[kN/m^3]$	24.5	24.5	21.7	21.3
γ_w $[kN/m^3]$	10.035	10.035	10.7	10.8
D $[m]$	15	15	15.6	15.5
t $[m]$	0.85	0.85	0.84	0.88
θ_R $[-]$	1	1	0.94	0.93
θ_S $[-]$	1	1	1.05	1.06

Table 6.6: Parameter results for correlated and uncorrelated diameter and thickness

6.3. Failure mechanism "Slackening of the tethers"

Since slackening depends on the structure's equilibrium, this criterion should first be investigated with the EQU-conditions from Eurocode.

6.3.1. Analysis

From the α-values in Table 6.2, six parameters turned out to be most important. Upward forces can be seen as resistance to slackening and downward forces can be seen as loading.

- Favorable permanent/ Buoyancy force: γ_w, D, θ_R

$$S_1 = \theta_R \cdot \frac{1}{4} \cdot \pi \cdot D^2 \cdot \gamma_w \cdot g \cdot L \tag{6.10}$$

- Unfavorable permanent load/ Self-weight of the tube: γ_c, D, t, θ_S

$$S_2 = \theta_S \cdot \left(\left(\frac{1}{4} \cdot \pi \cdot D^2 - \frac{1}{4} \cdot \pi \cdot (D - 2 \cdot t_c)^2 \right) \cdot \gamma_c \cdot L \cdot 1.1 + \right.$$
$$\left. q_{ballast} \cdot L + q_{asphalt} \cdot L + q_{equipment} \cdot L + q_{marine} \cdot L \right) \tag{6.11}$$

- Traffic load: $q_{traffic}$

$$S_3 = q_{traffic} \cdot L \tag{6.12}$$

- Other variable load/ Wave-current load: γ_w, D, θ_S

$$S_4 = \theta_S \cdot \frac{1}{2} \cdot \frac{\gamma_w}{g} \cdot C_L \cdot D \cdot u_c^2 \cdot L \tag{6.13}$$

The resistance is formed by the buoyancy force and acts as favorable loading. The load depends on multiple downward forces. This results in the following limit state function:

$$Z = S_1 - S_2 - S_3 - S_4 \tag{6.14}$$

6.3.2. Results

Model 3 is most similar to the earlier used model that resulted in β-value of 3.8. In Model 1 and 2 several parameters are given a deterministic value. They lead to a higher β-value, which makes a comparison with Eurocode invalid. For this reason, the results of Model 1 and 2 are displayed in gray.

In Model 1, only traffic load, water density and concrete density are taken as variable parameters. The FORM analysis resulted in a small α-value for traffic load. However, the factor from Eurocode for traffic load (1.35) should be examined briefly. In Model 1, 2 and 3A, it is assumed that D and t are fully uncorrelated. The traffic load is left out of Model 2, 3A and 3B, because of the low α-value. In Model 3B, it is assumed that D and t are correlated. Furthermore, Equation 6.4 is fulfilled for for Model 3A and 3B. This makes partial factors from these models comparable to the general partial factors from Eurocode.

Model	Stochasts	Deterministic values	D and t correlated?
Model 1	γ_w, γ_c, q_t	$D, t, L, C_D, C_L, u_c, q_{as}, q_{bal}, q_m, \theta_R, \theta_S$	No
Model 2	γ_w, γ_c, D, t	$L, C_D, C_L, u_c, q_{as}, q_{bal}, q_t, q_m, \theta_R, \theta_S$	No
Model 3A	$\gamma_w, \gamma_c, D, t, \theta_R, \theta_S$	$L, C_D, C_L, u_c, q_{as}, q_{bal}, q_t, q_m$	No
Model 3B	$\gamma_w, \gamma_c, D, t, \theta_R, \theta_S$	$L, C_D, C_L, u_c, q_{as}, q_{bal}, q_t, q_m$	Yes

Table 6.7: Stochasts and deterministic values per model

Parameter	Eurocode		Factor from Model 1:	Factor from Model 2:	Factor from Model 3A:	Factor from Model 3B:
	STR	EQU				
Favorable permanent loads	0.9	1	0.84	0.8	0.82	0.82
Unfavorable permanent loads	1.1	1.35	1.24	1.16	1.19	1.20
Traffic load	1.35	1.35	1.26	-	-	-
Other (unfavorable) variable load	1.05	1.5	0.84	0.84	1	1
β-value	3.8	3.8	5.6	4.9	3.8	3.8

Table 6.8: Comparison of partial factors from Eurocode with the models

For Model 1, the factors for favorable permanent load and other variable load both only depend on the water density. There is only one design point for y_W, which results in the same factor for favorable permanent load as well as other variable load. The water density turned out to be a resistance parameter (dominant in buoyancy force), and not a loading parameter. This factor of 0.84 has to be treated very carefully, because the design point can change from a resistance parameter to a loading parameter when a parameter is added. This can be seen in Model 3A and 3B.

In Table 6.9, it can be seen that the α-factor for traffic is low. This causes the other two α-values to be larger with respect to the other models. It can be seen that the partial factors come closer to unity when the model uncertainties are added.

The partial factor for the favorable permanent load and variable load are lower than Eurocode for both STR- and EQU-conditions. However, the unfavorable permanent load does not satisfy the EQU-conditions.

In the uncorrelated case, the α-values have an opposite sign, which causes the diameter to decrease in its design value and the thickness to increase. For the correlated case, the diameter and thickness both decreased. The corresponding α-values can be found in the table below.

Reliability model	α-values						
	γ_w	γ_c	q_t	D	t	θ_R	θ_S
1	0.70	-0.71	-0.08	-	-	-	-
2	0.60	-0.65	-	0.38	-0.26	-	-
3A	0.41	-0.51	-	0.27	-0.19	0.48	-0.48
3B	0.43	-0.52	-	0.11	0.08	0.56	-0.46

Table 6.9: The α-values of different models for slacking

The design values for these parameters can be found in Table 6.10.

Parameter	Mean value	Characteristic value	Uncorrelated Design values	Correlated Design values
γ_c $[kN/m^3]$	24.5	24.5	27.6	27.9
γ_w $[kN/m^3]$	10.035	10.035	9.5	9.4
D $[m]$	15	15	14.6	14.9
t $[m]$	0.85	0.85	0.86	0.848
θ_R $[-]$	1	1	0.91	0.89
θ_S $[-]$	1	1	1.09	1.09

Table 6.10: Parameter results for correlated and uncorrelated diameter and thickness

6.4. Failure mechanism "Longitudinal failure of the tube"

Longitudinal failure can be checked with the ULS design criteria. The STR-conditions of Eurocode would apply to this mechanism. The formulas for longitudinal failure have already been discussed in Chapter 5. Here, the formulas are organised and there most important variables are stated. Consequently, the resulting partial factors are presented.

6.4.1. Analysis

The loading types are divided into resistance, unfavorable-, favorable- and variable loading. The moment can be subdivided in the distributed force caused by three types of loading: the buoyancy force, the permanent downward forcing and the wave-current load.

From Table 6.2, it turned out that seven parameters have a significant influence. The rest of the parameters have been implemented as deterministic values.

- Resistance: f_s, D, $\theta_{\sigma R}$

$$R = \theta_{\sigma R} \cdot \left(\frac{f_s \cdot A_s}{A_c} + \frac{f_s \cdot A_s \cdot \frac{1}{3} \cdot D}{W} \right) \tag{6.15}$$

- Favorable permanent/ Self-weight of the tube and hydrostatic load: γ_c, γ_w, D, t, $\theta_{\sigma S}$

$$q_1 = \left((\frac{1}{4} \cdot \pi D^2 - \frac{1}{4} \cdot \pi \cdot (D - 2 \cdot t)^2) \cdot \gamma_c \cdot 1.1 \right) + q_{ballast} + q_{equipment} + q_{asphalt} + q_{marine} \tag{6.16}$$

$$S_1 = \theta_{\sigma S} \cdot \left(\frac{\frac{1}{12} \cdot q_1 \cdot L^2}{W} + \frac{\gamma_w \cdot D \cdot 40}{A_c} \right) \tag{6.17}$$

- Unfavorable permanent load/ Buoyancy force: γ_w, D, $\theta_{\sigma S}$

$$q_2 = \frac{1}{4} \cdot \pi \cdot D^2 \cdot \gamma_w \tag{6.18}$$

$$S_2 = \theta_{\sigma S} \cdot \frac{\frac{1}{12} \cdot q_2 \cdot L^2}{W} \tag{6.19}$$

- Variable load/ Wave-current force: γ_w, D, $\theta_{\sigma S}$

$$q_3 = \frac{1}{2} \cdot \frac{\gamma_w}{g} \cdot C_D \cdot D \cdot u_c^2 \tag{6.20}$$

$$S_3 = \theta_{\sigma S} \cdot \frac{\frac{1}{12} \cdot q_3 \cdot L^2}{W} \tag{6.21}$$

6.4.2. Results

Model 3 is most similar to the earlier used model that resulted in β-value of 3.8. In model 1 and 2 several parameters are given a deterministic value. They lead to a higher β-value, which makes a comparison with Eurocode invalid. For this reason, the results of Model 1 and 2 are displayed in gray.

In Model 1, 2 and 3A, it is assumed that D and t are fully uncorrelated. In Model 3B, it is assumed that they are correlated. The factors can be found in Table 6.12. When correlation between D and t increased, the β-value also increased (from 3.8 to 3.9). Furthermore, Equation 6.4 is fulfilled for for Model 3A and 3B. This makes partial factors from these models comparable to the general partial factors from Eurocode.

Model	Stochasts	Deterministic values	D and t correlated?
Model 1	f_s, γ_w, γ_c	$D, t, L, C_D, C_L, u_c, q_{as}, q_{bal}, q_m, \theta_{\sigma R}, \theta_{\sigma S}$	No
Model 2	$f_s, \gamma_w, \gamma_c, D, t$	$L, C_D, C_L, u_c, q_{as}, q_{bal}, q_t, q_m, \theta_{\sigma R}, \theta_{\sigma S}$	No
Model 3A	$f_s, \gamma_w, \gamma_c, D, t, \theta_{\sigma R}, \theta_{\sigma S}$	$L, C_D, C_L, u_c, q_{as}, q_{bal}, q_t, q_m$	No
Model 3B	$f_s, \gamma_w, \gamma_c, D, t, \theta_{\sigma R}, \theta_{\sigma S}$	$L, C_D, C_L, u_c, q_{as}, q_{bal}, q_t, q_m$	Yes

Table 6.11: Stochasts and deterministic values per model

Parameter	Eurocode STR	Factor from Model 1:	Factor from Model 2:	Factor from Model 3A:	Factor from Model 3B:
Resistance	1.15	1.08	1.04	1.08	1.11
Favorable permanent loads	1	0.86	0.90	0.86	0.87
Unfavorable permanent loads	1.35	1.09	1.08	1	1
Unfavorable variable load	1.5	1.09	1.12	1.04	1.03
β-value	3.8	4.3	4.0	3.8	3.9

Table 6.12: Comparison of partial factors from Eurocode with the models

All factors from the reliability model are lower than the factors from Eurocode, which means that if Eurocode would be used for this problem, it will be on the conservative side.
The α-values are stated in Table 6.13.

Reliability model	α-values						
	γ_w	γ_c	f_s	D	t	$\theta_{\sigma R}$	$\theta_{\sigma S}$
1	-0.55	0.55	0.63	-	-	-	-
2	-0.53	0.50	0.58	-0.35	0.14	-	-
3A	-0.50	0.48	0.44	-0.33	0.13	0.32	-0.32
3B	-0.51	0.50	0.50	-0.33	-0.20	0.34	-0.30

Table 6.13: The α-values of different models for longitudinal failure

The design values for these parameters can be found in Table 6.14. For the correlated case, the design points for the initial prestressing and the diameter are lower than the uncorrelated case. This increases the partial factor of the resistance from Model 3A to Model 3B.

Parameter	Mean value	Characteristic value	Uncorrelated Design values	Correlated Design values
$\gamma_c \ [kN/m^3]$	24.5	24.5	21.7	21.5
$\gamma_w \ [kN/m^3]$	10.035	10.035	10.7	10.8
$f_s \ [N/mm^2]$	1300	1152	1164	1141
$D \ [m]$	15	15	15.4	15.3
$t \ [m]$	0.85	0.85	0.84	0.87
$\theta_{\sigma R} \ [-]$	1	1	0.95	0.94
$\theta_{\sigma S} \ [-]$	1	1	1.05	1.05

Table 6.14: Parameter results for correlated and uncorrelated diameter and thickness

6.5. Conclusion

The sensitivity factors (α) for all parameters are presented in Table 6.15. These differ from the values stated in Table 6.2, because the total amount of variables was decreased. Only the most important parameters are taken into account in this analysis, and the other variables were implemented as deterministic values. The diameter and thickness have two possible α-values due to the correlated and uncorrelated case. For the correlated case, the α-values of D and t have the same sign. Moreover, when the case changes from uncorrelated to correlated, the sign of D does not change and the sign of t does change. This indicates that the diameter is dominant over the thickness, and that they serve as loading parameters for yielding and as resistance parameters for slacking. The α-value of D decreases significantly for the correlated case. The α-values of the other parameters increase slightly when changing from the correlated to uncorrelated case, however this is not presented in the table.

Parameter	α-values		
	Yielding	Slackening	Longitudinal failure
f_y [N/mm^2]	0.50	-	-
γ_w [kN/m^3]	-0.48	0.43	-0.52
γ_c [kN/m^3]	0.47	-0.52	0.52
f_s [N/mm^2]	-	-	0.55
D [m]	-0.46, -0.04	0.27, 0.11	-0.35, -0.11
t [m]	0.13, -0.34	-0.19, 0.08	0.14, -0.21
θ_R [-]	0.32	0.48	-
θ_S [-]	-0.29	-0.48	-
$\theta_{\sigma R}$ [-]	-	-	0.32
$\theta_{\sigma S}$ [-]	-	-	-0.32

Table 6.15: The α-values from FORM analysis

Most α-values are smaller than either 0.8 (dominant resistance parameter) and -0.7 (dominant loading parameter) or 0.28 (other resistance parameters) and -0.32 (other loading parameters). This means that the α-value multiplied with β-value results in a smaller distance between the design point and the mean value than Eurocode, which consequently leads to a smaller partial factor. This difference is proven in Appendix F. In a FORM analysis, no distinction is made upfront between dominant and non-dominant parameters. Furthermore, when more parameters are added, the lower the α-values become, because the sum of the α-values squared still needs to add up to one. In this analysis, the α-values converged to a certain value when more parameters were added. Thus, the partial factors converged as well. These converged factors can be seen in Table 6.16.

Parameter	Eurocode		Yielding	Slackening	Longitudinal failure
	STR	EQU			
Resistance	1.15	-	1.07	-	1.08
Unfavorable permanent load	1.35	1.1	1.23	1.19	1
Favorable permanent load	1	0.9	0.98	0.82	0.86
Unfavorable variable load	1.5	1.05	1.18	1	1.04

Table 6.16: Summary of the resulting partial factors from the models

3c. How can partial factors for resistance and loading be derived?
The partial factors for resistance and loading can be derived according to the procedure in Chapter 4.1. A flowchart is displayed to clarify the method. The condition of Equation 6.4 needs to be satisfied, and a β-value of 3.8 for the individual failure mechanisms should be met. First, the limit states and its parameters are defined. Consequently, the design points will be determined with the reliability analysis. Finally, this design point and the characteristic value are used to calculate the partial factor. A factor can be calculated for the resistance parameters as well as for the loading parameters. This method is executed in this chapter.

3d. What can be gained from the full probabilistic calibration of the partial factors?
Almost all general values from Eurocode are conservative over the values from the reliability analysis. Based on this analysis, the general partial factors for variable loading can be decreased with at least 20 %. Since the influence of variable loads on the structure is small, the adaptation of this factor will not result in significant changes in the design. Thus, the economic advantage is small.
In contrast, a change in water density will have a large influence on the design. Thus, decreasing the factor for unfavorable permanent load will have a significant effect on the design. According to this analysis, the factor of 1.35 could be decreased with almost 10 %.
For yielding and longitudinal failure, the STR-conditions can be applied and will result in a safe structure. However, for slackening, the EQU-conditions would result in an unsafe structure. For factor for unfavorable permanent load from the reliability model resulted in 1.2. This does not satisfy the factor of 1.1 from the EQU-condition.

Consequently, main research questions 2 and 3 from Chapter 1 can be answered as well. Both answers can be found below.

2. How can a full probabilistic design of an SFT be made?
In order to create a full probabilistic design of an SFT, many factors have to be taken into account. An overview of the necessary steps is given below. Step 1 is performed in this research. Step 2, 3 and 4 are partially performed. Step 5 is the final step, and can only be performed if all input from the previous steps is available. In this research, a reliability based design is made for a β-value of 3.8. The parameters for this design can be found in Table 5.2.

1. Find the most important failure mechanisms and find a suitable target β-value per mechanism

2. Quantify mean values and standard distributions for loading types, taking into account the local circumstances

3. Take into account correlations between parameters and between mechanisms

4. Perform a FORM analysis and MC simulation

5. Find the reliability of the system and compare this to an overall target β-value. If needed, adjust the system, or change the target β-values of the individual mechanisms.

3. How can a full probabilistic calibration of partial factors be performed?
First, a full probabilistic design has to be created. The method for this design was discussed in the section above. For the calibration of partial factors, a FORM analysis and MC simulation should be performed. The dominant parameters can be implemented as variables, and non-dominant parameters can be implemented as deterministic values. This results in design values for these different variables. The variables are assigned to a specific loading type. Consequently, a partial factor can be calculated for this loading type.
This research showed that general partial factors, recommended in the Eurocode EN 1990, can not be used for an accurate and economic design of an SFT. Although they may be safe when applied for STR cases, for EQU cases they can be unsafe. A semi-probabilistic calibration of partial factors, according to a full probabilistic design, will result in factors for a safe design. Thus, these calculated factors are directly applicable.

7

Robustness analysis

7.1. Introduction

In Chapter 5 and Chapter 6, the individual failure mechanisms were designed for a β-value of 3.8. For yielding and longitudinal failure, the area of the tethers and the amount of reinforcement in the concrete tube were tuned to reach this β of 3.8. For slackening, there was no material resistance involved. For this mechanism, the buoyancy force acts as resistance. This force could be increased by increasing the outer dimensions of the tube. However, this also negatively influences the other two mechanisms. Thus, the reliability of the SFT can be improved by making adaptations on the resistance side.

Robustness is the ability of a structure to withstand adverse and unforeseen events (like fire, explosion, impact) or consequences of human errors without being damaged to an extent disproportionate to the original cause [23]. The requirements for robustness aim at avoiding local damage developing to total collapse. Exposure to hazards can result in failure of events, and these events can then lead to other failures. In a robust system such cascading failures are prevented.

In order to check the system's robustness, a few scenarios could be considered. The following questions were asked:

- What influence does the spatial variability of waves have?

- What influence does failure of one tether and multiple tethers have?

- How is the structure able to prevent failure due to leakage?

7.2. Spatial variability of waves

Spatial variability of waves is important to consider. If the spatial variability is large, the probability of a high local wave load could also be large. This increases the total probability of failure of the system. However, it was investigated that loading on long structures shows a considerable reduction if wave directionality is taken into account instead of calculating with uniform long waves. [49]

In the case study, the mean value of the wave-current velocity was taken as 1.5 m/s. This parameter was implemented as a 50-year Gumbel distribution, which means that extreme values are taken into account. A wave has a vertical and horizontal component, which respectively causes a lift force and drag force on the tube. In the vertical plane, the governing situation would be when the maximum wave and current cause a large lift force. This could lead to yielding of the tether. The other way around, it could also cause slackening. Furthermore, an increase in wave force could cause a larger moment, which could lead to longitudinal failure.

In the longitudinal direction, the wave force can differ over the length. Battjes [5] concluded that due to the directional spreading and randomness of the waves, structures will never be fully loaded with the maximum wave force when they increase in size. Long structures experience a smaller total load at any point on time, than a less long, but further identical structure. An SFT element of 150 m can be calculated on a wave force of 100 %, however, an element of 5000 m can be calculated on a lower percentage of the wave force over the total length. This can be seen in Figure 7.1. In Chapter 6, one element of 150 m was calculated. This means that for the entire system, based on this theory, the reliability will be higher.
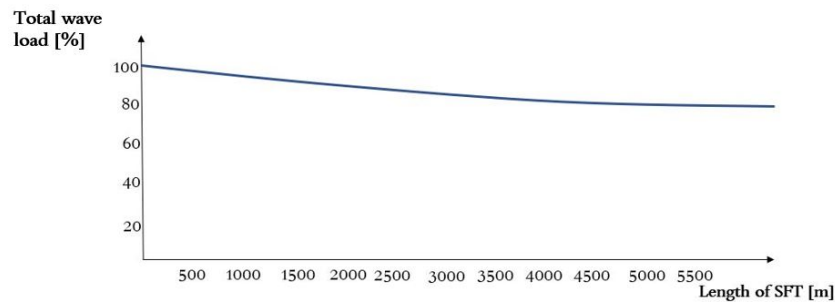
Figure 7.1: Length effect for wave load on SFT structure

The wave amplitude and length have their own distributions, which cause the distribution of the wave velocity (Chapter 3.2.4). The reliability can be recalculated with a larger spread of the wave velocity (u_c), in order to take into account different circumstances. Yielding, slackening and longitudinal failure should be considered. The spread could even be increased from 0.15 m/s to 1 m/s, without a noticeable decrease in β-value. An increase in mean-value from 1.5 m/s to 2 m/s gives a decrease in probability of failure (β-value from 3.8 to 3.7).

Considerations
The application of the research of Battjes [5] to an SFT should be investigated more thoroughly. When a structure can be calculated with less loading, the structure can be constructed more economically. Furthermore, it is important to look at the dominant direction of the waves or current. The shape of the tunnel should be adjusted to the situation. In this research, a straight shape was assumed. However, the tube can also be constructed in a C-shape or S-shape. This shape should be tuned to the geolocation and wave conditions. When the dominant wave direction is to the east side, the curve of the tunnel should be positioned in the opposite direction. This effect of the wave force on a curved tunnel can be compared to an arch bridge. The force perpendicular or parallel to the structure causes a normal force in the tube or arch respectively. The structure should be calculated for asymmetrical loading as well. Furthermore, the impact of the load can be decreased by creating a support structure. For example, barriers can be installed to decrease wave impact. This increases the total resistance as well. Lastly, the change of the direction of waves or currents can cause varying lateral displacements along the length. This could cause a violation of the traffic requirements. Thus, these motions should also be investigated.

7.3. Tether failure

In Chapter 5, all four tethers were simultaneously investigated for yielding. In this section, the tethers are investigated on element-level. Robustness is needed to avoid sequential damage of tethers after failure of one tether. The system should be able to redirect the loads.

The SFT is supported by four tethers every 150 m. If one of the tethers at one location fails, there are still three other tethers to take up the load. If all four tethers fail, the length which has to be supported by the remaining tethers doubles. This is schematised in Figure 7.2.
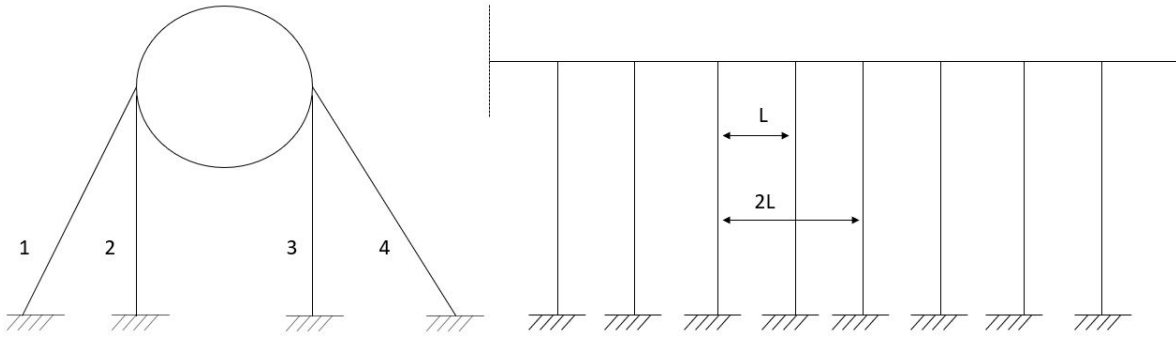
Figure 7.2: The front view (left) and side view (right) of the SFT

We now consider the front view on the left of Figure 7.2. When one tether fails due to yielding or due to external forcing or accidental loading, this does not have to lead to failure of the entire system. This has to be assessed, by making separate limit state functions for the four tethers. When a tether fails, the same load has to be carried by less tethers. The limit state for all four tethers together can be found in Chapter 5.2.1. The resistance (R) and the strength (S) can be written as:

$$R = \theta_R \cdot f_y \cdot A_{tether} \tag{7.1}$$

$$S = \frac{1}{4} \cdot \left(\frac{1}{4} \cdot \pi \cdot D^2 \cdot \rho_w \cdot g \cdot L + \frac{1}{2} \cdot \rho_w \cdot C_L \cdot u_c^2 \cdot D \cdot L + \frac{1}{2} \cdot \rho_w \cdot C_D \cdot u_c^2 \cdot D \cdot L - \right.$$
$$\left. \left(\frac{1}{4} \cdot \pi \cdot D^2 - \frac{1}{4} \cdot \pi \cdot (D - 2 \cdot t)^2 \right) \cdot \rho_c \cdot g \cdot L \cdot 1.1 - q_b \cdot L - q_{as} \cdot L - q_{eq} \cdot L - q_m \cdot L \right) \tag{7.2}$$

where: D = the diameter of the tube [m]
t = the thickness of the tube [m]
ρ_w = the density of water [kg/m^3]
ρ_c = the density of concrete [kg/m^3]
g = the gravitational acceleration [m/s^2]
L = the length of the tube [m]
C_L = the lift coefficient [-]
C_D = the drag coefficient [-]
u_c = the wave and current velocity [m/s]
q_b = the distributed force due to ballast [kN/m^2]
q_{as} = the distributed force due to asphalt [kN/m^2]
q_{eq} = the distributed force due to equipment [kN/m^2]
q_m = the distributed force due to marine load [kN/m^2]

Which gives the following equations for the four tethers separately:

$$Z_1 = R - S \; ; \; Z_2 = R - \frac{4}{3} \cdot S \; ; \; Z_3 = R - \frac{4}{2} \cdot S \; ; \; Z_4 = R - 4 \cdot S \tag{7.3}$$

Z_1 describes a situation where one tether fails. Z_2 describes the situation when one tether has already failed. Z_3 when two have already failed. Z_4 when three have failed. In the case that all four tethers are still in place, one tether carries $\frac{1}{4}$ of the load. When one tether fails, the other three tethers will carry $\frac{1}{3}$ of the load, etc. The probability of failure for one tether, according to Z_1, gives:

$$P_{f,Z_1} = P(\textit{1st tether fails}) = 6.98 \cdot 10^{-5} \tag{7.4}$$

For the second tether, when the first tether has already failed, the conditional probability can be written as:

$$P_{f,Z_{1,2}} = P(\textit{2nd tether fails | 1st tether fails}) = 1.48 \cdot 10^{-2} \tag{7.5}$$

This results in the following probability of failure of two tethers:

$$P_{f,Z_2} = P(\textit{2nd tether fails | 1st tether fails}) \cdot P_{f,Z_1} = 6.98 \cdot 10^{-5} \cdot 1.48 \cdot 10^{-2} = 1 \cdot 10^{-6} \quad (7.6)$$

For the third tether, when the first and second tether have already failed, the conditional probability can be written as:

$$P_{f,Z_{1,2,3}} = P(\textit{3rd tether fails | 1st and 2nd tether fail}) = 4.5 \cdot 10^{-1} \quad (7.7)$$

Consequently, this results in the following probability of failure of three tethers:

$$P_{f,Z_3} = P(\textit{3rd tether fails | 1st and 2nd tether fail}) \cdot P_{f,Z_{1,2}} \cdot P_{f,Z_1} = 4.5 \cdot 10^{-7} \quad (7.8)$$

For the fourth tether, when there is only one tether left that will carry the entire load, the failure probability resulted in 0.99. This means that if the third tether fails, the last tether will also fail. The total probability that four tethers fail is the same as the probability that three tethers fail. In Figure 7.3, the possible failures of the tethers can be seen in a so called "Venn diagram". The probabilities of failure are stated in the diagram.
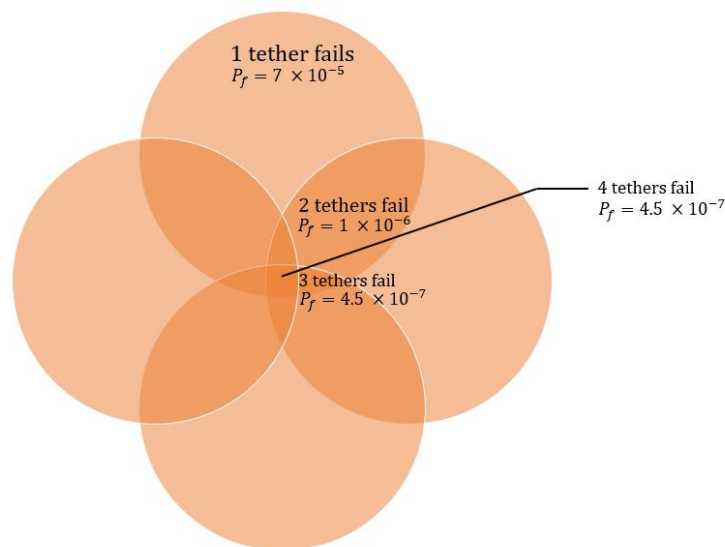
Figure 7.3: A Venn diagram for failure of tethers

In Table 7.1, the design points of the most important parameters are presented for limit states Z_1, Z_2 and Z_3. The design points of the different parameters get closer to the mean value when more tethers fail. This means that the structure becomes more prone to failure.

Parameter [unit]	Mean	Z_1	Z_2	Z_3
D [m]	15	15.59	15.52	15.03
f_y [N/mm^2]	285	241	269	285
t [m]	0.85	0.843	0.845	0.851
γ_c [kN/m^3]	24.5	21.8	22.8	24.5
γ_w [kN/m^3]	10.035	10.7	10.4	10.06
θ_R [-]	1	0.922	0.972	1.003
θ_S [-]	1	1.048	0.972	1.001

Table 7.1: Design points for three tether limit states

In the case that all four tethers on one location fail at the same time, for example by a terrorist attack or collision, the length which has to be supported by the remaining tethers doubles. Consequently, the two other sets of four tethers that need to carry more load. The remaining moment-capacity of the tube can be investigated. The extra capacity from the plastic calculation could be used to prevent the

structural failure when the element length doubles. The criterion $\sigma < 0$, no tension in the tube, was used as lower bound for the capacity. Tension in the tube may occur up to a certain height. In Chapter 5, it was shown that the plastic moment capacity resulted in a β of 6.7. For this mechanism, an element length of 180 m would lead to a β of 3.8. Thus, for a doubled length of 300 m when all tethers fail, this would definitely lead to longitudinal failure. The structure should warn in time to prevent a full collapse. Yielding serves as a warning mechanism. It will give large displacements before structural failure will occur. Concrete cracking is a brittle mechanism. Without reinforcement this is an abrupt mechanism without warnings.

Considerations

In this section, the failure of the first tether and the conditional failures of the other tethers were investigated. To take it a step further, a MC simulation could be performed for the total amount of failures, to examine the amount of tether failures for each individual failure case. When one tether fails, the same load will immediately be carried by three tethers instead of four. This characteristic has to be implemented in the calculation. Spatial variability and dependency should also be taken into account for future research into tether failure. Tethers can be dependent on each other due to the loading, but also due to their attachment point. Furthermore, research into fast reparation of tethers should be performed. The lifetime of the tethers should be considered, as well as the influence of a large length. A tether with a length of 500 m will have a significant weight. Furthermore, the variation of horizontal loads on tethers was not taken into account in this research.

Failure of all tethers at the same time does not have to be considered when the system is redundant. More or higher quality steel tethers can be applied to reach this. Furthermore, the failure of all tethers can be compared to failure of all cables of a cable-stayed bridge. For a bridge, the design is not calculated on this type of failure.

7.4. Leakage

In this section, the occurrence and consequences of leakage will be analysed and explained. Leakage could occur through the joints or through the tunnel wall. The following actions or compartments could lead to leakage in the tube:

- Impulse loading (by external accidental load; falling anchor/sinking ship/terrorist attack, or internal load; explosion, collision of trucks..)

- Material degradation

- Joints

The tube thickness is relatively large, so there is a low probability of an impulse load to create damage. For example for a dropping anchor, the resulting force is much lower than the force in a tether due to the distributed load acting on the tube. In Chapter 6, it was proven that shear failure does not occur due to the tether force. Thus, force due to an anchor will not result in shear failure either. However, there is still a possibility that it leads to water inflow in the tube. Finally, leakage could lead to sinking of the tube. The possible measures to prevent leakage from leading to tunnel failure are:

- Installation of a pumping system

- Installation of compartment doors

- Fast reparation

The amount of water which could leak in before the tube sinks depends on the buoyancy-weight ratio (BWR). For the case study, a BWR of 1.5 was found. Thus, when the weight increases with slightly more than 50 %, the resulting force is inverted and the system will sink.

For the Bjornafjorden case, the acceptable amount of in-leaked water was 0.1 $m^3/min/km$. This is considered a conservative estimate [35]. A tunnel length of 5 kilometers will be taken into account, which means that the acceptable amount becomes 500 L/min. The washing water drainage capacity is 18 m^3/h, which gives 300 L/min. Thus, an amount of 200 L/min is able to accumulate in the tube.

The distributed force from Chapter 5.4.1 gave a resulting upward force of around 600 kN/m, so 3000 MN over the tunnel length. Consequently, the amount of water to compensate for this force can be calculated. The amount of water, in order for the tube to sink, is $300 \cdot 10^6 \, L$. When 200 L/min would accumulate, it would take more than a thousand days for the tunnel to sink due to in-leaked water through joints and walls. For a large impulse load, the amount of in-leaked water can be much larger than 500 L/min. Consequently, accumulation can go much faster. However, the volume of water needed for the tunnel to sink is still very large.

Considerations
More research into probabilities of incidental loads should be conducted. A total failure probability could be calculated and the amount of measures could be determined. Specific calculations can be executed to find the necessary length in between compartment doors, and the most suitable amount and location of the pumping systems. A double shell could also be constructed. This guarantees extra safety, but can be difficult construction-wise. Furthermore, a warning system could be installed at the tunnel entrance, which does not allow traffic in the tunnel when a certain volume of water is detected within a certain time. The practical application of a warning system should be further developed. Escape routes should also be further developed. Finally, when the tunnel is not perfectly horizontal, but has a vertical gradient, water will accumulate at one location. As a result, the structure will bend locally, and even more water will accumulate at this location. This should also be considered.

7.5. Conclusion

For an SFT, there is more variation in loading vertically than horizontally. The spatial variability of waves (horizontally) has little influence, considering the construction depth. The spread of the wave velocity can be increased without a significant change in β-value. Furthermore, the wave load on the system can be taken as a lower value than the wave load on one element. This gives a higher reliability for the system.

If one tether fails, the other three tethers have to take on the same amount of load. The β-value for the failure of one tether is 3.8. When one tether has failed, the β-value of the failure of the second tether results in 2.2. This is called a "conditional probability". The total probability of failure of two tethers is lower than the probability of failure of one tether. Thus, this will not lead to progressive failure. However, when the third tether fails, the fourth tether will also fail immediately. When all four tethers fail at the same time, the moments will increase and longitudinal failure will occur. To increase robustness, tethers could be increased in diameter or the steel quality could be improved.

On the one hand, leakage has a very low probability of occurrence. On the other hand, the impact is gigantic. If the tunnel fills up with water and sinks, this could result in many deaths. If certain measures would be implemented, the chances of leakage to occur would become infinitesimally small.

These conclusions lead to the answers of sub questions $4a$ and $4b$ and main research question 4 from Chapter 1.

4a. What influence does the spatial variability have on the system's reliability?
A larger uncertainty and less good predictability of wave heights will lead to a smaller reliability of the structure. However, for structures having a length larger than e.g. 4 or 5 times the wave length, the length effect causes the total wave-current load on the entire structure to be lower than the load on one element. When one element is calculated for 100 % of the wave-current load, this results in an underestimation for the reliability of the entire system. Furthermore, for this case study, the wave-current force turned out to be non-dominant. The tube will be placed at a depth of - 30 m, where the wave-current impact is relatively low.

4b. Which methods can be used to make the structure more robust?
To reduce the impact of waves, the geolocation and wave conditions should be taken into account. When more about these conditions is known, the alignment of the tunnel can be optimized or a support structure can be built. For tether failure, the thickness or steel quality of the tethers can be increased. More tethers can also be installed to create a redundant system. In this case, failure of all tethers does not need to be addressed anymore and longitudinal failure as a consequence of tether failure will thus not occur. The attachment point of the tether to the tube could be improved. A larger attachment area reduces the local stresses in the tube. Furthermore, the structure could be made more robust by installing compartment doors, a pumping system or an outer shell.

4. How could the structure's robustness be assessed and improved?
Defining a β-value per mechanism implies a low level of risk of progressive collapse. This requires a robust structure that is able to remain its strength and equilibrium after it is damaged locally.
Within the scope of this research, the limit state functions met the requirement of a target value of $\beta = 3.8$ per failure mechanism. Besides this requirement, other requirements were not directly formulated. When the target value needs to be increased to $\beta = 4.3$, this will lead to increased margins between characteristic and design values of loads and resistances. These methods were addressed in the previous sub question. Furthermore, the amount of ballast, amount of reinforcement, the cross-sectional dimensions and the element-length can be adjusted.

8
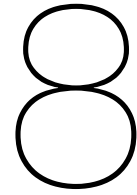
Conclusion, Discussion & Recommendations

8.1. Conclusion

This study aimed at describing the reliability of the SFT. To fulfill this aim, a suitable target reliability was selected, failure mechanisms of the SFT were described, partial safety factors for different loading types were calculated and the robustness of the structure was assessed. The following conclusions were drawn to answer the main research questions:

- The conventional reliability methods (i.e. FORM and MC) can be adopted in a reliability based design of an SFT. In this research, FORM and MC were applied to an SFT for the Bjørnafjorden-crossing. Permanent loads proved to be dominant, i.e. concrete and water density, and thus significantly influence the design of the SFT. The buoyancy force has to be large so that tension forces in the tethers are maintained. On the other hand, the tube has to be restricted in its diameter in order to limit the costs. An economic optimum between tethers and tube diameter can be found, which results in an optimized buoyancy-weight ratio. The same reliability methods can be applied to other SFTs, but they might result in different designs based on geolocation specific circumstances.

- A target reliability is required to perform the reliability analyses. The general partial factors from Eurocode are based on a β-value of 3.8. Therefore, in this research, a target β-value of 3.8 for 50 years was chosen as starting point for the individual failure mechanisms. For consistency, the lifetime of the SFT was assumed as 50 years as well. Design parameters were determined so that this target value was met. The actual β-values were computed using simplifications that are by definition safe. For the total probability of failure of the SFT, the individual cases were assumed to be uncorrelated. By adding failure probabilities and assuming independence of the mechanisms, the β-value of the system resulted in 3.3. It is debatable whether this is an acceptable target reliability for the system. A correct β-value for an SFT project should be based on an assessment of the length effect, dependency, lifetime, individual risk and group risk. For the individual failure mechanisms of the SFT, arbitrary β-values can be chosen and input parameters can be changed. However, the reliability method will be unchanged.

- Four important failure mechanisms for the SFT were derived using a fault tree analysis. These important mechanisms are yielding of the tethers, slackening of the tethers, longitudinal failure and transverse shear failure of the tube. It has been assumed within the scope and planning of this study that the additional failure mechanisms of corrosion, fatigue, geotechnical failure and accidental failure are not governing due to their complexity and expected research time needed. For geotechnical failure extensive research into the geolocation should be performed. Slackening proved to be the governing failure mechanism over the other three mechanisms. The resistance of slackening depends on the force equilibrium, whereas the resistance of the other mechanisms depends on structural strength.

- The influence factors (α-values) from the FORM analysis indicated that the most dominant parameters were the concrete density, water density, yield strength of the steel tethers, the diameter of the tube and the model uncertainties. The resulting α-values from FORM do not only depend on the coefficient of variation, but also on the absolute value of the mean of the parameter. The permanent loading parameters turned out to be dominant, because their relative contribution to the total load is large. The variable loads, i.e. traffic load and wind-current load, have relatively low α-values. The concrete and water density remained dominant even when the standard deviation of the variable loads was doubled.

- The general partial factors from Eurocode were never calibrated on SFT type of structures. They seem nevertheless safe to apply for the strength (STR) cases. They can be optimised based on this analysis. The favorable load and the material resistance factors fitted well. However, the general partial factors for the unfavorable permanent load and for the variable load turned out to be very conservative. Based on the case study, the general partial factors for variable loading can be decreased with at least 20 %. Since the influence of variable loads on the structure is small, the decrease of this factor will not result in significant changes in the design. Thus, the economic advantage is small. In contrast, a change in water density will have a large influence on the design. Thus, decreasing the factor for unfavorable permanent load will have a significant effect on the design. According to the case study, the factor of 1.35 could be decreased with almost 10 %. Conclusions cannot be too firm, since this calculation was performed for one case only.
The partial factors of the equilibrium (EQU) cases are not safe to be applied to the SFT. The factor for favorable load fitted well. However, the partial factor for the unfavorable permanent loading was insufficient.

- Leakage, wave loads and tether failure were analyzed to assess the robustness of the SFT. Excessive leakage has large consequences and will result in global structural failure. However, it has a low probability of occurrence. Mitigating measures are available to prevent failure due to leakage, e.g. installing a pumping system, installing compartment doors or fast reparation. Furthermore, the impact of waves was assessed. The magnitude of wave loading depends on the depth. At a depth of 30 meters, the wave load is small compared to the buoyancy force. When one SFT element is calculated on a maximum wave-current load, the entire length of an SFT can be calculated on a lower wave-current load. Lastly, failure of a single tether should not result in failure of adjacent tethers (i.e. progressive failure). The probability of failure of one tether is $7 \cdot 10^{-5}$, which is equal to a β-value of 3.8. However, when the first tether has failed, the probability for the second tether to fail is $1.5 \cdot 10^{-2}$. This is called a "conditional failure probability". When the requirements for conditional failure probability are tightened, a redundant system can be created by installing more or higher quality tethers. Consequently, when all four tethers of one element fail at the same time, this does not result in longitudinal failure.

8.2. Discussion

An engineer faced with the task of evaluating the reliability of structure must discuss four issues: the nature of the input uncertainties, the methodology for reliability analysis, the used analytical models and the interpretation of the output [9]. These four issues will be discussed in the sections below.

8.2.1. Input uncertainties

Reliability models require multiple input parameters. Research can increase the certainty of these parameters. However, complete certainty will not be reached, since values can still vary over time. In addition, variable loading will not be as certain as permanent loading.

A variable load can have a favorable as well as an unfavorable impact on the system. For yielding, the variable traffic loading was not taken into account since it was a favorable loading. This resulted in an underestimation of the reliability. Furthermore, the wave-current load resulted in an underestimation of the reliability for yielding, slackening and longitudinal failure, because the load can be directed upwards as well as downwards. Thus, for all failure mechanisms, all variable loads should be taken into account to draw a more firm conclusion.

Furthermore, model uncertainties were added to the model. For slackening, the model uncertainty nearly had the largest influence of all parameters. The mean and standard deviation of the model uncertainty were taken from the Probabilistic Model Code [24]. A smaller standard deviation could result in a significantly larger reliability. Research into the specific failure mechanisms of the SFT could be performed to decrease the model uncertainty.

Lastly, input parameters are calibrated on a β-value of 3.8 for the individual failure mechanisms, for a reference period of 50 years. The use of a β-value of 3.8 is debatable, because it results in a β_{system} of 3.3. Additionally, the lifetime of the structure could be 100 years instead of 50 years.

8.2.2. Methodology

A formal framework for assessing the structural reliability entailed by Eurocode is currently lacking [30]. In this study, a FORM and MC analysis are performed to assess the reliability of the structure and to calculate the partial factors. In practice, the partial factors are often obtained by a combination of historical developments, expert judgement, and calibrations to previous design methods. They are not obtained by a full probabilistic calibration [30]. In principle, it is questionable whether a design according to the partial factor method results in the same reliability level as a design according to the full probabilistic method. Calibration studies like this one are at least aiming for that.

In the FORM analysis, the individual α-values decrease when more parameters are added to the analysis. This is because α-values are relative values, and the sum of the squared α-values always adds up to one. However, this is not the case for α-values from Eurocode. They have standard values for dominant and non-dominant loads. Consequently, when more parameters are added, the sum of the squared α-values turns into a value larger than one. Thus, since α-values from the probabilistic calculation are generally smaller than Eurocode, their partial factors are also smaller.

8.2.3. Models

In this study, simplified but realistic models for SFT equilibrium and resistance are developed. Python and Prob2B can be used to perform a FORM and MC analysis. Python has a more workable interface, because the output can directly be used for displaying graphs and creating tables. In this research, Prob2B was only used to validate the output from Python. With the PyRe module from Python, a FORM analysis, distribution analysis, MC simulation and importance sampling can be performed. For a second-order reliability method (SORM) or numerical integration, Prob2B can be used. The amount of parameters should be closely monitored, since Prob2B allows for a maximum of 15 variables in its demo version.

Furthermore, the model results in one design point for each parameter. A parameter, for example the water density y_w, can be loading or a resistance parameter. The interpretation of this has to be

considered carefully, since a change in input parameters can change the design point. Consequently, a calculation results in other partial factors.

Certain limit states are not possible to investigate with a FORM or MC analysis. For example for structures under earthquake loads, the responses of the system become dynamic and nonlinear. This problem is generally not applicable to FORM or MC since it is difficult to determine the limit state function under these circumstances [59].

In order to reach a higher level of mechanics, probabilistic methods can be accompanied by advanced finite element methods (FEM). In Figure 8.1, the red dot indicates the level of this research, and the blue dot indicates the possible level for improvement. In case an analytical calculation is not exact, the output of an advanced FEM calculation will be more accurate. However, this will also take more time and effort.
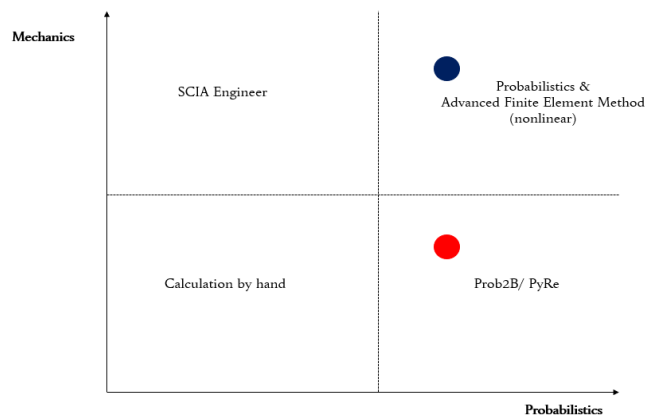

Figure 8.1: Scheme of level of probabilistics and mechanics: Bottom-left: analytical methods, based on basic theory, Top-right: numerical methods, based on more complex models

8.2.4. Interpretation

All reliability analyses in this study fulfill the requirement of $\beta = 3.8$, which indicates a sufficiently safe structure. Thus, within the scope and limitations of this research, the structure does not fail below that level of reliability. The fact that not all loads and load effects are included in the model is covered using model uncertainties. A more rigorous analysis of the structure of an SFT might result in different conclusions on the reliability parameters.

The partial factors from the reliability analysis were compared to the partial factors from Eurocode. These factors could be compared since both β-values were 3.8, and the condition of the limit state function from Eurocode was met. The input parameters from Chapter 5 result in safe partial safety factors for the STR cases. However, the factor for unfavorable permanent loading in the EQU case is not sufficient. Thus, the condition for the limit state function is possibly insufficient in guaranteeing a safe structure.

The correlation should also be taken into account while interpreting the results. By changing the correlation between parameters, α-values and the β-value change as well. In this research, correlation was only applied to the diameter D and the thickness t. This had a minor impact on the output. However, the magnitude of the correlation and other correlated parameters were not addressed. Thus, a concise conclusion about correlation should still be drawn.

Besides, the transverse shear failure mechanism was not taken into account for the partial factor method because of a large β-value. It was assumed that the force in the tethers could be modelled as a distributed load on the tube. The tethers were therefore assumed to be attached in the tangent line of the circular cross-section. However, this model needs more attention. To improve the reliability for shear, local reinforcement can be applied to the attachment-points.

8.3. Recommendations

The following recommendations are made for future research and development in reliability assessment of the SFT.

1. **Cost-benefit analysis**
   Costs are a dominant factor in realizing an SFT. This research showed that there is room for reliability based economic optimization of SFT concepts. For example, the buoyancy-weight ratio (BWR) can be optimized. When the BWR is high, the yield criterion will become critical. Many tethers will be necessary, which makes the construction less economical. Moreover, a larger tube cross-section will need more reinforcement. This can make a structure safer, but it will cost more. In order to determine the most optimal situation, there could be worked towards a Level IV calculation. In a Level IV calculation, the associated risk is used as a measure of the reliability. Uncertainty, costs and benefits are taken into account to compare different designs on an economic basis. Besides, the general partial factors from Eurocode are based on a cost-benefit analysis for standard structures. It is uncertain how this can be related to the economic effects of an SFT. Thus, a cost-benefit analysis could be performed for this specific case.

2. **Full probabilistic design**
   This research can serve as a basis for the full probabilistic design of an SFT. FORM and MC proved to be useful methods to calculate the probability of failure and the design points of the parameters. The accidental loads were out of scope for this research, but should be investigated for a specific case. For example, when an SFT is installed in an earthquake-prone area, this should be researched thoroughly.
   The simplifications of the used models should also be investigated. Methods to decrease the model uncertainty could be proposed. Furthermore, the applicable target reliability should be further analyzed. For a larger target reliability, larger general partial factors from Eurocode apply. The acceptable risk for a Level IV calculation should be further investigated as well.

3. **Construction**
   More research into the construction phase will be useful to increase the feasibility of an SFT. For SFTs, the installation of tethers at a large depth and the land-shore connection are different from other civil structures. The soil should be investigated, so that tethers can be placed at the most favorable locations. Furthermore, the tether diameters do not have to be consistent along the entire length of the tunnel because depths are differing and lengths are differing.
   For this research, all tethers were assumed to be made of steel, with steel quality S235. However, the inclined tethers do not need to have the same properties as the straight tethers. Potentially, the inclined tethers can be made of synthetic wire instead of steel, to save weight and costs. Synthetic wire has a high strength and low stiffness. The inclined tethers only have to resist the horizontal forces due to waves, so less resistance is required. The lifespans of tethers with different material types should be investigated. The method for attaching the tethers to the tunnel should be examined more in-depth as well.
   Lastly, the entire framework of the SFT should be addressed. Two parallel tubes with diagonals and crossbeams, as was designed for the Bjørnafjorden-crossing, should also be calculated. The interaction between two connected tubes should be studied. Furthermore, a suitable alignment for the tunnel has to be found. This depends on the wave-current loads, but also on the requirements of the geolocation.

4. **Robustness**
   For the robustness, recommendations have already been addressed in Chapter 7. Options to locally improve the structure should be investigated. Eccentric reinforcement can be used at specific locations in the cross-section. Furthermore, an outer shell or support structure can be developed to reduce leakage or decrease the impact of accidental loads. For tether failure, spatial variability and dependency should also be taken into account for future research. Furthermore, redundancy is an important aspect. More or higher quality tethers have to be applied if a higher reliability is required. Consequently, the system does not have to be calculated on failure of all four tethers and longitudinal failure will not occur. Finally, for an explosion in the tunnel, separate closing of tube elements can be researched. Escape routes have to be determined.

Bibliography

[1] Ahrens, D. and Gursoy, A. [1997], 'Immersed and floating tunnels, chapter 10: Submerged floating tunnels-a concept whose time has arrived', *Tunnelling and underground space technology, Special edition* **12**(2).

[2] Baker, G., Utstrand, J., Winberg, D., Sweco, A., Jönsson, A. and Brandskyddslaget, A. [2016], Probabilistic fire risk analysis in the nordic region, *in* '11th Conference on Performance-Based Codes and Fire Safety Design Methods, May 23-25, 2016, Warsaw, Poland', pp. 137–148.

[3] Baravalle, M. and Köhler, J. [2016], 'Risk and reliability based calibration of design codes for submerged floating tunnels', *Procedia engineering* **166**, 247–254.

[4] Baravalle, M. and Köhler, J. [2019], 'A risk-based approach for calibration of design codes', *Structural Safety* **78**, 63–75.

[5] Battjes, J. A. [1982], 'Effects of short-crestedness on wave loads on long structures', *Applied Ocean Research* **4**(3), 165–172.

[6] Binnenlandse Zaken en Koninkrijksrelaties, M. v. [2011], 'Bouwbesluit 2012'.

[7] BV, T. [2007], Multi-strand post-tensioning system, Technical report, UT Tensacciai.

[8] Chen, Y. and Zhang, D. [2017], 'Response-based analysis for tension leg platform', *Journal of Marine Science and Application* **16**(1), 87–92.

[9] Christian, J. T. [2004], 'Geotechnical engineering reliability: How well do we know what we are doing?', *Journal of geotechnical and geo-environmental engineering* **130**(10), 985–1003.

[10] Courage, W. and Steenbergen, H. [2007], 'Prob2b: variables, expressions and excel installation and getting started', *Delft: TNO Built Environment and Geosciences* .

[11] Den Heijer, C. [2012], 'Reliability methods in openearthtools. communications on hydraulic and geotechnical engineering 2012-01', *Delft University of Technology* .

[12] DNV [2000], 'Submarine pipeline systems', *DNV-OSF101, DNV* .

[13] EN1990 [2011], Eurocode 0: Basis of structural design, Standard, European Committee for Standardization.

[14] EN1991-2 [2015], Eurocode 1: Actions on structures - Part 2: Traffic loads on bridges , Standard, European Committee for Standardization, Delft, NL.

[15] EN1992 [2005], En 1992-1-1 eurocode 2: Design of concrete structures - part 1-1: General rules and rules for buildings, Standard, European Committee for Standardization.

[16] EN1993 [2004], Eurocode 3: Design of steel structures, Standard, European Committee for Standardization.

[17] ENW [2017], *Grondslagen voor hoogwaterbescherming*, second edn.

[18] Faber, M. H. [2009], 'Basics of structural reliability', *DRAFT, Swiss Federal Institute of Technology ETH, Zürich, Switzerland* .

[19] Gokce, A., Koyama, F., Tsuchiya, M. and Gencoglu, T. [2009], 'The challenges involved in concrete works of marmaray immersed tunnel with service life beyond 100 years', *Tunnelling and underground space technology* **24**(5), 592–601.

[20] Gomes, L. and Vickery, B. [1978], 'Extreme wind speeds in mixed wind climates', *Journal of Wind Engineering and Industrial Aerodynamics* **2**(4), 331–344.

[21] Grierson, D., Xu, L. and Liu, Y. [2005], 'Progressive-failure analysis of buildings subjected to abnormal loading', *Computer-Aided Civil and Infrastructure Engineering* **20**(3), 155–171.

[22] Ibrahim, S. E. B. [2011], Risk-based design of horizontal curves with restricted sight distance, PhD thesis, University of British Columbia.

[23] ISO2394 [2015], General principles on reliability for structures, Standard, International Organization for Standardization, Geneva, CH.

[24] JCSS, J. [2001], 'Probabilistic model code', *Joint Committee on Structural Safety* .

[25] Jonkman, S., Steenbergen, R., Morales-Nápoles, ., Vrouwenvelder, A. and Vrijling, J. [2017], *Probabilistic Design: Risk and Reliability Analysis in Civil Engineering*, Vol. 4, Delft University of Technology.

[26] Journée, J. and Massie, W. [2001], 'Offshore hydromechanics, chapter 12 wave forces on slender cylinders', *Offshore Hydromechanics, Delft University of Technology* .

[27] Jusoh, I. and Wolfram, J. [1996], 'Effects of marine growth and hydrodynamic loading on offshore structures', *Jurnal Mekanikal* **1**(1).

[28] Lunniss, R. and Baber, J. [2013], *Immersed tunnels*, CRC Press.

[29] Martire, G. [2010], The development of Submerged Floating Tunnels as an innovative solution for waterway crossings, PhD thesis, Università degli Studi di Napoli Federico II.

[30] Meinen, N. and Steenbergen, R. [2018], 'Reliability levels obtained by eurocode partial factor design-a discussion on current and future reliability levels', *HERON* **63**(3), 243.

[31] Melcher, J., Kala, Z., Holický, M., Fajkus, M. and Rozlívka, L. [2004], 'Design characteristics of structural steels based on statistical analysis of metallurgical products', *Journal of Constructional Steel Research* **60**(3-5), 795–808.

[32] Moan, T. [2005*a*], 'Reliability-based management of inspection, maintenance and repair of offshore structures', *Structure and Infrastructure Engineering* **1**(1), 33–62.

[33] Moan, T. [2005*b*], 'Safety of offshore structures', *Center for Offshore Research and Engineering, National University of Singapore, Singapore, Report* **4**.

[34] NORSOK [2007], 'N-003 action and action effects'.

[35] Reinertsen, Dr. Techn. Olsen, O. and Norconsult [2016], Bjørnafjord submerged floating tube bridge, Technical report.

[36] Rijkswaterstaat [2016], 'Systeemspecificatie rws tunnelsysteem', **1.2 SP2**.

[37] Ronold, K. O. [1990], 'Random field modeling of foundation failure modes', *Journal of geotechnical engineering* **116**(4), 554–570.

[38] Roubos, A., Steenbergen, R., Schweckendiek, T. and Jonkman, S. [2018], 'Risk-based target reliability indices for quay walls', *Structural Safety* **75**, 89–109.

[39] Schweckendiek, T., Vrouwenvelder, A., Calle, E., Kanning, W. and Jongejan, R. [2012], 'Target reliabilities and partial factors for flood defenses in the netherlands', *Modern Geotechnical Codes of Practice-Code Development and Calibration* pp. 311–328.

[40] Shanmugam, G. [2012], Bottom-current reworked sands, *in* 'Handbook of Petroleum Exploration and Production', Vol. 9, Elsevier, pp. 129–219.

[41] Siddiqui, N. A. and Ahmad, S. [2000], 'Reliability analysis against progressive failure of tlp tethers in extreme tension', *Reliability Engineering & System Safety* **68**(3), 195–205.

[42] Skorpa, L. [2010], 'Developing new methods to cross wide and deep norwegian fjords', *Procedia Engineering* **4**, 81–89.

[43] Steenbergen, H., Lassing, B., Vrouwenvelder, A. and Waarts, P. [2004], 'Reliability analysis of flood defence systems', *Heron, 49 (1)* .

[44] Steenbergen, R. D., Sỳkora, M., Diamantidis, D., Holickỳ, M. and Vrouwenvelder, T. [2015], 'Economic and human safety reliability levels for existing structures', *Structural Concrete* **16**(3), 323–332.

[45] Steenbergen, R., De Boer, A. and Van der Veen, C. [2012], 'Calibration of partial factors in the safety assessment of existing concrete slab bridges for shear failure', *Heron, 57 (2012) 1* .

[46] Steenbergen, R. and Vrouwenvelder, A. [2010], 'Safety philosophy for existing structures and partial factors for traffic loads on bridges', *Heron, 55 (2), 2010* .

[47] Steenbergen, R. and Vrouwenvelder, A. [2014], 'Reliability based assessment of buildings under earthquakes due to gas extraction', *HERON* **59**(2/3), 129.

[48] Thoft-Christensen, P. [1999], *Estimation of bridge reliability distributions*, Thomas Telford, London.

[49] Van Heteren, J., Botma, H., Roskam, A. and Battjes, J. [1987], Verification of the consequences of wavedirectionality on the loading of long coastal structures by field experiments, *in* 'Coastal Engineering 1986', pp. 2435–2444.

[50] van Kinderen, S. [1995], Risicoanalyse van een geboorde tunnel, Master's thesis, TU Delft.

[51] Vierth, I., Berell, H., McDaniel, J., Haraldsson, M., Hammarström, U., Yahya, M. R., Lindberg, G., Carlsson, A., Ögren, M. and Björketun, U. [2008], *The effects of long and heavy trucks on the transport system: Report on a government assignment*, Statens väg-och transportforskningsinstitut.

[52] Voorendt, M. and Molenaar, W. [2019], *Manual Hydraulic Structures*, Delft University of Technology.

[53] Vrijling, J., Schweckendiek, T. and Kanning, W. [2011], 'Safety standards of flood defenses', *Keynote paper at ISGSR* pp. 67–84.

[54] Vrouwenvelder, A. [2001], L550 betrouwbaarheidsaspecten boortunnels, Technical report, COB.

[55] Vrouwenvelder, A. and Siemes, A. [1987], 'Probabilistic calibration procedure for the derivation of partial safety factors for the netherlands building codes', *HERON, 32 (4), 1987* **32**.

[56] Walraven, J. [2010], *Gewapend beton: dictaat CT2052/3150*, TU Delft.

[57] Wardhana, K. and Hadipriono, F. [2003], 'Analysis of recent bridge failures in the united states', *Journal of performance of constructed facilities* **17**(3), 144–150.

[58] Welleman, J. W., Dolfing, A. and Hartman, J. [2011], *Basisboek toegepaste mechanica*, ThiemeMeulenhoff.

[59] Wen, Y.-K. [2001], 'Reliability and performance-based design', *Structural safety* **23**(4), 407–428.

[60] Won, D., Seo, J., Kim, S. and Park, W.-S. [2019], 'Hydrodynamic behavior of submerged floating tunnels with suspension cables and towers under irregular waves', *Applied Sciences* **9**(24), 5494.

[61] Xiang, Y. and Yang, Y. [2016], 'Challenge in design and construction of submerged floating tunnel and state-of-art', *Procedia engineering* **166**, 53–60.

[62] Yang, M., Cai, Z., Li, C. and Guan, J. [2014], An improved jade algorithm for global optimization, pp. 806–812.

[63] Zhang, L., Tang, W. H. and Ng, C. W. [2001], 'Reliability of axially loaded driven pile groups', *Journal of Geotechnical and Geoenvironmental Engineering* **127**(12), 1051–1060.

[64] Zhou, X. J., Wang, J. H. and Luo, G. [2012], Study on reliability of submerged floating tunnel with single span under vortex-induced vibration, *in* 'Advanced Materials Research', Vol. 446, Trans Tech Publ, pp. 2168–2171.

A
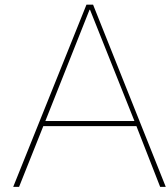
Tables from Eurcode and JCSS

A.1. Partial factors from Eurocode EN1990

A.1.1. ULS (EQU) Set A

For check tension in tethers

Action	Description	Load factor
G	Permanent load	0.95 if favorable, 1.05 if unfavorable
Q	Leading variable action	Traffic 1.35 Other 1.50
Q	Accompanying variable action	$1.50 \cdot \psi_{0,i}$

Table A.1: Factors ULS (EQU) Set A [13]

A.1.2. ULS (STR) Set B

Check yielding and longitudinal capacity

Action	Description	Load factor
G	Permanent load	1.0 if favorable, 1.35 if unfavorable
Q	Leading variable action	Traffic 1.35 Other 1.50
Q	Accompanying variable action	$1.50 \cdot \psi_{0,i}$

Table A.2: Factors ULS (STR) Set B, 6.10 [13]

Action	Description	Load factor
G	Permanent load	1.0 if favorable, 1.35 if unfavorable
Q	Main variable action	Traffic $1.35 \cdot \psi_{0,i}$ Other $1.50 \cdot \psi_{0,i}$
Q	Other accompanying variable actions	$1.50 \cdot \psi_{0,i}$

Table A.3: Factors ULS (STR) Set B 6.10a [13]

Action	Description	Load factor
G	Permanent load	1.0 if favorable, 0.85 · 1.35 if unfavorable
Q	Leading variable action	Traffic 1.35 Other 1.50
Q	Accompanying variable actions	1.50 $\cdot \psi_{0,i}$

Table A.4: Factors ULS (STR) Set B 6.10b [13]

A.1.3. ULS (STR) Set C

Action	Description	Load factor
G	Permanent load	1.0 if favorable, 1.0 if unfavorable
Q	Leading variable action	Traffic 1.15 Other 1.3
Q	Accompanying variable actions	1.50 $\cdot \psi_{0,i}$

Table A.5: Factors ULS (STR) Set C [13]

A.1.4. SLS Characteristic

Action	Description	Load factor
G	Permanent load	1.0
Q	Lead variable action	1.0
Q	Accompanying variable action	0.7

Table A.6: Factors SLS [13]

A.2. Model uncertainties from JCSS

A.2.1. Materials

Material	Mean value [kN/m³]	Coefficient of variation
Steel	77	< 0.01
Concrete		
Ordinary concrete [2]	24	0.04
High strength concrete	24-26 [4]	0.03
Lightweight aggregate concrete	[4]	0.04-0.08
Cellular concrete	[4]	0.05-0.10
Heavy concrete for special purposes	[4]	0.01-0.02
Masonry	-	≈ 0.05
Timber [3]		
Spruce, fir (Picea)	4.4	0.10
Pine (Pinus)	5.1	0.10
Larch (Larix)	6.6	0.10
Beech (Fagus)	6.8	0.10
Oak (Quercus)	6.5	0.10

Figure A.1: Mean value and coefficient of variation for weight density [24]

A.2.2. Wave characteristics

X	Designation	μ	V	Dist type	ρ_{ij}
	Measurement H_s	nom	0.10	-	-
H_s	Significant wave height	Local	Local	W/L	-
$T_z \mid H_s$	Mean period for given H_s	Local	Local	L/N	-
ϕ_s	Mean wave direction	Local	Local	Local	-
T_d	Duration of sea state	3-6 hrs	1.0	E	-
$H_{max} \mid H_s$	Max wave in given sea state	Calculation	Local	G	-
θ_w	Wave model	Depends	$0.05 - 0.3$	-	-
θ_{MG}	Marine growth model	1	0.2 - 0.5	W	0.9
C_D	Drag force coefficient	0.6-1.3	$0.2 - 0.3$	L	0.9
C_M	Inertia force coefficient	1.6-2.5	$0.10 - 0.15$	L	0.9
p_1	Horizontal pressure on wall	0.90	0.20	L	-
	Moment due to horizontal pressure on wall	0.81	0.37	L	-
p_4	Uplift pressure	0.77	0.20	L	-
	Moment due to uplift pressure	0.72	0.34	L	-

Figure A.2: Mean value and coefficient of variation for basic variables for waves [24]

A.2.3. Load and resistance effects

	Model type	Distr	mean	CoV	correlation
	load effect calculation				
	moments in frames	LN	1.0	0.1	
	axial forces in frames	LN	1.0	0.05	
	shear forces in frames	LN	1.0	0.1	
	moments in plates	LN	1.0	0.2	
	forces in plates	LN	1.0	0.1	
	stresses in 2D solids	N	0.0	0.05	
	stresses in 3D solids	N	0.0	0.05	
	resistance models steel (static)				
	bending moment capacity [1]	LN	1.0	0.05	
	shear capacity	LN	1.0	0.05	
	welded connectio capacity	LN	1.15	0.15	
	bolted connection capacity	LN	1.25	0.15	
	resistance models concrete (static)				
	bending moment capacity [1]	LN	1.2	0.15	
	buckling	LN	1.4	0.25	
	shear capacity	LN	1.0	0.1	
	connection capacity				

Figure A.3: Mean value and coefficient of variation for model uncertainties [24]

A.3. Immersed tunnels

Table A.4 follows from the book "Immersed tunnels", by Baber and Lunniss. [28]

	Ultimate limit state			
	Load combinations[a]			
	I	II[a]	II[b]	III
Load	Temporary	In-service		Accidental/ seismic
Permanent Loads (G)				
Self-weight of structure	1.2	0.9/1.25	1.0/1.35	1.0
Ballast concrete	1.2	0.9/1.25	1.0/1.35	1.0
Road pavement, furniture		0.9/1.25	1.0/1.35	1.0
Hydrostatic load (MWL)	1.2	1.0/1.25	0.9/1.35	1.0
Earth pressure	1.2	1.0/1.25	0.9/1.4	1.0
Settlements	1.2	1.0/1.25	0.9/1.4	1.0
Prestressing, creep and shrinkage[b]	1.0	1.0	1.0	1.0
Variable Loads (Q)				
Earth pressure (surcharge)	1.35	1.5		1.0
Road traffic		1.5		1.0
Wind	1.35	1.5		1.0
Water level variation	1.2	1.2		1.0
Temperature				
Wave and current loads	1.35			
Temporary construction loads	1.35			
Accidental Loads (A): One of the following actions				
Explosion				1.0
Collision from road traffic				1.0
Sunken ship				1.0
Falling anchor				1.0
Earthquake				1.0
Tunnel flooding				1.0
Extreme high water and waves				1.0

[a] For all loads, the factors given in the column are to be multiplied by the corresponding load in all load combinations. If no value is given, the load shall not be taken into account.
[b] Effects of creep and shrinkage only included if these create an unfavorable effect for the element under consideration.

Figure A.4: Partial factors for the Ultimate Limit State [28]

B

Verification FORM analysis

B.1. Input

A structure is assumed to be loaded by S1 and S2, and it has a resistance of R. The goal is to illustrate how to derive the influence factors α for S1, S2 and R by using a hand calculation. The methodology shown in this Appendix is fundamentally equal to the methods in computer programs as Prob2B and Python.

In order to be able to add up or subtract variables, all variables should be normally distributed. In case of a Gumbel or lognormal distributed variable, this should be transformed into a normally distributed variable. The explanation for this can be found in Appendix E. For this example, three normally distributed variables are chosen.

Parameter	Mean	St.dev.
Resistance (R)	600	10
Permanent load 1 ($S1$)	425	25
Permanent load 2 ($S2$)	65	25

Table B.1: Input parameters

The probability density functions of these three distributions are plotted in Figure B.1.
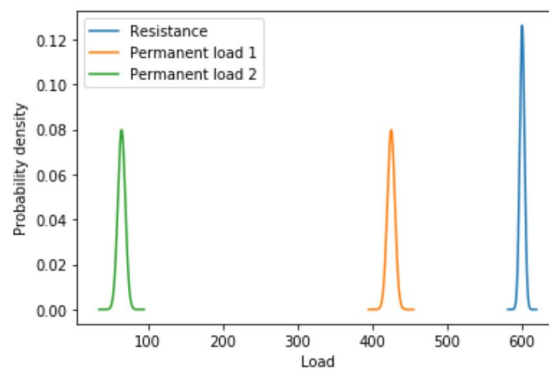
Figure B.1: Probability density of three parameters from Python

The probability densities are calculated with the following formula:

$$f(x) = \frac{1}{\sigma\sqrt{2 \cdot \pi}} \cdot \exp\left(-\frac{1}{2} \cdot \left(\frac{x - \mu}{\sigma}\right)^2\right) \tag{B.1}$$

where: μ = the mean value
σ = the standard deviation

101

The limit state function for this mechanisms can be written as:

$$Z = R - S1 - S2 \tag{B.2}$$

The mean and standard deviation of this Z-function have to be determined, in order to calculate the reliability index (β-value).

$$\mu_Z = 600 - 425 - 65 = 110 \qquad\qquad \sigma_Z = \sqrt{10^2 + 25^2 + 25^2} = 36.7 \tag{B.3}$$

According to the formulation for β, this gives:

$$\beta = \frac{\mu_Z}{\sigma_Z} = \frac{110}{36.7} = 3 \tag{B.4}$$

The Z-function is plotted in Figure B.2. The red line indicates the failure line, $Z = 0$.
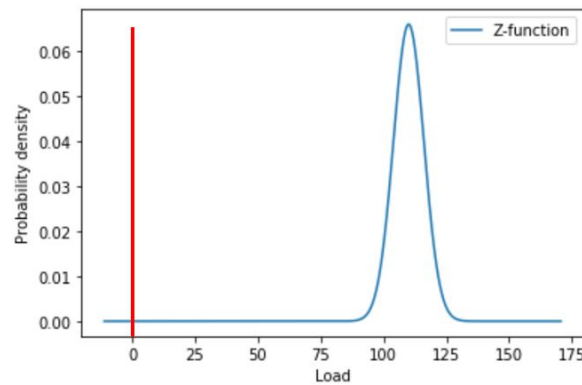
Figure B.2: The probability density of the Z-function from Python

B.2. Graphical display

To display three parameters in a two or three dimensional plot, the two loading parameters ($S1$ and $S2$) should be added up to one loading parameter (S).

$$\mu_S = 425 + 65 = 490 \qquad\qquad \sigma_S = \sqrt{25^2 + 25^2} = 35.4 \tag{B.5}$$

The limit state function can be formulated as:

$$Z = R - S \tag{B.6}$$

The probability density of R was multiplied by the probability density of S, to create Figure B.3. For the line $Z = 0$ the resistance is equal to the load. This line can be drawn in a 2D plot, so that the design points can be read. This can be seen in Figure B.4. This gives the same value for resistance as loading:
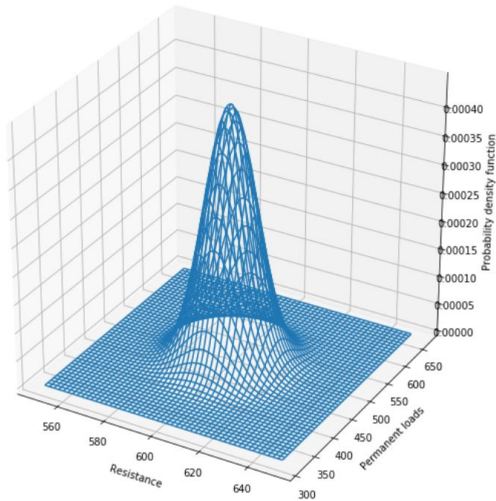
$$R_{design} = S_{design} = 591 \tag{B.7}$$
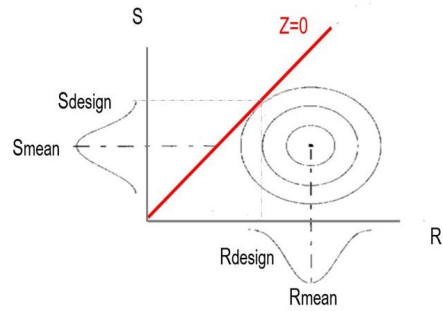
Figure B.3: 3D probability density function from Python

Figure B.4: Top view of the 3D plot of R and S

Now, the loading (S) can again be subdivided into $S1$ and $S2$. In the same way as before, the probability density of S1 was multiplied by the probability density of S2, to create Figure B.5.

The structure will fail if both loads add up to 591, according to the previously calculated design point. Thus, the limit state can be formulated as:

$$Z = S1 + S2 = 591 \tag{B.8}$$

In the 2D plot of Figure B.6, the line $Z = 591$ was plotted and the design points could be read.
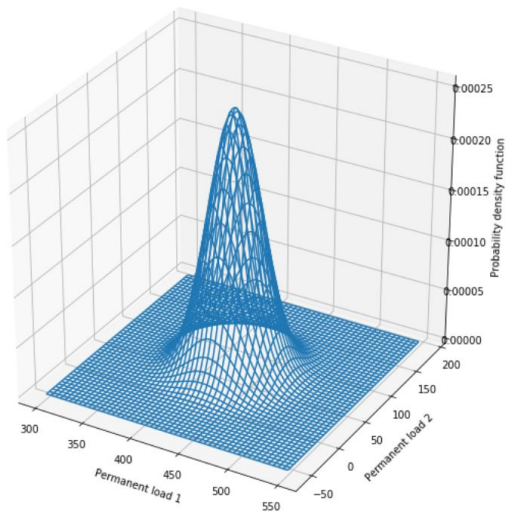
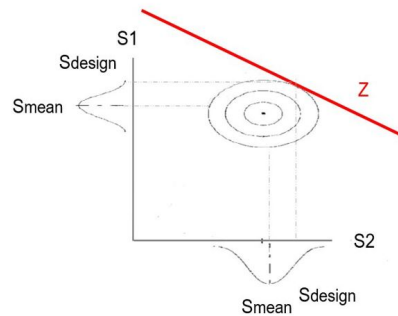Figure B.5: 3D probability density function from Python

Figure B.6: Top view of the 3D plot of S1 and S2

This gives the following design points:

$$S1_{design} = 475 \qquad\qquad S2_{design} = 116 \tag{B.9}$$

B.3. Calculations

The distance between the mean value and the design point can be formulated as:

$$R_{mean} - R_{design} = \alpha_R \cdot \beta \cdot \sigma_R \tag{B.10}$$

$$S_{mean} - S_{design} = \alpha_S \cdot \beta \cdot \sigma_S \tag{B.11}$$

From the graphs, the design points could be read. The mean values and standard deviations are given as well. In this way, the α-values can be calculated for the first case:

$$\alpha_R = \frac{\frac{600-591}{10}}{3} = 0.3 \tag{B.12}$$

$$\alpha_S = \frac{\frac{490-591}{35.4}}{3} = -0.95 \tag{B.13}$$

And for the second case:

$$\alpha_{S1} = \frac{\frac{425-475}{25}}{3} = -0.67 \tag{B.14}$$

$$\alpha_{S2} = \frac{\frac{65-116}{25}}{3} = -0.68 \tag{B.15}$$

B.4. Conclusion

The α-values of the three parameters resulted in:

$$\alpha_R = 0.3 \qquad\qquad \alpha_{S1} = -0.67 \qquad\qquad \alpha_{S2} = -0.68 \tag{B.16}$$

The squared sum of these values adds up to one, which indicates that this is a correct calculation. Furthermore, when this output is compared to Prob2B or Python, the same output follows.
Thus, separations of loads and resistances can be made in order to display them in 2D plots. With more than two parameters, this takes more effort. This is why Prob2B or Python is used in this research.
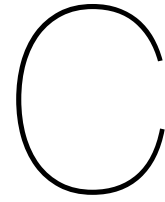
Compressive stress in transverse direction

C.1. Analysis of failure mechanism

For this analysis, a cross sectional element with a 1 meter width will be considered. This element fails when the applied compressive stress is larger than the compressive strength of concrete. Compressive stress on the tube is caused by hydrostatic pressure, which acts around the entire perimeter of the tube. The pressure depends on the water depth: pressure is larger at a larger depth. The pressure around the tube can be schematised as a uniform pressure and a deviating pressure (Figure C.1).
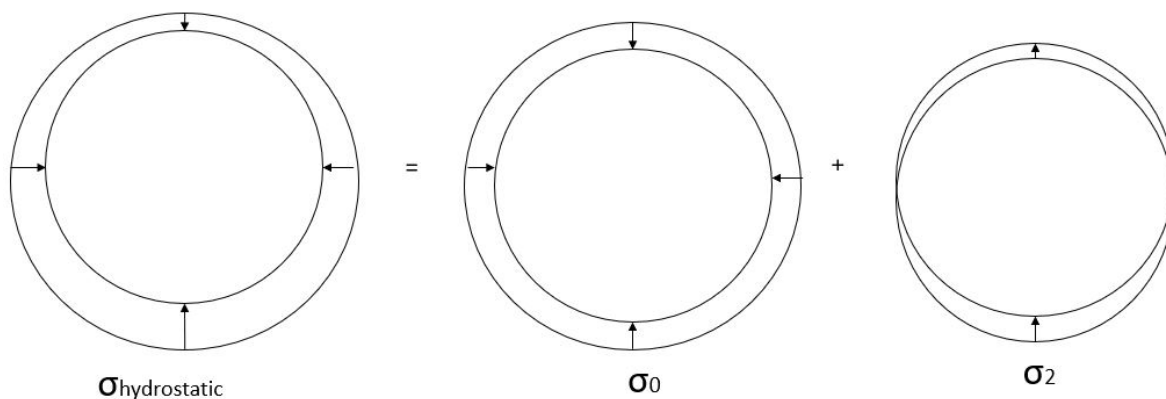

$\sigma_{hydrostatic}$ = σ_0 + σ_2

Figure C.1: Forces in ring due to hydrostatic pressure

For simplification, only the uniform pressure (σ_0) will be used for calculation. The deviating pressure is relatively small, and can be taken into account by incorporating a larger uncertainty of the pressure. The σ_0 value will be taken as the average value of the hydrostatic pressure, which can be found in the middle of the tube. According to Figure C.2, the equilibrium situation can be formulated as:

$$2N_h = q \cdot D = q \cdot 2 \cdot R$$

In turn, this can be rewritten as:

$$N_h = q \cdot R = d_{w,avg} \cdot \gamma_w \cdot R$$

where: N_h = the force on the tube caused by hydrostatic pressure $[kN]$
$d_{w,avg}$ = the average water depth of the tube $[m]$
γ_w = the weight of the tube $[kN/m^2]$
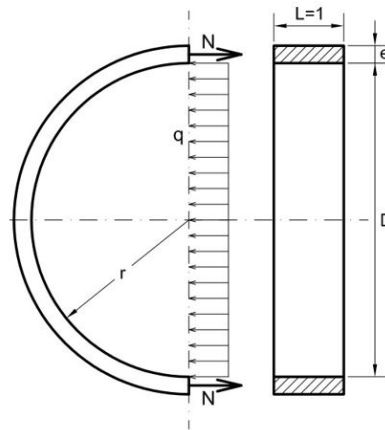R = the tube radius $[m]$

105

Figure C.2: Forces in ring due to hydrostatic pressure

C.2. Limit state function

The pressure on the cross section of the tube needs to be smaller than the concrete compressive strength. The following limit state can be formulated:

$$Z = \theta_1 \cdot f_c - \frac{N_h}{A_c}$$

(C.1)

where: σ_c = the compressive stress [N/mm]
A_c = the cross section of the tube: $A_c = b_c \cdot t_c$ [mm^2]
f_c = the concrete compressive strength [N/mm^3]
θ_1 = the model uncertainty for resistance of concrete in compression [-]

Concrete C45/55 has a characteristic value, f_{ck}, of 45 N/mm^2. This gives a design value, f_{cd}, of $\frac{f_{ck}}{1.5} = 30$, and a mean value of $f_{cm} = f_{ck} + 8 = 53N/mm^2$.

C.3. Conclusion

The compressive stress ($\frac{N_h}{A_c}$) will be at its maximum for a maximum water depth and maximum tube radius, and minimum tube thickness. The situation would become critical when the reliability index β is below 3.8. This would occur for a depth larger than 100 meters and a radius larger than 20 meters, which is highly unrealistic. The thickness-radius ratio should also not be smaller than 1:50. Construction-wise, this is almost impossible. These are reasons for not taking this failure mechanism into account.

D
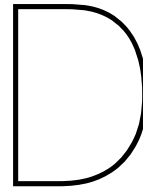
Tether behaviour

D.1. Mechanism analysis

The stiffness of the tether can be calculated with the equations for springs, Hooke's Law:

$$k = \frac{E \cdot A}{L}$$

(D.1)

where: k = the stiffness of the spring $[N/m]$
E = the modulus of elasticity or Youngs modulus $[N/m^2]$
A = the cross sectional area of the spring $[m^2]$
L = the length of the spring $[m]$

Tether lengths vary from 90 to 520 meters, because of the changing depth of the fjord. Since the steel class and cross sectional area are the same for all tethers, the shortest tethers result in the largest stiffness. The spring system is a parallel system. The equivalent stiffness can be written as:

$$k_{eq} = k_1 + k_2 + \dots$$

(D.2)

The angle of inclination can be varied, which changes the length of the tether (L) as well as the displacement (u). The force in the spring can be calculated with Formula D.3.

$$F = k \cdot u$$

(D.3)

A larger stiffness means that a certain forcing results in a smaller displacement, and yielding will take place for a smaller displacement compared to a longer tether. To visualize the behaviour of the tethers, force-displacement diagrams can be made. These are shown from Figure D.1 to Figure D.8. Two boundaries are defined in all graphs: the yielding limit and slackening limit. The structure is 'safe' in between yielding and slackening. The resistance of one tether against yielding is calculated as approximately 30 MN, for fy=284 N/mm2 and A = 0.129 m^2. This is demonstrated as dark blue line. Slackening occurs when the force in the tether is equal to zero, and can be seen as light blue line. In these diagrams, a positive force means tension force. First, the force-displacement diagram for both a 90 meter tether and 520 meter tether will be shown, to demonstrate the difference between the longest and shortest tether. For a length of 90 meters, yielding occurs at a vertical displacement around 0.1 meters (Figure D.1). For a length of 520 meter, yielding occurs only around 0.6 meters (Figure D.2). Thus, the shortest cables are governing in case of purely vertical displacement.
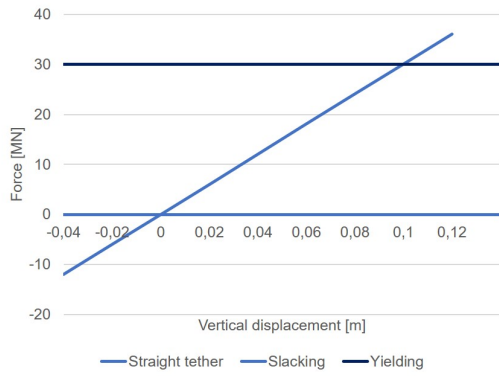
Figure D.1: Force-Displacement Diagram for vertical displacement of straight tether with L=90m
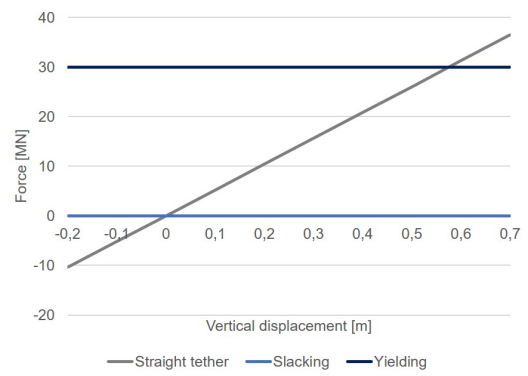

Figure D.2: Force-Displacement Diagram for vertical displacement of straight tether with L=520m

Second, the simultaneously occurring vertical and horizontal displacement will be examined. The horizontal displacement will be small relative to the vertical displacement, because downward loading cases have much larger values than the load due to waves and currents. The large values of horizontal displacement shown on the x-axis in Figure D.3 and Figure D.4 have a low possibility of occurrence. Subsequently, the inclined tethers need to be examined for the combined horizontal and vertical displacement, again for 90 and 520 meters. For the tether length of 90 meters, vertical displacements of 0.07, 0.08 and 0.09 meters are chosen, because these are close to the limit for yielding. For the tether length of 520 meters, values of 0.4, 0.5 and 0.6 meters are chosen for the same reason.
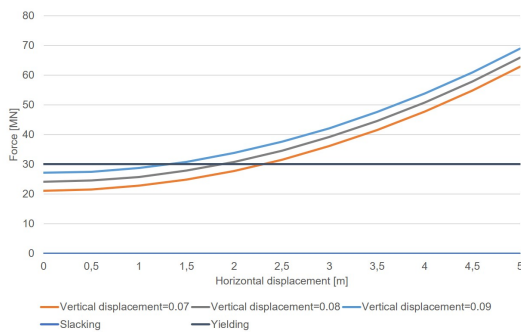

Figure D.3: Force-Displacement Diagram for horizontal displacement given a variable vertical displacement, for a straight tether with L=90m
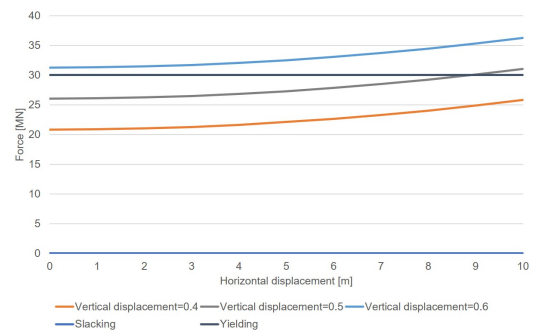

Figure D.4: Force-Displacement Diagram for horizontal displacement given a variable vertical displacement, for a straight tether with L=520m

Lastly, the behaviour of the inclined tethers is shown. For the inner tether of 90 meters (on the left side/ the side of the incoming wave), the 80 degrees inclined tether will yield before the 60 degrees inclined tether for a horizontal displacement (Figure D.5). For the outer tether of 90 meters (on the right side), the 20 degrees inclined tether will slack before the 40 degrees inclined tether for a horizontal displacement (Figure D.6). This proves that an angle of 20 or 80 degrees is not the most favorable for the tether configuration. Due to the net buoyancy force, a certain level of tension has already been assured in the starting situation. This ensures a certain capacity to withstand an increase in downward loading. For horizontal loading, the limit can also be set as the yielding limit. The capacity should be examined and a safety range should be formulated. The actual occurrence of failure depends on the load cases.
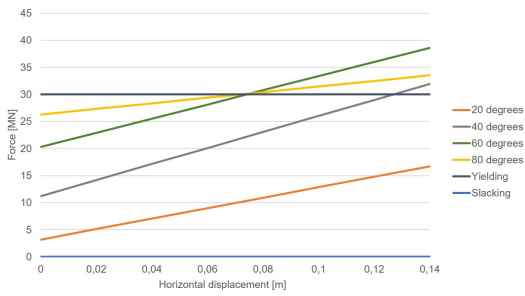
Figure D.5: Force-Displacement Diagram for horizontal displacement given a vertical displacement of 0.09m, for the inner inclined tether with L=90m

Figure D.6: Force-Displacement Diagram for horizontal displacement given a vertical displacement of 0.09m, for the outer inclined tether with L=90m

Figure D.7: Force-Displacement Diagram for horizontal displacement given a vertical displacement of 0.5m, for the inner inclined tether with L=520m
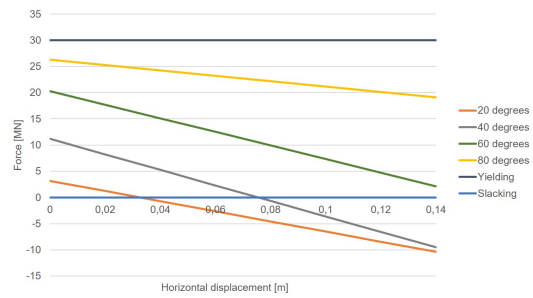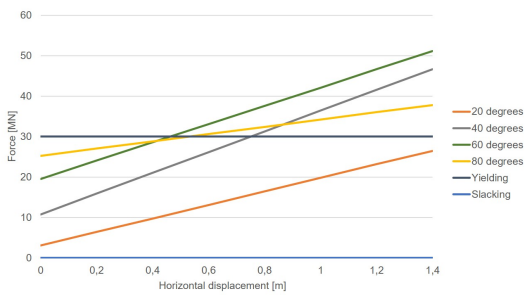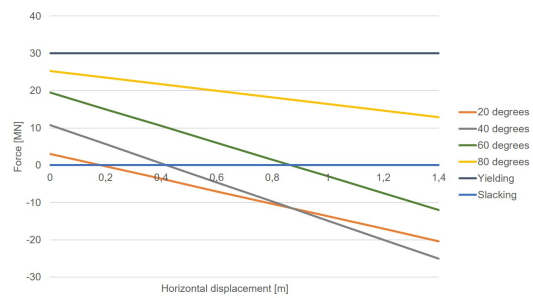

Figure D.8: Force-Displacement Diagram for horizontal displacement given a vertical displacement of 0.5m, for the outer inclined tether with L=520m

D.2. Lift force

When the straight tether is elongated with 1 meter, the inclined tether is elongated with 1.15 meters (for 60 degrees) or 1.55 meters (for 40 degrees). When the stiffness of the inclined tether is smaller than the straight tether, the force in all tethers can still be the same. So the lift force, a purely vertical force, is equally spread over the four tethers. The lift coefficient depends on the shape and the type of waves and currents.

D.3. Drag force

The drag force is a horizontal force, which is only taken by the inclined tethers. When the tether is displaced by 1 meter in the horizontal direction, the straight tethers are elongated by only 0.005 meters. The inclined tether is elongated by 0.5 meters (60 degrees) or 0.76 meters (40 degrees).

E
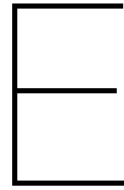
Parameter transformations

E.1. General

For the normal distribution in Prob2B, the mean (μ) and standard deviation (σ) are used as input parameters. However, for the lognormal and Gumbel distribution, this is not the case. A lognormal distribution uses λ and ζ- parameters and a Gumbel distribution has a and u parameters. This will be explained in the following sections. Furthermore, formulas for design points for lognormal and Gumbel distributions will be explained. For time dependent loads, Gumbel distributions are applied. The transformation formulas are shown.

Additionally, the rules for adding and multiplying mean values and standard deviations are explained. Lognormal and Gumbel distributions have to be transformed to normal distributions in order to add, subtract or multiply them. Finally, the multivariate normal distribution is shown.

E.2. Lognormal distribution

For the lognormal distributions, the λ and ζ- parameters are necessary as input for Prob2B. These values can be found in Table E.1.

Parameter	Mean	Standard deviation	λ	ζ
C_D	0.7	0.2	-0.396	0.28
C_L	0.1	0.02	-2.322	0.198
y_w	10.035	0.4	2.305	0.0398
y_c	24.5	1.7	3.196	0.0693
f_y	285	20	5.648	0.07
f_s	1300	50	7.19	0.069
f_c	53	8	3.96	0.15
θ_1	1	0.05	-0.00125	0.0499
θ_2	1	0.1	-0.00498	0.0997

Table E.1: Lognormal distribution: Input for Prob2B

The probability density function can be written as:

$$f(x) = \frac{1}{x\sigma\sqrt{2 \cdot \pi}} \cdot \exp{-\frac{(\ln{(x)} - \mu)^2}{2\sigma^2}}$$ (E.1)

The cumulative density function can be written as:

$$F(x) = \Phi\left(\frac{(\ln{x}) - \mu}{\sigma}\right) = $$ (E.2)

$$\delta = \frac{\sigma}{\mu} \tag{E.3}$$

$$\zeta = \sqrt{\ln 1 + \delta^2} \tag{E.4}$$

$$\lambda = \ln \mu - \frac{\zeta^2}{2} \tag{E.5}$$

From $F_{x_i}(x_i^*) = \Phi(-\alpha_i \cdot \beta)$ follows the following formula for the design point:

$$x_i^* = \frac{\mu_{x_i}}{\sqrt{1 + V_{x_i}^2}} \cdot \exp\left(-\alpha \cdot \beta \sqrt{\ln 1 + V_{x_i}^2}\right) \tag{E.6}$$

E.3. Gumbel distribution

For the Gumbel distributions, the parameters a and u are needed as input values. These values can be found in Table E.2.

Parameter	Mean	Standard deviation	u	a
u_c	1.5	0.15	1.433	8.55
q_t	50	7.5	46.65	0.17

Table E.2: Gumbel distribution: Input for Prob2B

The probability density function can be written as:

$$f(x) = \alpha \cdot \exp\left[-\alpha(x - u) - \exp\left(-\alpha(x - u)\right)\right] \tag{E.7}$$

The cumulative density function can be written as:

$$F(x) = \exp\left[-\exp(-\alpha(x - u))\right] \tag{E.8}$$

$$\mu_x = u + \frac{\gamma}{\alpha} = u + \frac{0.5772}{\alpha} \tag{E.9}$$

$$\sigma_x = \frac{\pi}{\alpha \cdot \sqrt{6}} = \frac{1.282}{\alpha} \tag{E.10}$$

From $F_{x_i}(x_i^*) = \Phi(-\alpha_i \cdot \beta)$ follows the following formula for the design point:

$$x_i^* = u - \frac{1}{\alpha} \cdot \ln\left[-\ln \Phi(-\alpha_i \cdot \beta)\right] \tag{E.11}$$

For time dependent loads, a Gumbel distribution can be used. When scaling from 50 years to 1 year, the standard deviation does not change. The mean and coefficient of variation do change. This can be seen in Figure E.1.
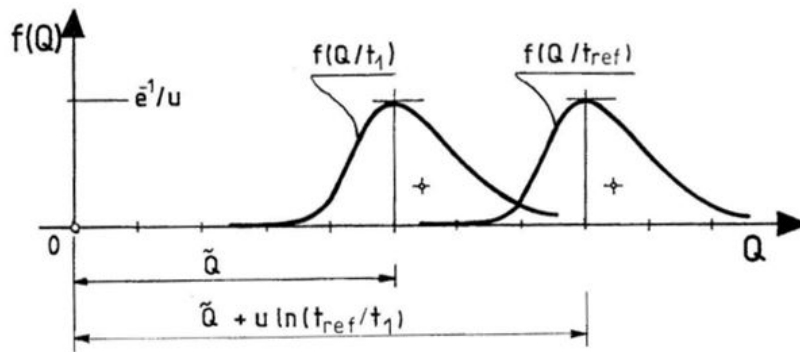

Figure E.1: Gumbel distribution of the maximum over a time period t_1 and t_{ref} [25]

The following formulas need to be used:

$$u_n = u_1 + \frac{\ln n}{a} \tag{E.12}$$

$$\mu_n = \mu_1 + \frac{\ln n}{a} \tag{E.13}$$

Where n is the amount of years, and a can be calculated with Equation E.9.

E.4. Rules for adding and multiplying mean values and standard deviations

E.4.1. Normal distributions

The mean, or expected value, written as $E[X]$ has the property that:

$$E[aX + b] = a \cdot E[X] + b \tag{E.14}$$

So, if the mean of X is μ, then the mean of $aX + b$ is $a \cdot \mu + b$.

The variance, or standard deviation squared, written as $Var[X]$ has the property that $Var[aX + b] = a^2 \cdot Var[X]$ If the standard deviation of X is σ, then the standard deviation of $aX + b$, is $|a| \cdot \sigma$

If one parameter has a standard deviation of σ_1 and the other parameter of σ_2, the added standard deviation is:

$$\sigma_{total} = \sqrt{\sigma_1^2 + \sigma_2^2} \tag{E.15}$$

E.4.2. Lognormal and Gumbel distributions

Non-normally distributed base variables have to be transformed to normally distributed base variables in order to add or subtract them. This transformation assumes that the values of the real and the approximated probability density function and probability distribution function are equal in the design point.
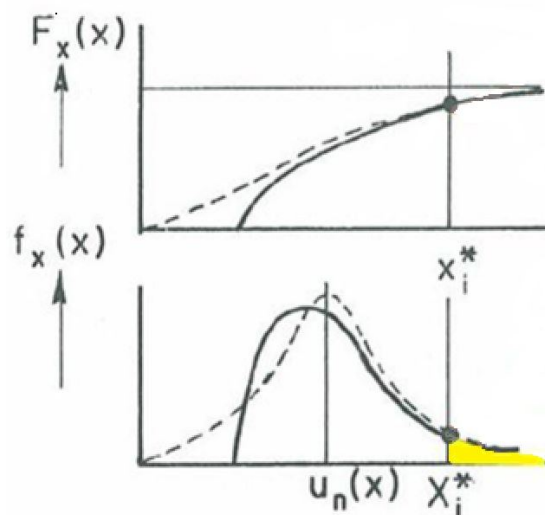

Figure E.2: Transformation to Normal distribution in design point

E.5. Multivariate normal distribution

When a phenomenon is described by more than one random variable, the probability density function of this phenomenon is multi-dimensional. When the two parameters are independent, the joint probability density is:

$$f(x, y) = \frac{1}{\sigma_{x1} \cdot \sigma_{x2} 2 \cdot \pi} \cdot \exp\left(-\frac{1}{2} \cdot \left(\frac{x - \mu}{\sigma_{x1}}\right)^2 + \frac{y - \mu}{\sigma_{x2}}\right) \qquad \text{(E.16)}$$

A multivariate normal distribution, or joint normal distribution, is a generalization of the one-dimensional (univariate) normal distribution to higher dimensions. When this involves two variables, it can be called a bivariate normal distribution, which in turn has two dimensions. The probability density function of a bivariate normal distribution is given as:

$$f_x(x_1, \ldots, x_n) = \frac{1}{\sqrt{(2\pi)^n \cdot |\Sigma|}} \cdot \exp\left(-\frac{1}{2} \cdot (x - \mu)' \cdot \Sigma^{-1} \cdot (x - \mu)\right) \qquad \text{(E.17)}$$

For this equation, the covariance matrix (Σ) has to be determined.

$$\Sigma = \left\{ \begin{matrix} \sigma_1^2 & \rho\sigma_1\sigma_2 \\ \rho\sigma_1\sigma_2 & \sigma_2^2 \end{matrix} \right\} \qquad \text{(E.18)}$$

The covariance is a measure of linear dependence. A concept directly related to the covariance is the Pearson's product moment correlation coefficient ρ_{XY}, which is defined as follows:

$$\rho_{XY} = \frac{cov(XY)}{\sigma(X) \cdot \sigma(Y)} \qquad \text{(E.19)}$$

If X and Y are independent, the value for ρ_{XY} is zero.

$$\mathsf{F}$$
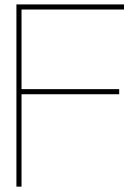
Verification of partial factors from Eurocode

F.1. Parameters from Eurocode

The goal of this chapter is to recalculate the partial factors from Eurocode, by calculating the characteristic value and the design value with the α-values from Eurocode. These α-values can be found in Table F.1.

Thus, the question is whether the α-values from Eurocode really lead to the partial factors stated for the STR cases and EQU cases.

X_i	α_i
Dominating resistance parameter	0.8
Other resistance parameters	0.32
Dominant load parameter	-0.7
Other load parameters	-0.28

Table F.1: Sensitivity factors from Eurocode [23]

The following equation has to hold in order to be able to apply the α-values from Table F.1:

$$0.16 < \frac{\sigma_S}{\sigma_R} < 7.6 \tag{F.1}$$

The design point for normally distributed values is found by using Equation F.2. For Gumbel and lognormal distributions, the design point can be calculated according to the formula in Appendix E.

$$X_d = \mu(X) - \alpha_X \cdot \beta \cdot \sigma(X) \tag{F.2}$$

The characteristic value of the resistance is taken as the 5%-value. The characteristic value of a permanent loading parameter is taken as the 50%-value. For a variable load, this is taken as the 98%-value.

The design value and the characteristic value will be used to calculate the partial factor for yielding of the tethers as well as slackening of the tethers. The STR-conditions of Eurocode would apply to yielding, and the EQU-conditions would apply to slackening.

F.2. Failure mechanism "Yielding of tethers"

For yielding of the tethers, the limit state function can be found in Chapter 5.2. The formulation was written as follows:

$$Z = \theta_R \cdot f_y \cdot 10^3 \cdot A_t \cdot n_{tethers} - \theta_S \cdot \left(\frac{1}{4} \cdot \pi \cdot D^2 \cdot \gamma_w \cdot L + \frac{1}{2} \cdot \frac{\gamma_w}{g} \cdot C_L \cdot u_c^2 \cdot D \cdot L + \right.$$

$$\frac{1}{2} \cdot \frac{\gamma_w}{g} \cdot C_D \cdot u_c^2 \cdot D \cdot L - \left(\frac{1}{4} \cdot \pi \cdot D^2 - \frac{1}{4} \cdot \pi \cdot (D - 2 \cdot t)^2 \right) \cdot \gamma_c \cdot L \cdot 1.1 -$$

$$\left. q_{ballast} \cdot L - q_{asphalt} \cdot L - q_{equipment} \cdot L - q_{marine} \cdot L \right) \quad \text{(F.3)}$$

For this recalculation of the partial factors from Eurocode, only four parameters will be used as variables. The other parameters will be taken as deterministic variables.

Here, f_y and y_c function as resistance and y_w and u_c function as load. They can be dominant as well as not-dominant parameters. The yield strength of steel and the unit weight of water are chosen to be the most dominant parameters, because in this study, they turned out to have the largest influence. With these four parameters, a simple calculation can be done. The results can be seen in Table F.2. The criterion of Equation F.1 should be checked:

$$\frac{\sigma_S}{\sigma_R} = \frac{22195}{13400} = 1.7 \quad \text{(F.4)}$$

The β-value for this limit state function resulted in 4.9. However, a β-value of 3.8 was used for the calculation of the design point. This resulted in the following output:

Parameter	Mean	Standard deviation	α	X_d according to formula	X_{char}	Partial factor γ
f_y - dominant	285	20	0.8	224	252	1.13
y_c - not dominant	24.5	1.7	0.32	22.4	24.5	0.91
y_w - dominant	10.035	0.4	-0.7	11	10.035	1.1
u_c - not dominant	1.5	0.15	-0.28	1.66	1.75	0.95

Table F.2: Design and characteristic values for yielding and longitudinal failure

These partial factors can be compared with the STR-factors from Eurocode:

Force	Partial factor based on X_d formula	Partial factor according to Eurocode
Resistance steel	1.13	1.15
Permanent downward load	0.91	1
Buoyancy force	1.1	1.35
Variable load	$1.1 \cdot 0.95 = 1.05$	1.5

Table F.3: Partial factors for yielding according to recalculation and Eurocode [23]

The material factor for steel and the factor for favorable downward loading are close to the partial factors from Eurocode. However, the buoyancy force and variable load seem conservative. These partial factors could increase, due to a relatively high β-value for this case. The standard deviation of the wave-current velocity could increase, and the buoyancy force could also be increased.

F.3. Failure mechanism "Slackening of tethers"

Another test can be performed for the slackening criterion. Slackening is different from yielding, because parameters have another influence on the system. For slackening of the tethers, the limit state function can be found in Chapter 5.3, and could be written as follows:

$$Z = \theta_R \cdot \frac{1}{4} \cdot \pi \cdot D^2 \cdot \gamma_w \cdot L + \theta_S \cdot \left(-\frac{1}{2} \cdot \frac{\gamma_w}{g} \cdot C_L \cdot u_c^2 \cdot D \cdot L - \left(\frac{1}{4} \cdot \pi \cdot D^2 - \frac{1}{4} \cdot \pi \cdot (D - 2 \cdot t)^2 \right) \cdot \gamma_c \cdot L \cdot 1.1 \right.$$

$$\left. - q_{ballast} \cdot L - q_{asphalt} \cdot L - q_{equipment} \cdot L - q_{traffic} \cdot L - q_{marine} \cdot L \right) \quad \text{(F.5)}$$

For this recalculation of the partial factors from Eurocode, only three parameters will be used as variables. The other parameters will be taken as deterministic variables.

For this criterion, y_w functions as resistance. The unit weight of concrete (y_c) and the traffic load (q_t) have been taken as loading parameters. The y_c or q_t can either be a dominant or not dominant loading parameter.

The criterion of Equation F.1 should be checked:

$$\frac{\sigma_S}{\sigma_R} = \frac{33934}{10603} = 3.2 \quad \text{(F.6)}$$

The β-value for this limit state function resulted in 5.6. However, a β-value of 3.8 was used for the calculation of the design point. With only three parameters as variables, this resulted in the following output:

Parameter	Mean	Standard deviation	α	X_d according to formula	X_{char}	Partial factor γ
y_w - dominant	10.035	0.4	0.8	8.82	10.035	0.88
y_c - dominant	24.5	1.7	-0.7	29.02	24.5	1.18
y_c - not dominant	24.5	1.7	-0.28	26.3	24.5	1.07
q_t - dominant	50	7.5	-7	69.95	62.33	1.12
q_t - not dominant	50	7.5	-0.28	57.98	62.33	0.93

Table F.4: Design and characteristic values for slackening

These partial factors can be compared with the EQU-factors from Eurocode:

Force	Partial factor based on X_d formula	Partial factor according to Eurocode
Buoyancy force	0.88	0.9
Permanent load	1.07-1.18	1.1
Variable load	0.93-1.12	1.35

Table F.5: Partial factors for slackening according to recalculation and Eurocode [23]

The partial factors for buoyancy force turned out to be close to predicted factor from Eurocode. However, the other two factors depend on which parameter is dominant and not dominant.

When the traffic load is not dominant, this partial factor turns out to be significantly lower than the factor from Eurocode. On the other hand, when the unit weight of concrete is dominant, this partial factor is larger than the factor from Eurocode. For another type of limit state calculation, with a β-value closer to 3.8, the results could be closer to the factors from Eurocode.